

WISCONSIN

UNIVERSITY OF WISCONSIN • MADISON, WISCONSIN

39th Annual Gaseous Electronics Conference
October 7-10, 1986

GEC 86

UNIVERSITY OF WISCONSIN

Thirty-Ninth Annual Gaseous Electronics Conference

GEC86

October 7-10, 1986
Madison, Wisconsin

Program and Abstracts

A topical conference of The American Physical Society

Hosted by:

The University of Wisconsin-Madison
The American Physical Society, Division of Electron and Atomic Physics

Executive Committee

Joseph T. Verdeyen, Chairman
University of Illinois

Douglas W. Ernie
University of Minnesota

William P. Allis, Honorary Chairman
Massachusetts Institute of Technology

Raymond Flannery
Georgia Tech

L. Wilmer Anderson, Secretary
University of Wisconsin

Richard Gottscho
AT&T Bell Laboratories

David L. Huestis, Treasurer
SRI International

Gerald Hays
Sandia National Laboratories

Joseph Proud, Chairman Elect
GTE Laboratories

Mark Kushner
Spectra Technology

Oscar Biblarz
Naval Postgraduate School

Local Arrangements Committee

L. W. Anderson
S. Chung
J. E. Lawler
Chun C. Lin
Jack Schneider
Francis A. Sharpton
James C. Weisshaar

Acknowledgments

•

The Gaseous Electronics Conference gratefully acknowledges the support of the University of Wisconsin and the Wisconsin Center where the Conference is held. Financial support for the Gaseous Electronics Conference has been graciously provided by:

The National Science Foundation

The Office of Naval Research

The Air Force Office of Scientific Research

The General Electric Company

The Gaseous Electronics Conference is a Topical Conference of the American Physical Society with sponsorship by the Division of Electron and Atomic Physics.

•

CONTENTS

	Page
ACKNOWLEDGMENTS	2
TECHNICAL PROGRAM	4
SESSIONS	
AA: Electron-Atom/Molecule Collisions I	25
AB: Sheaths: Theory and Experiment	29
BA: Ion-Neutral Collisions	34
BB: Transient Discharge Phenomena	38
CA: Electron Recombination and Attachment	42
CB: D. C. Glows	48
DA: Heavy-Particle Collisions and Clusters	52
DB: R. F. Glows	57
EA: Radiation Transport in Arcs	62
EB: Laser Diagnostic Techniques	67
FA: Posters; Processing	72
FB: Posters; Diagnostics	77
FC: Posters; Spectroscopy	82
GA: Posters; Electron-Atom/Molecule Collisions	88
GB: Posters; Breakdown and Transport	95
GC: Posters; Sheaths	100
HA: Spectroscopy of Atoms, Molecules, Ions	105
HB: Discharges in Electronegative Gases	109
JA: Electron-Atom/Molecule Collisions II	114
JB: Spectroscopy of Arc Lamps	118
KA: Modeling of Transport and Kinetics	122
KB: Laser Diagnostics of Sheaths	126
LA: Posters; Spectroscopy	130
LB: Posters; Lasers and R. F. Discharges	134
LC: Posters; Recombination	140
LD: Posters; Ion-neutral Collisions	147
LE: Posters; Electron-atom/Molecule Collisions	154
MA: Laser Kinetics	157
MB: Plasma Chemistry	161
N: Recent Developments in Excimer Kinetics	164
INDEX OF AUTHORS	167

PROGRAM
THIRTY-NINTH ANNUAL
GASEOUS ELECTRONICS CONFERENCE

RECEPTION AND REGISTRATION

6:00 PM - 8:00 PM
Monday, October 6
Wisconsin Center

Room 213 is available throughout the Conference for use as a discussion room.

SESSION AA. ELECTRON-ATOM/MOLECULE COLLISIONS I

8:00 AM - 9:50 AM, Tuesday, October 7

Lakeshore Room - Wisconsin Center

Chairperson: R. M. St. John, University of Oklahoma

- AA- 1 OPTICAL EXCITATION FUNCTIONS: WHAT CAN ONE BELIEVE (25 min presentation + 5 min discussion)
D. W. O. Heddle (Invited Paper)
- AA- 2 ELECTRON EXCITATION OF METASTABLE RARE GAS ATOMS (20+5)
Chun C. Lin, L. W. Anderson, Francis A. Sharpton, M. Bruce Schulman, and David L. A. Rall (Invited Paper)
- AA- 3 ELECTRON-POLARIZED PHOTON COINCIDENCE STUDIES OF THE EXCITATION OF Ne, Ar and Kr (20+5)
M. A. Khakoo, P. Hammond, and J. W. McConkey (Long Paper)
- AA- 4 V.U.V. ELECTRON IMPACT EXCITATION CROSS-SECTIONS IN Ar AND N₂ (10+3)
J. L. Forand, J. M. Woolsey and J. W. McConkey
- AA- 5 ELECTRON EXCITATION AND INTERSYSTEM QUENCHING OF N₂(a¹Π) BY N₂ (10+3)
W. J. Marinelli, B. David Green, and W. A. M. Blumberg

SESSION AB. SHEATHS: THEORY and EXPERIMENT

8:00 AM - 9:50 AM, Tuesday, October 7

Room 313 - Wisconsin Center

Chairperson: T. Benson, General Electric Company

- AB- 1 TIME EVOLUTION OF COLLISIONLESS SHEATHS (20+5)
N. Hershkowitz, M. H. Cho, E. Y. Wang, and T. Intrator
(Long Paper)
- AB- 2 THE CATHODE SHEATH IN HIGH PRESSURE GLOW DISCHARGES, (10+3)
M. von Dadelszen
- AB- 3 THEORETICAL ASPECTS OF SHEATH PHENOMENA IN GLOW DISCHARGES
(20+5)
K. U. Riemann (Invited Paper)
- AB- 4 A SELF-CONSISTENT CALCULATION OF rf SHEATH PROPERTIES ((10+3)
S. E. Savas
- AB- 5 THEORETICAL INVESTIGATION OF THE CATHODE FALL IN A NEON GLOW
DISCHARGE (10+3)
T. J. Moratz
- AB- 6 INFLUENCE OF COLLISIONS INSIDE THE CATHODE SHEATH UPON THE
ELECTRON ENERGY SPECTRUM IN A HOLLOW CATHODE DISCHARGE (10+3)
B. Shi, Z. Yu, J. Meyer and G. J. Collins
- AB- 7 CHARACTERIZATION OF AN ELECTRICALLY CONDUCTING SPHERE IN A
PLASMA (10+3)
G. L. Rogoff

SESSION BA. ION-NEUTRAL COLLISIONS

10:10 AM - 11:50 AM, Tuesday, October 7

Lakeshore Room - Wisconsin Center

Chairperson: W. A. M. Blumberg, Air Force Geophysics Laboratory

- BA- 1 STATE-TO-STATE VIBRATIONAL ENERGY TRANSFER IN SINGLE MOLECULAR
COLLISIONS (20+5)
W. Ronald Gentry (Invited Paper)
- BA- 2 MICROSCOPIC PERSPECTIVE TO TERMOLECULAR ION-MOLECULE REACTIONS
(10+3)
M. R. Flannery
- BA- 3 STATE-TO-STATE CHANGE TRANSFER CROSS SECTIONS FOR $\text{Ar}^+ + \text{N}_2$
COLLISIONS (10+3)
E. A. Gislason and G. Parlant
- BA- 4 MEASUREMENT OF THE CHARGE TRANSFER RATE CONSTANT FOR $\text{D}_3^+ + \text{SiH}_4$
(10+3)
P. D. Haaland and A. Garscadden

- BA- 5 COLLISIONAL EXCITATION OF Na TO THE 3p AND 3d LEVELS BY FAST H^+ , H_2^+ , H_3^+ , H^0 and H^- (20+5)
L. W. Anderson, James S. Allen, Chun C. Lin, A. M. Howald and R. E. Miers (Long Paper)

SESSION BB. TRANSIENT DISCHARGE PHENOMENA

10:10 AM - 11:50 AM, Tuesday, October 7

Room 313 - Wisconsin Center

Chairperson: J. Dutton, University College of Swansea

- BB- 1 EXCITATION AND IONIZATION BY ELECTRONS AND FAST NEUTRALS AT EXTREMELY HIGH E/N IN Ar (20+5)
A. V. Phelps and B. M. Jelenkovic (Long Paper)
- BB- 2 IONIZATION AND EXCITATION RATE COEFFICIENTS AND INDUCTION TIMES IN MOLECULAR GASES AT HIGH E/n (20+5)
G. N. Hays, J. B. Gerardo, J. T. Verdeyen, L. C. Pitchford, and Y. M. Li (Long Paper)
- BB- 3 RELAXATION TIME MODELING OF ELECTRON TRANSPORT IN RAPIDLY VARYING FIELDS (10+3)
C. Wu, B. M. Penetrante, and E. E. Kunhardt
- BB- 4 DYNAMICS OF AN ASSEMBLY OF ELECTRONS DESCRIBED BY INTERPOLATING BETWEEN THE BOLTZMANN AND FLUID FORMULATIONS (10+3)
E. E. Kunhardt, B. M. Penetrante and C. Wu
- BB- 5 HV BREAKDOWN OF THE SHORT GAP: MODEL (10+3)
J. P. Novak and R. Bartnikas
- BB- 6 DETERMINATION OF $N_2(v)$ DISTRIBUTIONS PRODUCED IN He/ N_2 MICROWAVE DISCHARGES (10+3)
L. G. Piper and W. J. Marinelli

SESSION CA. ELECTRON RECOMBINATION AND ATTACHMENT

1:00 PM - 2:50 PM, Tuesday, October 7

Lakeshore Room - Wisconsin Center

Chairperson: R. S. Freund, AT&T Bell Laboratories

- CA- 1 ELECTRON-ION RECOMBINATION RATES IN AN ATMOSPHERIC PRESSURE PLASMA (10+3)
S. M. Jaffe, M. Mitchner, and S. A. Self
- CA- 2 THE ELECTRON-TEMPERATURE DEPENDENCE OF THE RECOMBINATION OF ELECTRONS WITH NO^+ IONS (10+3)
J. L. Dulaney, M. A. Biondi and R. Johnsen

- CA- 3 DISSOCIATIVE RECOMBINATION OF ELECTRONS WITH HYDRONIUM CLUSTER IONS (10+3)
B. M. Penetrante and J. N. Bardsley
- CA- 4 PHOTOENHANCED ELECTRON ATTACHMENT TO ELECTRONICALLY EXCITED METASTABLE MOLECULES (10+3)
Michel J. Rossi, Hanspeter H. Helm, and Donald C. Lorents
- CA- 5 OPTICALLY ENHANCED ELECTRON ATTACHMENT FROM ELECTRONICALLY EXCITED MOLECULES (10+3)
S. R. Hunter, L. G. Christophorou and L. A. Pinnaduwege
- CA- 6 ELECTRON ATTACHMENT TO NF_3 REVISITED (10+3)
S. R. Hunter
- CA- 7 VARIATION WITH TEMPERATURE OF THE DISSOCIATIVE AND NONDISSOCIATIVE ELECTRON ATTACHMENT TO $n\text{-C}_4\text{F}_{10}$ (10+3)
P. G. Datskos and L. G. Christophorou
- CA- 8 ELECTRON-ION RECOMBINATION OF BENZENE IONS
D. J. Eckstrom, J. S. Dickinson, and M. N. Spencer
- CA- 9 TWO-PHOTON IONIZATION OF BENZENE AT 248 nm AT HIGH BUFFER GAS PRESSURES
J. S. Dickinson, M. N. Spencer and D. J. Eckstrom
- ((Total time allotted for CA-8 and CA-9 (15+3))

SESSION CB. DC GLOWS

1:00 PM - 2:50 PM, Tuesday, October 7

Room 313 - Wisconsin Center

Chairperson: G. L. Rogoff, GTE Laboratories

- CB- 1 KINETIC FORMALISM FOR THE ROLE OF VIBRATIONAL AND ELECTRONIC PROCESSES IN PARTICLE-BEAM SUSTAINED PLASMAS DISCHARGES (20+5)
N. Peyraud (Long Paper)
- CB- 2 GENERATION OF INTENSE LARGE AREA ELECTRON BEAMS BY GLOW DISCHARGES (10+3)
H. F. Ranea-Sandoval, N. Reesor, B. Szapiro, B. Wernsman and J. J. Rocca
- CB- 3 ABNORMAL GLOW DISCHARGE ELECTRON BEAM SPATIAL PROFILE AND ELECTRON ENERGY DISTRIBUTION STUDIES (10+3)
Z. Yang, L. Li, J. Meyer, Z. Yu and G. Collins,
- CB- 4 A NOVEL LOW PRESSURE DISCHARGE WITH PARTITIONS CONTAINING AN ORIFICE (20+5)
V. Godyak, R. Lagushenko, J. Maya, and R. Pai (Long Paper)

- CB- 5 THE RADIAL DISTRIBUTIONS OF CHARGED PARTICLE DENSITIES AND ELECTRIC FIELD STRENGTH IN THE POSITIVE COLUMN (10+3)
D. W. Ernie, H. J. Oskam, and A. Metze
- CB- 6 MOVING AND STANDING STRIATIONS IN HELIUM-NEON LASER (10+3)
R. J. Blair and J. P. Hauck

SESSION DA. HEAVY-PARTICLE COLLISIONS AND CLUSTERS

3:10 PM - 5:00 PM, Tuesday, October 7

Lakeshore Room - Wisconsin Center

Chairperson: J. P. Doering, Johns Hopkins University

- DA- 1 REACTIONS OF ELECTRONIC STATE-SELECTED TRANSITION METAL CATIONS CREATED BY MULTIPHOTON IONIZATION (20+5)
L. Sanders, R. Tonkyn and J. C. Weisshaar (Long Paper)
- DA- 2 COLLISIONAL DESTRUCTION OF $H_2(c^3\Pi_u)$ METASTABLES BY H_2 (10+3)
A. B. Wedding and A. V. Phelps
- DA- 3 ARGON METASTABLE ATOM INTERACTIONS WITH THE CADMIUM HALIDES (10+3)
C. L. Bohler, L. D. Schearer, I. M. Littlewood and S. Abayarathna
- DA- 4 TRANSPORT, EXCHANGE AND QUENCHING OF RESONANCE EXCITATION IN CESIUM VAPOR (10+3)
C. L. Chen, C. S. Liu and P. J. Chantry
- DA- 5 RATE COEFFICIENTS FOR REACTIONS OF NITROGEN METASTABLES WITH SILANE (10+3)
L. G. Piper and G. E. Caledonia
- DA- 6 ION/MOLECULE REACTIONS OF CARBON CLUSTER IONS USING FOURIER TRANSFORM MASS SPECTROMETRY
S. W. McElvany and A. O'Keefe
- DA- 7 REACTIONS OF SILICON CLUSTER IONS AND SILICON SURFACES STUDIED USING FOURIER TRANSFORM MASS SPECTROMETRY
W. R. Creasy and A. O'Keefe
((Total time allotted for DA-6 and DA-7 (30+5))

SESSION DB. RF GLOWS

3:10 PM - 5:00 PM, Tuesday, October 7

Room 313 - Wisconsin Center

Chairperson: D. Graves, University of California-Berkeley

- DB- 1 EQUIVALENT CIRCUITS OF ARBITRARY GEOMETRY RF GAS DISCHARGES
(20+5)
C. B. Zarowin (Long Paper)
- DB- 2 COMPARISON BETWEEN A SIMPLE CIRCUIT MODEL AND THE ELECTRICAL
CHARACTERISTICS OF A RF PARALLEL PLATE DISCHARGE (10+3)
P. Bletzinger and Mark J. Flemming
- DB- 3 A CALCULATION OF SELF-BIAS VOLTAGE AS A FUNCTION OF ELECTRODE
AREA RATIO IN THE ION FLUID MODEL (10+3)
S. E. Savas
- DB- 4 THE ELECTRIC FIELD IN A RF DISCHARGE (10+3)
G. A. Hebner and J. T. Verdeyen
- DB- 5 EFFECT OF RF FIELDS ON THE DYNAMICS OF AN ISOLATED PLASMA (10+3)
R. G. Beeler, H. L. Chen, P. Gabriele, E. Fehring, J. Beard,
J. Wooldridge and J. DeGroot
- DB- 6 MEASURED AND PREDICTED LIGHT EMISSION FROM RF DISCHARGES IN CH₄
(10+3)
L. E. Kline, W. D. Partlow and W. D. Bies
- DB- 7 α and γ RF DISCHARGES IN N₂ AT INTERMEDIATE PRESSURES (10+3)
P. Vidaud, S. M. A. Durrani and D. R. Hall

October 7, Tuesday 7:30 PM - 8:30 PM

Popular Lecture - Geysers

L. W. Anderson

1300 Sterling Hall

SESSION EA. RADIATION TRANSPORT IN ARCS

8:00 AM - 10:00 AM, Wednesday, October 8

Lakeshore Room - Wisconsin Center

Chairperson: P. A. Vicharelli, GTE Laboratories

- EA- 1 DEPARTURES FROM LTE OF FREE-BURNING ARCS IN ARGON (20+5)
G. N. Haddad, A. J. D. Farmer, L. E. Cram, and J. J. Lowke
(Long Paper)
- EA- 2 GENERALIZED MULTITHERMAL EQUILIBRIUM DIAGNOSTICS OF ARGON AND
HYDROGEN ARCS (10+3)
T. L. Eddy

- EA- 3 GMTE ANALYSIS OF ARGON ARC PLASMA AT VARIOUS PRESSURES (10+3)
A. Sedghinasab and T. L. Eddy
- EA- 4 GENERALIZED MULTI-TEMPERATURE RELATIONS FOR HYDROGEN PLASMA
(10+3)
K. Y. Cho and T. L. Eddy
- EA- 5 DETERMINATION OF THE Cd $5^1D_2 \rightarrow 5^1P_1$ ($\lambda=643.8\text{nm}$) TRANSITION
PROBABILITY FROM A CADMIUM-DOPED HIGH PRESSURE MERCURY ARC
(10+3)
T. P. Benson and A. K. Bhattacharya
- EA- 6 SPECTROSCOPIC INVESTIGATION OF A FLOW STABILIZED DC-ARC WITH A
METAL VAPOR CORE (10+3)
R. Sielker, and J. Mentel
- EA- 7 K-SHELL ALUMINUM RESONANCE LINE RATIOS FOR PLASMA DIAGNOSIS
USING SPOT SPECTROSCOPY (10+3)
J. P. Apruzese, J. Davis and D. Duston
- EA- 8 RECOVERY PHENOMENA OF HIGH-CURRENT VACUUM ARCS (10+3)
E. Schade, E. Dullini, B. Gellert

SESSION EB. LASER DIAGNOSTIC TECHNIQUES

8:00 AM - 10:00 AM, Wednesday, October 8

Room 313 - Wisconsin Center

Chairperson: B. N. Ganguly, Wright Patterson Air Force Base

- EB- 1 OPTICAL DIAGNOSTICS OF RF PLASMAS (20+5)
Terry A. Miller (Invited Paper)
- EB- 2 A STUDY OF MOLECULAR ION DISTRIBUTION IN THE POSITIVE COLUMN OF
D.C. GLOW DISCHARGES BY DIODE LASER SPECTROSCOPY (10+3)
Fu-Shih Pan and Takeshi Oka
- EB- 3 OBSERVATION OF THE REVERSAL OF THE OPTOGALVANIC SIGNAL USING
COUNTERPROPAGATING BEAMS (10+3)
Wayne Richardson and L. Maleki
- EB- 4 MEASUREMENT OF H-ATOM DENSITY IN A HYDROGEN DISCHARGE (10+3)
A. S. Schlachter, G. Stutzin, K. N. Leung, J. W. Stearns,
W. B. Kunkel, R. Stevens, G. Worth, E. M. Bernstein,
P. Gohil, and W. G. Graham
- EB- 5 APPLICATIONS OF LASER SPECTROSCOPY IN GASEOUS ELECTRONICS (20+5)
P. J. Hargis, Jr. (Invited Paper)
- EB- 6 NOVEL INTERSECTING LASER BEAM TECHNIQUE FOR FLUORESCENT LAMP
DIAGNOSTICS (10+3)
P. Moskowitz

EB- 7 LASER ABSORPTION MEASUREMENT OF SODIUM DENSITY IN A METAL-HALIDE DISCHARGE LAMP (10+3)

G. Allen, R. Lagushenko, W. Keeffe and J. Maya

SESSION. POSTERS

10:30 AM - 3:45 PM, Wednesday, October 8

Robert P. Lee Lounge and Alumni Lounge - Wisconsin Center

All posters are to be up from 10:30 AM - 3:30 PM. Even numbered posters must be manned from 10:30 AM - 12:30 PM; odd numbered posters must be manned from 1:30 PM - 3:30 PM. All posters must be removed by 4:00 PM.

SESSION FA. PROCESSING

Robert P. Lee Lounge - Wisconsin Center

Chairperson: J. Ingold, General Electric Company

- FA- 1 NOVEL HEAT PIPE DEVICE PRODUCING STABLE DISCHARGE IN CORROSIVE METAL VAPORS
S. B. Hutchison
- FA- 2 TUNABLE DIODE LASER DETECTION OF ATOMS AND MOLECULES IN PROCESS PLASMAS
J. Wormhoudt
- FA- 3 EXCITED STATES IN N₂ REACTIVE PLASMAS FOR STEEL SURFACE NITRIDING
A. Ricard
- FA- 4 ULTRAVIOLET AND VISIBLE CHEMILUMINESCENCE OBSERVED FROM FLUORINE AND XENON DIFLUORIDE ETCHING OF SILICON
M. J. Mitchell, M. Suto, L. C. Lee and T. J. Chuang
- FA- 5 PLASMA SOURCE ION IMPLANTATION
J. R. Conrad and T. Castagna
- FA- 6 PARTICLE SIMULATION OF PLASMA IN A DENSE NEUTRAL BACKGROUND
W. N. G. Hitchon
- FA- 7 PRODUCTION OF GOLD OXIDE IONS DURING SPUTTER DEPOSITION OF GOLD FILMS IN ARGON-OXYGEN DISCHARGES
Carolyn Rubin Aita

SESSION FB. DIAGNOSTICS

Alumni Lounge - Wisconsin Center

Chairperson: S. Chung, University of Wisconsin-Madison

- FB- 1 INFLUENCE OF ELECTRICAL RESONANCE UPON INTERPRETATION OF OPTOGALVANIC DATA
Seong-Pong Lee, Erhard W. Rothe, and Gene P. Reck

- FB- 2 EFFECT OF PHOTODETACHMENT ON A RADIO FREQUENCY DISCHARGE THROUGH BCl_3
Carl E. Gaebe, Todd R. Hayes and Richard A. Gottscho
- FB- 3 STUDY OF THE DIRECT ELECTRON IMPACT IONIZATION PROCESS IN Ne/Hg HCD TUBE BY THE PULSED OPTOGALVANIC TECHNIQUE
M. Hakham-Itzhaq and R. Shuker
- FB- 4 ELECTRONIC TEMPERATURE MEASUREMENTS OF HELIUM MICROWAVE DISCHARGES
J. Hopwood, M Kubinec, J. Asmussen and M. L. Brake
- FB- 5 DETERMINATION OF TWO-DIMENSIONAL TEMPERATURE AND ADDITIVE DENSITY DISTRIBUTIONS IN AN ARC
G. L. Rogoff, A. E. Feuersanger, J. P. Drummey
H. L. Rothwell, Jr.
- FB- 6 PLASMA POTENTIAL DIAGNOSTIC BASED ON EMITTING PROBES
E. Y. Wang, N. Hershkowitz, T. Intrator, M. H. Cho, C. Forest
- FB- 7 MEASUREMENT OF DISCHARGE PLASMA CONDUCTIVITY WITH RF EXTERNAL COIL PROBE
A. M. Pointu and P. Zeller

SESSION FC. SPECTROSCOPY

Robert P. Lee Lounge - Wisconsin Center
Chairperson: J. Ingold, General Electric Company

- FC- 1 PROMPT AND DELAYED PHOTOLYSIS OF SIMPLE MOLECULES
F. Davanloo, C. B. Collins
- FC- 2 ArZn EXCIMER
Y. Tamir and R. Shuker
- FC- 3 THE UV-VISIBLE SPECTROSCOPY OF LASER PRODUCED ALUMINUM PLASMAS
J. T. Knudtson, W. B. Green and D. G. Sutton
- FC- 4 MEASUREMENT OF BARIUM ION DENSITY IN THE VICINITY OF FLUORESCENT LAMP ELECTRODES BY LASER INDUCED FLUORESCENCE
P. G. Hlahol and A. K. Bhattacharya
- FC- 5 TEMPORAL BEHAVIOR OF AN RF DISCHARGE IN SILANE
L. Overzet and J. Verdeyen
- FC- 6 STUDY OF AN OXYGEN D.C. GLOW DISCHARGE BY V.U.V. ABSORPTION SPECTROSCOPY
G. Gousset, P. Panafieu, M. Touzeau, M. Vialle
- FC- 7 ABSORPTION IN LONG-PULSED, ELECTRON-BEAM GENERATED HELIUM PLASMAS
L. W. Downes, S. D. Marcum and W. E. Wells

- FC- 8 POSSIBLE ORIGIN OF HIGH TEMPERATURE SOLAR CORONAS
J. G. Winans
- FC- 9 DECAY OF Cd(II) 441.6nm LINE INTENSITY IN A HOLLOW CATHODE
He-Cd⁺ LASER DISCHARGE
T. Arai, U. K. Nihira, T. Iijima and T. Goto
- FC-10 MEASUREMENTS OF THE BALMER LINE RATIOS EMITTED FROM A DISCHARGE
IN A HYDROGEN THYRATRON AT HIGH CURRENT DENSITIES
J. Fuhr, Th. Aschwanden, B. M. Penetrante, S. Kuo and
E. E. Kunhardt

SESSION GA. ELECTRON-ATOM/MOLECULE COLLISIONS

Alumni Lounge - Wisconsin Center

Chairperson: S. Chung, University of Wisconsin-Madison

- GA- 1 VACUUM ULTRAVIOLET STUDIES OF ELECTRON IMPACT CROSS SECTIONS FOR
H₂ IN THE THRESHOLD ENERGY REGION
J. M. Ajello and D. E. Shemansky
- GA- 2 VUV POLARIZATION STUDIES OF THE EXCITATION OF THE RARE GAS ATOMS
BY ELECTRON IMPACT
P. Hammond, A. G. McConkey and J. W. McConkey
- GA- 3 CROSS SECTIONS FOR EXCITATION OF LONG-WAVE INFRARED EMISSION OF
NITROGEN ATOMS BY ELECTRON IMPACT ON NITROGEN MOLECULES
Sunggi Chung, Chun C. Lin and Edward T. P. Lee
- GA- 4 ELECTRON-EXCITATION CROSS SECTIONS OF THE 5p⁵6p STATES OF XENON
AND THEIR PRESSURE DEPENDENCE
John E. Gastineau, Chun C. Lin, L. W. Anderson, and
Keith G. Walker
- GA- 5 ELECTRON EXCITATION OF THE SECOND NEGATIVE BAND SYSTEM OF THE
OXYGEN MOLECULE
R. Scott Schappe, M. Bruce Schulman, Francis A. Sharpton, and
Chun C. Lin
- GA- 6 EMISSION OF ATOMIC NITROGEN SPECTRAL LINES PRODUCED BY
ELECTRON-IMPACT DISSOCIATION
David L. A. Rall, Albert R. Filipelli, Francis A. Sharpton,
and Chun C. Lin
- GA- 7 OPTICAL EXCITATION FUNCTIONS: STUDY OF THRESHOLD EXCITATION OF
HELIUM AUTOIONIZING STATES
P. J. M. Van Der Burgt, J. Van Eck and H. G. M. Heideman
- GA- 8 RESONANCES IN LOW ENERGY ELECTRON IMPACT ON MAGNESIUM
D. Chen and G. A. Gallup
- GA- 9 ELECTRON ENERGY LOSS SPECTRA OF DISILANE FROM 5-25 eV
M. A. Dillon, H. Tanaka and D. Spence

- GA-10 ELECTRONIC AND VIBRATIONAL EXCITATION OF N_2 IN A GLOW DISCHARGE
J. Loureiro and C. M. Ferreira
- GA-11 COLLISION CROSS SECTIONS AND EXCITATION RATE COEFFICIENTS IN ARGON
V. Puech and L. Torchin
- GA-12 NEW SEMI-EMPERICALLY DERIVED ABSORPTION POTENTIALS FOR e^+ -MOLECULE (ATOM) COLLISIONS FROM Ps THRESHOLD TO UP TO 600 eV
A. Jain

SESSION GB. BREAKDOWN AND TRANSPORT

Robert P. Lee Lounge - Wisconsin Center
Chairperson: J. Ingold, General Electric Company

- GB- 1 THEORY OF RUNAWAY ELECTRONS IN WEAKLY IONIZED PLASMAS
K. U. Riemann
- GB- 2 TRANSPORT PROPERTY OF ELECTRONS IN RAMSAUER GAS
K. Yamamoto and N. Ikuta
- GB- 3 EFFECT OF RAMSAUER MINIMUM FOR TRANSPORT OF ELECTRONS
A. Takeda and N. Ikuta
- GB- 4 EXCITATION MECHANISMS IN ARGON AT VERY HIGH E/n
D. A. Scott and A. V. Phelps
- GB- 5 ELECTRICAL BREAKDOWN INDUCED IN SPARK GAPS BY AN X-RAY PULSE
R. V. Hodges, L. E. McCoy and J. F. Riley
- GB- 6 OPTICAL SWITCHING OF GLOW DISCHARGE WITH AN EXCIMER LASER
M. Saporoschenko, M. J. Rossi and H. Helm
- GB- 7 THE EFFECT OF HUMIDITY AND GAS DENSITY ON SWITCHING-IMPULSE BREAKDOWN OF AIR
A. J. Davies, J. Dutton, R. Turri and R. T. Waters

SESSION GC. SHEATHS

Alumni Lounge - Wisconsin Center
Chairperson: S. Chung, University of Wisconsin-Madison

- GC- 1 PLASMA PRE-SHEATH IN A COLLISIONAL PLASMA
J. T. Scheuer, and G. A. Emmert
- GC- 2 THE PROPERTIES OF PLASMA SHEATHS IN THE PRESENCE OF NEGATIVE IONS
M. F. Toups, D. W. Ernie and H. J. Oskam
- GC- 3 PLASMA-SHEATH STRUCTURE FOR AN ELECTRODE CONTACTING AN ISOTHERMAL PLASMA: III. CATHODES
L. D. Eskin and S. A. Self

- GC- 4 THICKNESS OF THE ION-SHEATH SURROUNDING A LANGMUIR PROBE
G. Goyette and M. Nachman
- GC- 5 SPACE CHARGE, DOUBLE SHEATHS AND PARTICLE EMISSION AT PLASMA BOUNDARIES
T. Intrator, M. H. Cho, E. Y. Wang
- GC- 6 DYNAMICS OF AN IONIC NON COLLISIONAL SHEATH CREATED BY A R.F. POTENTIAL
A. M. Pointu
- GC- 7 MEASUREMENT OF PLASMA POTENTIAL PROFILES WITH RF APPLIED TO CONDUCTING BOUNDARIES
M. H. Cho, N. Hershkowitz, E. Y. Wang, T. Intrator

SESSION HA. SPECTROSCOPY OF ATOMS, MOLECULES, AND IONS

4:00 PM - 5:30 PM, Wednesday, October 8

Lakeshore Room - Wisconsin Center

Chairperson: F. A. Sharpton, University of Wisconsin-Madison

- HA- 1 METASTABLE AUTODETACHING STATES OF NEGATIVE IONS (20+5)
Y. K. Bae and J. R. Peterson (Long Paper)
- HA- 2 THE HOPFIELD HELIUM CONTINUUM AND $\text{He}_2(X^1\Sigma_g^+)$ POTENTIAL (10+3)
J. R. Peterson and H. H. Michels
- HA- 3 RADIATIVE LIFETIMES OF THE O_u^- SUBLEVELS OF THE RARE GAS EXCIMERS (10+3)
David L. Huestis
- HA- 4 ATOMIC TRANSITION PROBABILITIES FOR ScI AND ScII (10+3)
E. A. Den Hartog, G. Marsden, J. E. Lawler, J. T. Dakin
and V. Roberts
- HA- 5 A SOLUTION TO THE PROBLEM OF MISSING INFRARED BRANCHES (10+3)
D. W. Duquette, E. A. Den Hartog, and J. E. Lawler
- HA- 6 THE ABSOLUTE ACCURACY OF THE ELECTRON-IMPACT PHOTOEMISSION CROSS SECTIONS FOR THE VUV RADIOMETRIC STANDARD (10+3)
R. C. G. Ligtenberg, P. J. M. Van Der Burgt, W. B. Westerveld
and J. S. Risley

SESSION HB. DISCHARGES IN ELECTRONEGATIVE GASES

4:00 PM - 5:30 PM, Wednesday, October 8

Room 313 - Wisconsin Center

Chairperson: S. R. Hunter, Oak Ridge National Laboratory

- HB- 1 ELECTRON ATTACHMENT IN WEAKLY ATTACHING GASES (10+3)
J. Dutton, A. K. Lucas and A. W. Williams
- HB- 2 THE INFLUENCE OF TRANSVERSE MAGNETIC FIELDS ON THE
CURRENT-VOLTAGE CHARACTERISTICS OF GLOW DISCHARGES (10+3)
K. H. Schoenbach, S. T. Ko, T. J. Powers and V. K. Lakdawala
- HB- 3 SWITCHING OF CONDUCTION CURRENT BY PHOTODETACHMENT AND
PHOTODISSOCIATION PROCESSES OCCURRING IN THE $\text{SOCl}_2\text{-N}_2$ GAS
MIXTURE (10+3)
W. C. Wang and L. C. Lee
- HB- 4 BREAKDOWN OF A WIRE-TO-PLANE DISCHARGE - TIME-WISE DEVELOPMENT
(10+3)
K. Ramakrishna, I. M. Cohen, and P. S. Ayyaswamy
- HB- 5 OXYFLUORIDE YIELDS FROM CORONA DISCHARGES IN GAS MIXTURES OF SF_6
WITH O_2^{18} AND H_2O^{18} (10+3)
R. J. Van Brunt and M. C. Siddagangappa
- HB- 6 LIMIT-FIELD BEHAVIOR OF VARIOUS GAS MIXTURES DESCRIBED IN TERMS
OF THE RELEVANT MICROSCOPIC COLLISIONAL PROCESSES (10+3)
M. F. Fréchette and J. P. Novak
- HB- 7 EFFECT OF O_2 ON BY-PRODUCT FORMATION IN SPARK DECOMPOSITION OF
 SF_6 (10+3)
I. Sauers

I. Lakeshore Room and 313 are available Wednesday evening

SESSION JA. ELECTRON-ATOM/MOLECULE COLLISIONS II

8:00 AM - 9:45 AM, Thursday, October 9

Lakeshore Room - Wisconsin Center

Chairperson: P. D. Burrow, University of Nebraska

- JA- 1 PARTIAL CROSS SECTIONS FOR Na 3S-3P EXCITATION BY ELECTRONS
(20+5)
X. L. Han, G. W. Schinn and A. Gallagher (Long Paper)
- JA- 2 ELASTIC 3P-3P EXCITED STATE SCATTERING OF ELECTRONS BY SODIUM
(10+3)
M. Zuo, G. F. Shen, B. Stumpf, L. Vuskovic and B. Bederson

- JA- 3 ELECTRON SCATTERING FROM ATOMIC OXYGEN (20+5)
J. P. Doering, E. E. Gulcicek and S. O. Vaughan (Long Paper)
- JA- 4 EXCITATION OF THE ELECTRONIC STATES OF HELIUM BY ELECTRON IMPACT
(20+5)
D. C. Cartwright, Gy. Csanak, S. Trajmar and D. Register
(Long Paper)
- JA- 5 FURTHER MEASUREMENTS OF SMALL-ANGLE SCATTERING BY ALKALI HALIDES
(10+3)
G. F. Shen, M. Zuo, B. Stumpf, L. Vusković, and B. Bederson

SESSION JB. SPECTROSCOPY OF ARC LAMPS

8:00 AM - 9:45 AM, Thursday, October 9

Room 313 - Wisconsin Center

Chairperson: J. J. Lowke, CSIRO

- JB- 1 SELF-REVERSED LINES, AND WHAT WE CAN LEARN FROM THEM (20+5)
D. O. Wharmby (Invited Paper)
- JB- 2 LINE AND CONTINUUM EMISSION FROM OPTICALLY DENSE SODIUM (Na + Hg
+ Xe) PLASMAS (20+5)
J. J. De Groot, J. Schlejen and J. P. Woerdman (Invited Paper)
- JB- 3 EXTENSIONS TO BARTELS' THEORY OF RADIATIVE TRANSFER (10+3)
P. A. Reiser and P. A. Vicharelli
- JB- 4 SENSITIVITY ANALYSIS OF LINESHAPE DIAGNOSTICS IN OPTICALLY THICK
PLASMAS (10+3)
P. A. Vicharelli, W. P. Lapatovich and C. Struck
- JB- 5 MODEL AND DIAGNOSTICS OF THE HIGH PRESSURE MERCURY ARC WITH
SODIUM AND SCANDIUM IODIDE ADDITIVES (10+3)
R. P. Gilliard and J. T. Dakin
- JB- 6 ESTIMATION OF THE BROADENING CONSTANTS FOR THE 3S-3P SODIUM
RESONANCE LINE IN A SODIUM-MERCURY ARC (10+3)
P. A. Reiser and E. F. Wyner

SESSION KA. MODELING OF TRANSPORT AND KINETICS

10:00 AM - 11:30 AM, Thursday, October 9

Lakeshore Room - Wisconsin Center

Chairperson: J. N. Bardsley, University Pittsburgh

- KA- 1 A NOVEL METHOD FOR SOLVING A BOLTZMANN EQUATION (10+3)
N. Ikuta, A. Takeda and Y. Murakami

- KA- 2 MICROWAVE TRANSIENT CONDUCTIVITY OF ELECTRONS IN HELIUM (10+3)
B. Shizgal and S. Ranganathan
- KA- 3 A DIFFUSION LENGTH FORMULA MODIFICATION ACCOUNTING FOR PARTICLE REFLECTION AND LONG MEAN FREE PATHS (10+3)
P. J. Chantry
- KA- 4 USE OF THE PROPORTIONALITY CONDITION FOR SIMPLIFYING AMBIPOLAR DIFFUSION COEFFICIENTS (10+3)
G. L. Rogoff
- KA- 5 EFFECT OF A HIGH FREQUENCY FIELD ON THE DIFFUSION RATE OF ELECTRONS IN MOLECULAR NITROGEN (10+3)
D. F. Hudson and P. H. E. Meijer
- KA- 6 TIME-DEPENDENCE OF THE ATOMIC LEVEL POPULATIONS IN A PULSED, HIGH-CURRENT HYDROGEN DISCHARGE (10+3)
B. M. Penetrante, E. E. Kunhardt, S. C. Kuo, J. Fuhr and Th. Aschwanden

SESSION KB. LASER DIAGNOSTICS OF SHEATHS

10:00 AM - 11:30 AM, Thursday, October 9

Room 313 - Wisconsin Center

Chairperson: J. B. Gerardo, Sandia National Laboratory

- KB- 1 SPECTROSCOPIC STUDIES OF THE CATHODE FALL REGION (20+5)
J. E. Lawler and D. A. Doughty (Invited Paper)
- KB- 2 MEASUREMENT OF ELECTRIC FIELD PROFILE IN A GLOW DISCHARGE CATHODE FALL REGION (10+3)
B. N. Ganguly, J. Shoemaker, B. L. Preppernau and A. Garscadden
- KB- 3 STARK SPECTROSCOPY OF A DOUBLE SHEATH AT A DISCHARGE CONSTRICTION (10+3)
B. N. Ganguly and A. Garscadden
- KB- 4 DOUBLE LAYERS, BREATHING SHEATHS, AND CHEMISTRY IN BCl_3 /RARE GAS RADIO FREQUENCY DISCHARGES (20+5)
Richard A. Gottscho and Geoffrey R. Scheller (Long Paper)
- KB- 5 TEMPORAL AND SPATIAL ELECTRIC FIELD MEASUREMENTS IN A 15KHz GLOW DISCHARGE (10+3)
B. L. Preppernau and B. N. Ganguly

BUSINESS MEETING - 11:30 AM - 12:00 PM, Thursday, October 9 in the Lakeshore Room

POSTERS

1:00 PM - 4:00 PM, Thursday, October 9

Robert P. Lee Lounge and Alumni Lounge - Wisconsin Center
Chairperson: J. E. Lawler, University of Wisconsin-Madison

All posters are to be up from 1:00 PM - 3:30 PM. All posters in LA, LB and LC must be manned from 1:00 - 2:15. All posters in LC and LE must be manned from 2:15 PM - 3:30 PM. All posters must be removed by 4:00 PM.

SESSION LA. SPECTROSCOPY

Robert P. Lee Lounge - Wisconsin Center

- LA- 1 LASER DOUBLE RESONANCE MEASUREMENTS OF THE VIBRATIONAL ENERGY TRANSFER RATES AND MECHANISMS OF $DF(v=1,2)$
J. M. Robinson, K. J. Rensberger, M. A. Muyskens and F. F. Crim
- LA- 2 STUDIES OF VIBRATIONAL-ROTATIONAL POPULATIONS IN NITROGEN DISCHARGES USING CROSSED-BEAM CARS
P. P. Yaney, C. J. Emmerich, D. D. Hodson and S. W. Kizirnis
- LA- 3 COLLISIONAL RELAXATION OF $DF/HF(v=1)$ BY THE DF DIMER THROUGH COMPLEX FORMATION
K. J. Rensberger, J. M. Robinson and F. F. Crim
- LA- 4 MAGNETICALLY INDUCED CIRCULAR POLARIZATION
K. L. Stricklett, D. J. Burns, and P. D. Burrow
- LA- 5 EFFECT OF RADIATION TRAPPING ON THE POLARIZATION OF AN OPTICALLY PUMPED ALKALI METAL VAPOR
D. Tupa, L. W. Anderson, D. L. Huber, and J. E. Lawler

SESSION LB. LASERS AND R.F. DISCHARGES

Alumni Lounge - Wisconsin Center

- LB- 1 DIRECT OBSERVATION OF 157.5 nm "LASER" PHOTONS FROM THE $f\ 3\Pi_g$ STATE OF F_2
D. Spence, H. Tanaka, M. A. Dillon and K. Lanik
- LB- 2 LITHIUM PLASMA GENERATION BY ArF^* LASER
S. Lin, K. Y. Tang and R.O. Hunter, Jr.
- LB- 3 LASER DIAGNOSTIC IN SURFACE WAVE HELIUM DISCHARGE
C. Boisse-Laporte, G. Gousset and A. Granier
- LB- 4 SPATIALLY RESOLVED EMISSION PROFILES OF A PARALLEL PLATE RF GLOW DISCHARGE
R. M. Roth
- LB- 5 A FLUID MODEL OF THE R. F. DISCHARGE AT 13.56 MHz
D. B. Graves

- LB- 6 DIFFUSION THEORY OF SURFACE WAVE PRODUCED PLASMAS WITH IONIZATION FROM METASTABLE STATES
C. M. Ferreira and A.B. Sa
- LB- 7 MICROWAVE DISCHARGES SUSTAINED BY SURFACE WAVE IN ARGON-OXYGEN MIXTURES
C. Boisse-Laporte, P. Leprince, R. Darchicourt, J. Marec, S. Pasquiers
- LB- 8 STANDING WAVE DISCHARGE (SWD) APPLICATION TO ION ARGON LASER
Z. Rakem, P. Leprince, J. Marec and S. Saada
- LB- 9 EFFECTS OF ALKALI-METAL SEEDING ON THE PERFORMANCE OF THE CuCl Laser
S. W. Kim, J. B. Atkinson and L. Krause

SESSION LC. RECOMBINATION

Robert P. Lee Lounge - Wisconsin Center

- LC- 1 DETAILED INVESTIGATION OF THE THOMSON MODEL OF TERMOLICULAR RECOMBINATION
E. J. Mansky and M. R. Flannery
- LC- 2 ION-ION RECOMBINATION IN SF₆ AND IN MIXTURES OF CH₄ AND SF₆
M. C. Cornell and I. M. Littlewood
- LC- 3 ION-PAIR PRODUCTION IN Li-Cs COLLISIONS
S. Y. Tang, D. P. Wang and R. H. Neynaber
- LC- 4 CONTRIBUTIONS OF ATOM-ATOM COLLISIONS IN WEAKLY-IONIZED ARGON PLASMAS
C. Braun and J. A. Kunc
- LC- 5 STEADY-STATE TOWNSEND EXPERIMENT: MEASURED AND PREDICTED ELECTRON SWARM PROPERTIES OF CCl₂F₂ AND CCl₂F₂/N₂ MIXTURES
M. F. Fréchette and J. P. Novak
- LC- 6 DISSOCIATIVE ELECTRON ATTACHMENT TO THE ISOTOPES OF MOLECULAR HYDROGEN
J. M. Wadehra
- LC- 7 Cs ION-ELECTRON RECOMBINATION IN THE PRESENCE OF THE RARE GASES
A. T. Pritt, Jr.
- LC- 8 DISSOCIATIVE ATTACHMENT IN THE CHLOROMETHANES
S. C. Chu, K. L. Stricklett and P. D. Burrow
- LC- 9 ASSESSMENT OF THE He₂⁻ POTENTIAL FROM THE AUTODETACHMENT SPECTRUM
Y. K. Bae, J. R. Peterson and H. H. Michels
- LC-10 ANGULAR AND ENERGY DISTRIBUTIONS OF ELECTRONS DETACHED IN H⁻ - He COLLISIONS (50 eV-2 keV)
F. Penent, J. P. Grouard, R. I. Hall and J. L. Montmagnon

- LC-11 RATE FOR F^- EXCHANGE IN $SF_6^- + SOF_4$ COLLISIONS
I. Sauers, L. W. Sieck, R. J. Van Brunt and
M. C. Siddagangappa

SESSION LD. ION-NEUTRAL COLLISIONS

Alumni Lounge - Wisconsin Center

- LD- 1 IONIZATION OF RYDBERG ATOMS IN THERMAL COLLISIONS WITH POLAR MOLECULES.
Toshizo Shirai
- LD- 2 THERMAL-ENERGY CHARGE TRANSFER IN Ar-Zn SYSTEM
Y. Tamir and R. Shuker
- LD- 3 COLLISIONAL PROCESSES IN $XeF(X)$
G. Black, L. E. Jusinski and D. L. Huestis
- LD- 4 LASER-PUMPED He^4 AS A SPIN-DEPENDENT PROBE OF ATOMIC AND MOLECULAR COLLISIONS
L. D. Schearer, C. L. Bohler and M. Leduc
- LD- 5 REACTIONS OF He_2^+ AND $He(2^3S)$ WITH Ne, Ar, Kr, Xe, H_2 , N_2 , O_2 , CO_2 , AND N_2O AT ATMOSPHERIC PRESSURES
J. M. Pouvesle, A. Khacef, J. Stevefelt, V. T. Gyls,
H. Jahani and C. B. Collins
- LD- 6 S AND P STATE EXCITATION DURING HARD COLLISIONS IN THE Ar^+ ON Kr SYSTEM - METASTABLE PRODUCTION
K. B. McAfee, Jr and R. S. Hozack
- LD- 7 CLUSTERING REACTIONS OF H_2CN^+ IONS WITH HCN
B. Chatterjee and R. Johnsen
- LD- 8 EXCITATION MECHANISMS IN keV He^+ - H_2/D_2 COLLISIONS
C. L. Engelhardt and D. H. Jaecks
- LD- 9 THREE-BODY REACTION OF $XeCl^*$ TO FORM Xe_2Cl
D. C. Lorents, R. L. Sharpless, D. L. Huestis
- LD-10 DISSOCIATION OF DIATOMIC MOLECULES
Philip C. Cosby and Hanspeter Helm
- LD-11 TOTAL QUENCHING CROSS SECTIONS OF METASTABLE ATOMS AND MOLECULES BY MERCURIC HALIDES
J. L. Daniels
- LD-12 POLARIZATION OF THE Na $3d+3p$ AND THE Na $3p+3s$ RADIATION INDUCED BY THE COLLISIONAL EXCITATION OF Na BY FAST H^+ AND H^- IONS
James S. Allen, L. W. Anderson, Chun C. Lin

SESSION LE. ELECTRON-ATOM/MOLECULE COLLISIONS

Robert P. Lee Lounge - Wisconsin Center

- LE- 1 ELECTRON-SILENE INTERACTIONS AT 30-500 eV USING A PARAMETER-FREE ENERGY-DEPENDENT SPHERICAL-COMPLEX-OPTICAL-POTENTIAL (SCOP) MODEL
A. Jain
- LE- 2 EFFECTS OF HELIUM UPON ELECTRON BEAM EXCITATION OF N_2^+ AT 391.4 nm AND 427.8 nm
M. L. Brake, T. Repetti, K. Pearce, R. M. Gilgenbach, R. F. Lucey, Jr., and P. Sojka
- LE- 3 THE GENERALIZED OSCILLATOR STRENGTH FOR ONE-ELECTRON DIATOMIC MOLECULES
M. Kimura
- LE- 4 DISSOCIATION OF ETCHANT GAS PLASMA CONSTITUENTS BY CONTROLLED ELECTRON IMPACT
A. E. Tabor and K. Becker

Banquet

Lowell Hall 6:30 - 10:00

After Dinner Speaker, Prof. Robert Greenler
University of Wisconsin-Milwaukee
"Optical Phenomena in the Atmosphere"

SESSION MA LASER KINETICS

8:45 AM - 10:15 AM, Friday, October 10

Lakeshore Room - Wisconsin Center

Chairperson: H. T. Powell, Lawrence Livermore National Laboratory

- MA- 1 ANALYTICAL TIME-DEPENDENT TREATMENT OF ELECTRON DEGRADATION: ELECTRONIC EXCITATION OF N_2 MOLECULE BY SUBEXCITATION ELECTRON IN He OR Ne GASES (10+3)
M. A. Dillon, M. Kimura and M. Inokuti
- MA- 2 EXCITED-STATE LIFETIME MEASUREMENTS IN NITROGEN AT HIGH PRESSURES (10+3)
P. Bletzinger and D. F. Grosjean
- MA- 3 QUENCHING OF $NF(b^1\Sigma)$ BY F_2 , IF, AND I_2 FROM 330K TO 572K (10+3)
R. A. Young, R. Bower, C. L. Lin and J. Blauer
- MA- 4 CRITERIA FOR THE TRANSIENT GENERATION OF HOMOGENEOUS OZONE-SYNTHESIS PLASMAS (10+3)
L. A. Rosocha

- MA- 5 PUMP RATE DEPENDENCE OF RARE-GAS HALIDE EXCIMER LASER EFFICIENCIES USING SELF-SUSTAINED DISCHARGE PUMPING OF Ne DILUENT MIXTURES (10+3)
M. Ohwa and M. Obara
- MA- 6 NON-UNIFORM OPTICAL EXTRACTION AS A SOURCE OF DISCHARGE INSTABILITY IN E-BEAM SUSTAINED DISCHARGE EXCIMER LASERS (10+3)
Mark J. Kushner

SESSION MB. PLASMA CHEMISTRY

8:45 AM - 10:15 AM, Friday, October 10
Room 313 - Wisconsin Center
Chairperson: C. Zarowin, Perkin-Elmer Corporation

- MB- 1 PLASMA CHEMISTRY IN METAL ETCHING (20+5)
D. W. Hess (Invited Paper)
- MB- 2 REACTIONS LEADING TO THE FORMATION OF LARGE CLUSTERS IN SiH_4/Ar RF PLASMAS (10+3)
Mark J. Kushner
- MB- 3 THE SURFACE OF GROWING HYDROGENATED AMORPHOUS SILICON FILMS (10+3)
J. R. Doyle, G. H. Lin, M. Z. He and A. Gallagher
- MB- 4 OXYGEN SPECIES IN Ne-O_2 and Ar-O_2 rf SPUTTER DEPOSITION DISCHARGES AND THEIR EFFECT ON Pt-O ALLOY FILM GROWTH (20+5)
Carolyn Rubin Aita (Long Paper)

SESSION N. RECENT DEVELOPMENTS IN EXCIMER KINETICS

10:30 AM - 11:40 AM, Friday, October 10
Lakeshore Room - Wisconsin Center
Chairperson: J. J. Ewing, Mathematical Sciences Northwest Inc.

- N- 1 ELECTRON DENSITY MEASUREMENTS OF XeCl , XeF AND KrF LASER MIXTURES (10+3)
W. D. Kimura, D. R. Guyer, S. E. Moody, J. F. Seamans, and D. H. Ford
- N- 2 MODEL COMPARISONS OF ELECTRON DENSITY MEASUREMENTS IN KrF , XeF , AND XeCl (10+3)
E. T. Salesky and W. D. Kimura
- N- 3 IMPLICATION OF ATTACHMENT RATES ON KrF LASER PERFORMANCE IN LIGHT OF RECENT MEASUREMENTS OF ELECTRON DENSITY (10+3)
Mark J. Kushner

N- 4 CURRENT UNDERSTANDING OF THE XeCl LASER (20+5)
D. L. Huestis (Long Paper)

SESSION AA

8:00 - 9:50 AM, Tuesday, October 7

Lakeshore Room - Wisconsin Center

ELECTRON-ATOM/MOLECULE COLLISIONS I

Chairperson: R. M. St. John, University of Oklahoma

AA-1 Optical Excitation Functions: What can one believe,
D W O HEDDLE, Royal Holloway & Bedford New College --
Measurements have been reported of the optical excitation
function of at least one spectrum line for more than 45
neutral atoms and two dozen positive ions. Despite the
large amount of data, the extent of our knowledge of
optical excitation functions is quite limited because so
many papers omit discussion of factors which are crucial
to the assessment of the quality of the results. In
this paper I shall very briefly review the factors which
matter and give examples of measurements by different
authors which, because they are well documented, can be
combined to give more information than either separately.
My faith in theoretical excitation cross-sections is
very limited and, unless confirmed by experiment extends
only to the Bethe approximation and I shall discuss the
proper application of this to normalisation. While we
all deplore papers which give insufficient information
about the experimental or analysis procedure what can one
say about papers which do not even give the results?
There are a surprising number of these and some are very
strange indeed.

AA-2 Electron Excitation of Metastable Rare Gas
Atoms* CHUN C. LIN, L. W. ANDERSON, FRANCIS A. SHARPTON,
M. Bruce SCHULMAN, David L. A. RALL, U. of
Wisconsin--The optical method for measuring electron
excitation cross sections by monitoring the radiation
emitted by the excited atoms is not directly applicable
to metastable levels. However, with a cw laser beam
perpendicular to the electron beam to pump the
metastable atoms produced by electron excitation to a
higher level, it is possible to utilize the
laser-induced fluorescence intensity to determine the
excitation cross section of the metastable levels.
Furthermore the number density of the metastable atoms
can be determined by a similar experiment using a pulsed
laser. These methods have been applied to neon.
Experiments for measuring the cross sections of exciting
the atoms from the metastable level to a higher level
are reported.

* Supported by the AFOSR.

AA-3 Electron-Polarized Photon Coincidence Studies of the Excitation of Ne, Ar and Kr* M.A. KHAKOO, P. HALMOND† and J.W. McCONKEY††, U. of Windsor, Ontario, Canada - Polarization correlations have been measured for electron impact excitation of the heavy rare gases at impact energies of 80 eV (Ne and Ar) and 60 eV (Kr) and for electron scattering angles up to 45°. Circular polarization measurements have been obtained and are the first to be reported for the resonance lines of these targets. The angular momentum transfer to all targets is found to be positive at small scattering angles and is in fact surprisingly helium-like. Less than 10% incoherence in the radiation emitted perpendicular to the scattering plane is observed.

* Supported by the Natural Sciences and Engineering Research Council of Canada.

† U.K. S.E.R.C. Fellow.

†† Canada Council Killam Fellow.

AA-4 V.U.V. Electron Impact excitation cross-sections in Ar and N₂ J.L. FORAND, J.M. WOOLSEY† and J.W. McCONKEY††, U. Windsor, Ont., Canada -- Absolute emission cross-sections have been measured for the resonance lines of Ar (104.8 and 106.7 nm) Ar⁺ (92 and 93.8 nm) and for a variety of emissions from N and N₂ following 200 eV electron impact on Ar and N₂. Calibration of the detection equipment has been accomplished using the Lyman series excited following electron impact on atomic H produced in an RF source and also molecular emissions following e-H₂ collisions when the source is switched off. Full details of the technique, errors involved and data obtained will be presented at the Conference.

* Supported by the Natural Sciences and Engineering Research Council of Canada and NATO Division of Scientific Affairs.

† Permanent address: University of Stirling, Scotland.

†† Canada Council Killam Fellow.

AA-5 Electron Excitation and Intersystem Quenching of $N_2(a^1\Pi)$ by N_2 . W.J. MARINELLI and B.D. GREEN, Physical Sciences Inc. and W.A.M. Blumberg Air Force Geophysics Lab.-We report results of experiments on the large LABCEDE facility at AFGL on excitation and quenching of $N_2(a)$. Beams of 4.5 keV electrons excite $N_2(a)$ in pure N_2 at pressures from 0.25-72 mTorr. Emissions observed between 165-220 nm are analyzed by a least-squares spectral fitting code to determine vibrational populations. $N_2(C-B)$ emission intensities correct LBH intensities for pressure scaling and fluctuations in excitation source intensity. Our low-pressure (0.25 mT) $N_2(a)$ vibrational distributions are consistent with a Franck-Condon type excitation of $N_2(X, v''=0)$ by high energy electrons. The vibrational distribution in the $N_2(a)$ state changes considerably between 0.25 and 6 mT. Weak emission from the $N_2(a', v'=0 \rightarrow X, v)$ transition also is been observed. This rapid vibrational redistribution may be a result of pure vibrational redistribution or collisional coupling with the near-resonant $a'^1\Sigma_u^-$ state. At higher pressures (up to 72 mT) slower electronic quenching becomes the important.

This work was supported by the Air Force Office of Scientific Research and the Defense Nuclear Agency.

SESSION AB

8:00 - 9:50 AM, Tuesday, October 7

Room 313 - Wisconsin Center

SHEATHS: THEORY AND EXPERIMENT

Chairperson: T. Benson, General Electric Company

AB-1 Time Evolution of Collisionless Sheaths,* N. HERSHKOWITZ, M.H. CHO, E.Y. WANG, T. INTRATOR, University of Wisconsin-Madison -- Experimental measurements are made of the time evolution of the spatial profile of the plasma potential near negatively biased electrodes in collisionless multidipole plasmas. Plasma is produced by electrons emitted from hot filaments located far from the biased electrode and confined by a surface magnetic field. The biased electrode does not play a significant role in plasma production or in determining the background plasma potential. Representative argon plasma density and electron and ion temperatures are $n = 10^8 - 10^9 \text{ cm}^{-3}$ and $T_e \approx 2 \text{ eV}$ and $T_i \approx 0.2 \text{ eV}$. Low densities are studied in order to achieve good spatial resolution. At $t = 0$ the electrode bias potential is switched from ground to $-|V_{\text{bias}}|$. The sheath is found to initially form close to the electrode, to expand to a maximum separation and to contract to a steady state value. Data are obtained using emissive probes with fast time resolution achieved with a boxcar averager. Scaling with plasma density, ion mass and electrode bias voltage is discussed. Results are compared to Child-Langmuir and matrix sheaths.
*Supported by NSF Grant ECS-8314488.

AB-2 The Cathode Sheath in High Pressure Glow Discharges, M. VON DADELSZEN,* U. of Washington --The results of a series of experiments undertaken to investigate the general nature of the cathode sheath in externally-sustained, long pulse, high pressure glow discharges will be presented. The experiments include double pulse holographic interferometry of the sheath driven thermal layer, surface heating experiments to investigate the observed density profiles, and open shutter photographs of the distributed nature of the sheath (cathode spots) and filamentary discharges originating from these spots. The effects of supersonic flow on the filaments were also observed. It is concluded that the cathode spots are regions of self-sustained cathode fall operating in the normal glow regime and are independent of the external source. In discharges without flow, a transition to an arc is always associated with a filament crossing the discharge gap, whereas in discharge with supersonic flow the filaments are not observed to cross the gap. These results led to the analysis of cathode spot distributions, presented at the 1985 GEC.

*Current affiliation: Spectra Technology, Inc.

AB-3

Theoretical Aspects of Sheath Phenomena
Glow Discharges -

K.-U. RIEMANN, Ruhr-University, Bochum, FRG.

We consider the plasma sheath transition of a weakly ionized plasma in front of a negative wall. Due to Bohm's criterion the ions entering the space charge region ("sheath") must be preaccelerated to ion sound velocity in the quasineutral plasma boundary layer ("presheath"). The presheath is strongly affected by the inhomogeneous electric field and requires a selfconsistent kinetic analysis. We discuss the presheath mechanism and the influence of several effects (elementary processes, geometry, magnetic field, etc.). In the case of moderate wall potentials the subsequent "thin" sheath (extension some Debye lengths) may be considered collision free. For highly negative walls, however, the sheath becomes "thick" and is influenced by collisional effects. We present a simplified theory of a thick sheath based on the classical model of Davis and Vanderslice [1]. The problems mentioned so far refer to stationary sheath theory. However, if certain frequency requirements are met ($\omega \ll \omega_{pi}$ resp. $\omega_{pi} \ll \omega \ll \omega_{pe}$, where $\omega_{pi,e}$ is the ion - resp. electron plasma frequency) the analysis can be extended to describe sheath phenomena in RF discharges.

[1] W.D. Davis, T.A. Vanderslice, Phys.Rev.131 (219), 1963

AB-4 A Self-Consistent Calculation of rf Sheath Properties. S.E. SAVAS, Lawrence Berkeley Lab.--The ion density, electric field and complex impedance have been calculated self-consistently for the sheaths of capacitive rf discharges. This numerical work assumes that: ions take \geq two full rf cycles to transit the sheath; that electrons "slosh" with small inertia and temperature; and that the sheath potential varies sinusoidally from 0. Volts to twice the rf amplitude, V_0 . We find that in the collisionless case: the ion density is well approximated by the function $\rho = \rho_0 (1 + (Z/Z_0)^2)^{-1/2}$ (where ρ_0 is the ion density at the point of maximum sheath width and Z_0 is a scale length depending on V_0 and initial ion energy.); the spatial dependence of the electric field becomes nearly linear as the ion's initial energy is increased; and sheath impedance becomes more reactive with increasing current density, j , and with decreasing V_0 . Finally, j dependence on V_0 and d , the sheath width, is found to be close to Child's Law. For the collisional case charge exchange is assumed to dominate. Here, the ion density function from the collisionless case is modified by Z_0 becoming a function of the parameter, $P \equiv n\sigma_c x d$, where n is the gas density.

AB-5 Theoretical Investigation of the Cathode Fall in a Neon Glow Discharge, T.J. MORATZ, U. of Pittsburgh-- A theoretical analysis of the cathode fall experiments of Doughty et. al.^{1,2} is presented, based on a Monte Carlo simulation of the electrons in the discharge. The non-local aspects of the electron kinetics (i.e. the average energy and the ionization coefficient) are emphasized and the connection is made to the work of Davies and Evans³. The light output in the negative glow and the electron energy distribution at the anode are described and the electron energy deposition is seen to be non-local. The good agreement with the experiments verifies the usefulness of the method. The ion kinetics concentrate on the ion drift velocity and the molecular ion (Ne_2^+) formation.

¹D.K. Doughty, S. Salih and J.E. Lawler, Phys. Lett. A, 103, 41 (1984).

²D. K. Doughty, E.A. DenHartog and J.E. Lawler, Appl. Phys. Lett., 46, 352 (1985).

³A.J. Davies and J.G. Evans, J. Phys. D, 13, L161 (1980).

AB-6 Influence of Collisions Inside the Cathode Sheath Upon the Electron Energy Spectrum in a Hollow Cathode Discharge,* B. SHI, Z. YU, J. MEYER, and G. J. COLLINS, Colorado State U.--Computer models(1) make Boltzmann equation calculations of the energy spectrum both inside and outside the cathode sheath. Electron collisions inside the cathode sheath occurring during electron acceleration explain the origin of the peak structure of the electron energy spectrum measured in a bulk hollow cathode discharge. The relative role of elastic, inelastic-excitation and inelastic-ionization collisions on the $N(E)$ spectrum are examined by the computer model. Good agreement was obtained between our $N(E)$ calculation and previous experiments done by Gill and Webb(2) as well as by Olson and Nordlund(3).

*Work supported by NSF

¹B. Shi, J. Meyer, Z. Yu and G. J. Collins, IEEE, J. Plasma Science (to be published) Aug. 1986.

²P. Gill and C. E. Webb, J. Phys. D, 10, 229 (1977).

³R. A. Olson and D. R. Nordlund, 1973, Wright-patterson AFB, Technical Report.

AB-7 Characterization of an Electrically Conducting Sphere in a Plasma. G.L. ROGOFF, GTE Laboratories Inc.--
Since an electrically-floating particle in a plasma can collect no net current, its potential relative to the surrounding plasma and the conditions in the neighborhood adjust accordingly. A simplified analysis is being developed to describe the electrical conditions for a spherical particle located in a collisional, thermal plasma with an electric field present. Charged particle densities are sufficiently high for the sheath to be collisionless and to be thin compared with the particle size, allowing the region near the particle surface to be treated in planar geometry. The particle distorts the surrounding plasma potential distribution to that required for the integrated electron flux to the surface to equal the integrated ion flux. However, since the electron flux is nonuniform, current flows through the particle. Expressions for the distorted plasma potential distribution, the particle potential, the electron flux distribution, the location of particle flux balance, the electric field at the surface, the surface charge density distribution, and the current through the particle have been obtained. These relationships provide bases for assessing the importance of momentum- and energy-transfer processes associated with charged-particle fluxes and surface charging.

SESSION BA

10:10 AM - 11:50 AM, Tuesday, October 7

Lakeshore Room - Wisconsin Center

ION-NEUTRAL COLLISIONS

Chairperson: W. A. M. Blumberg, Air Force Geophysics Laboratory

BA-1 State-to-State Vibrational Energy Transfer in Single Molecular Collisions,* W. RONALD GENTRY, Department of Chemistry, U. of Minnesota -- Molecular energy transfer processes play an important role in virtually all gas-phase dynamical phenomena. The detailed, microscopic dynamics of such processes may be studied at the most fundamental level by observing the quantum state-resolved transfer of energy in single bimolecular collisions at controlled kinetic energy. Making use of both molecular beam and laser spectroscopic techniques, such experiments have now been carried out for a variety of chemical systems. The lecture will summarize the dynamic insights which these experiments reveal and indicate likely avenues of future progress.

*Research supported by the U.S. Department of Energy, Division of Chemical Sciences.

BA-2 Microscopic Perspective to Termolecular Ion-Molecule Reactions,* M. R. FLANNERY, School of Physics, Georgia Tech--Current chemical kinetics of various ion-molecule reactions and of termolecular recombination, $A+B+M \rightleftharpoons AB+M$, in a gas M invokes simplified macroscopic schemes so as to predict the general variation with gas density of such processes. In this paper a non-equilibrium microscopic treatment of the various energy-transfer and stabilization sequences is provided, and connection is established with the previous macroscopic treatments. Expressions for the three-body rate for stabilization of complexes AB^* by collision with M are derived. This rate is, in general, dependent on the gas density. For moderate-high gas densities, the effect of transport, while important for ion-ion recombination, is not important for termolecular ion-atom and atom-atom association at most gas densities of practical interest.

*Research supported by U. S. Air Force Office of Scientific Research under Grant No. AFOSR-84-0233.

BA-3 State-to-State Charge Transfer Cross Sections for $\text{Ar}^+ + \text{N}_2$ Collisions, E.A. GISLASON, U. of Illinois-Chicago, and G. PARLANT, U. of Paris-South--Theoretical cross sections for the process $\text{Ar}^+ + \text{N}_2 \rightarrow \text{Ar} + \text{N}_2^+$ in the energy range 1-4000 eV(cm) are presented and compared with available experimental results. The method ^{1,2} treats the translational motion classically while solving the time-dependent Schrodinger equation exactly for the vibronic states. Ab initio potential energy surfaces³ are used. State-to-state charge transfer cross sections are obtained for both spin-orbit states of Ar^+ . In addition, the cross section for direct transition between the two Ar^+ states is shown to be surprisingly large. Energy resonance considerations determine the product state distribution at low energy; the results become Franck-Condon-like at high energy.

¹M.R. Spalburg and E.A. Gislason, Chem. Phys. 94,327,339(1985).

²G.Parlant and E.A. Gislason, Chem. Phys. 101,227(1986).

³P. Archirel and B. Levy, Chem. Phys. 106,51(1986).

BA-4 Measurement of the Charge Transfer Rate Constant for $\text{D}_3^+ + \text{SiH}_4$, P. D. Haaland and A. Garscadden, Air Force Wright Aeronautical Laboratories, Wright-Patterson Air Force Base. -- Studies of dissociative charge transfer in silane collisions with SiH_2^+ and SiH_3^+ ions have indicated that H^+ is transferred. In silane deposition reactor plasmas, H^+ and H_2^+ also are formed and are expected to rapidly form H_3^+ . The reaction of H_3^+ on silane is therefore of interest. In order to resolve ambiguities in the reaction, the measurements were made using D_3^+ . The experiment utilized a modified Nicolet Fourier Transform Mass Spectrometer. A mixture of deuterium and silane was ionized by an electron beam. The silane ions were then ejected from the trap. The deuterium molecular ions react rapidly with background deuterium to form D_3^+ . The D_3^+ reacts with the background silane to give SiH_3^+ and neutral products. This rate constant is estimated as approximately $2 \times 10^{-9} \text{ cm}^3 \text{ s}^{-1}$.

BA-5 Collisional Excitation of Na to the 3p and 3d Levels by Fast H^+ , H_2^+ , H_3^+ , H^0 , and H^- .* L. W. ANDERSON, JAMES S. ALLEN, CHUN C. LIN, A. M. HOWALD, and R. E. MIERS, Department of Physics, University of Wisconsin, Madison, WI 53706--Apparent cross sections are reported for the excitation of Na from the ground 3s level to the 3p and 3d levels by incident fast H^+ , H_2^+ , H_3^+ , H^- , or H^0 with velocities in the range $0.5-2.2 \times 10^6$ m/s. The cross section to the 3p level for H^+ ions has a maximum of 3.8×10^{-15} cm² at $v = 1.7 \times 10^6$ m/s, and the cross section to the 3p level for H^- ions has a maximum of 3.8×10^{-15} cm² at $v = 1.7 \times 10^6$ m/s. The cross section for incident H^0 atoms decreases from 1.3×10^{-15} cm² at $v = 0.5 \times 10^6$ m/s to 2.7×10^{-16} cm² at $v = 2.2 \times 10^6$ m/s. The cross section to the 3d level for H^+ ions has a maximum value of 4.9×10^{-16} cm² at $v = 1.7 \times 10^6$ m/s and the cross section for H^- ions is less than the cross section for H^+ ions by about 45% for velocities above 1.7×10^6 m/s. The polarization of the radiation from these excitation collisions will be presented. The ion excitation cross sections can be related to the corresponding electron excitation cross sections at high velocities.

*Supported in part by the AFOSR.

SESSION BB

10:10 AM - 11:50 AM, Tuesday October 7

Room 313 - Wisconsin Center

TRANSIENT DISCHARGE PHENOMENA

Chairperson: J. Dutton, University College of Swansea

BB-1 Excitation and Ionization by Electrons and Fast Neutrals at Extremely High E/N in Ar,* A. V. Phelps and B. M. Jelenković,† JILA, Univ. of Colo. and NBS -- An analysis is made of 811.5 nm line emission from steady-state, uniform electric field discharges in Ar at E/N up to 43 kTd. Beam-like electron motion is calculated using number and energy balances. The Ar⁺ drift is controlled by charge exchange collisions and results in >10 times as many fast neutrals as ions. At E/N > 25 kTd ionization and excitation by fast neutrals exceeds that by electrons. Theory is compared with spatially dependent emission measurements from <10⁻³ A/m² discharges at E/N up to 43 kTd. At E/N > 10 kTd the calculated spatial dependences, including the cathode directed avalanche present at the higher E/N, are in agreement with experiment for the ≥60% of the 40 mm discharge gap nearest the cathode. The magnitude of the calculated 811.5 nm emission due to fast neutrals is about 40% of the observed values at 43 kTd. The discrepancy increases with decreasing E/N.

*Work supported in part by Lawrence Livermore National Laboratories.

†On leave from Institute of Physics, Belgrade, Yugoslavia during 1983-85.

BB-2 Ionization and Excitation Rate Coefficients and Induction Times in Molecular Gases at High E/n,* L. C. PITCHFORD and Y. M. LI, GTE Laboratories, G. N. HAYS, J. B. GERARDO, Sandia National Laboratories, J. T. VERDEYEN, U. of Illinois -- Steady-state ionization and excitation rate coefficients and the induction times for these rates to reach steady-state have been measured and calculated in nitrogen, hydrogen and oxygen over a range of E/n from several hundred to over 10,000 Td by monitoring the time-dependence of the electron density and the light output after application of a high-power, fast-rising microwave field at cyclotron resonance. Under these conditions, there is one-to-one correspondence between the microwave heating and a D.C. pulsed excitation without the complication of electrode effects. Time-dependent Boltzmann calculations of the rate coefficients and the induction times are in good agreement with the experiment. Even at the highest values of E/n, regions of exponential growth of the electron density and the light output were found, and the induction time can be directly related to the inverse of the ionization rate coefficient.

*This work performed at Sandia National Laboratories, supported by the U. S. Department of Energy under contract number DE-AC04-76DP00789.

BB-3 Relaxation Time Modeling of Electron Transport in Rapidly Varying Fields, * C. Wu, B. M. Penetrante, E. E. Kunhardt Weber Research Institute, Polytechnic University --Relaxation time (RT) models provide a simple way of accounting for transient transport by using static characteristics to approximately describe the electron dynamics. In the usual formulation of the RT model, both the energy relaxation time τ_ϵ and the momentum relaxation time τ_p are assumed to depend only on the mean energy $\bar{\epsilon}$. However, from analysis of the moment equations we show that τ_p should depend on the mean velocity \bar{v} , whereas τ_ϵ should depend on $\bar{\epsilon}/\bar{v}$. Comparisons between these RT models, and the response obtained from the time-dependent Boltzmann equation, are performed. Results will be presented for fields varying in time with a ramp character.

*Work supported by the Office of Naval Research.

BB-4 Dynamics of an Assembly of Electrons Described by Interpolating between the Boltzmann and Fluid Formulations,* E. E. Kunhardt, B. M. Penetrante and C. Wu, Weber Research Institute, Polytechnic University -- It is desirable to find a description of the dynamics of an assembly of electrons in a gas, that is simpler than the Boltzmann eq., but does not sacrifice the physics of the problem. To achieve this, we have used characteristic-time scales to order the fluid equations. This ordering is used to derive from the Boltzmann equation a kinetic equation valid in the time scale of the fluid variables. This kinetic equation and a finite set of fluid equations form a closed system. The appeal of this system lies in the fact that the kinetic equation need only be solved once. This solution, together with the fluid equations, describe the dynamics of the electrons under various transient conditions. Comparisons between this formulation and the Boltzmann formulation will be presented.

*Work supported by the Office of Naval Research.

BB-5 HV Breakdown of the Short Gap: Model,* J.P. NOVAK and R. BARTNIKAS, IREQ, Varennes, Québec, Canada. A model of the channel formation in HV breakdown in He has been formulated, consisting of the Poisson eq. and conservation eqs. for electrons, ions and metastable atoms. Direct, Penning and stepwise ionization are included, but volume recombination is neglected. Cathode emission includes ion and metastable induced emission and photo-emission. It is assumed that mutual interactions of the excited and charged particles are negligible. Time development of the densities and field is calculated in two dimensions from the moment of the release of the initial electrons ($t=0$) until the maximum ion density reaches about 10^{12} cm^{-3} ($t=1 \mu\text{s}$). In early development, radial density profiles are well described by the $\exp(-r^2/d(z))$ dependence (r and z being radial and axial distance) and time variation of the density integrals is very nearly exponential. At later stages it is mainly distortion of the field by the space charges which increases ionization, leading to local enhancement of the densities, channel constriction and rapid growth in time. Penning ionization contributes increasingly, while stepwise ionization remains small.

* This work was supported by the CEA (Canada).

BB-6 Determination of $N_2(v)$ Distributions Produced in He/ N_2 Microwave Discharges,* L.G. PIPER and W.J. MARINELLI, Physical Sciences Inc.-We have developed a technique for studying the vibrational distributions of ground-electronic-state, molecular nitrogen in the afterglow of a microwave discharge through mixtures of helium and nitrogen. The technique is based upon adding metastable helium atoms to the afterglow. The He^* excites the $N_2(X,v)$ to $N_2^+(B, {}^2\Sigma_u^+)$ in a Penning-ionization reaction. Since Penning ionization is a Franck-Condon process, the vibrational distribution of the $N_2^+(B)$ emission mirrors that of the $N_2(X,v)$ from which it was produced. The measurements show that the ground-state nitrogen distribution is highly non-Boltzmann, with vibrationally hotter distributions being produced with lower mole fractions of nitrogen in the discharge. We have also observed the production of $N_2^+(C^2\Sigma_u^+)$ from He^* Penning ionization of molecular nitrogen. This process is energetically allowed only if the vibrational energy in the ground-electronic-state nitrogen exceeds 3.8 eV.

*Work supported by Los Alamos National Laboratories under subcontract no. 9X25-X451-2.

SESSION CA

1:00 PM - 2:50 PM, Tuesday, October 7

Lakeshore Room - Wisconsin Center

ELECTRON RECOMBINATION AND ATTACHMENT

Chairperson: R. S. Freund, AT&T Bell Laboratories

CA-1 Electron-Ion Recombination Rates in an Atmospheric Pressure Plasma, S.M. JAFFE, M. MITCHNER, S.A. SELF, Mech. Engr. Dept., Stanford Univ. --The results of experiments to measure the rate of the three body recombination reaction $e + Cs^+ + N_2 \rightarrow Cs + N_2$ will be presented. The experiment employs the afterglow of a mixture of 20 torr of partially ionized cesium and 1000 torr of nitrogen at a temperature of 1200 K. Selective photoionization of the cesium with radiation from a Xenon flashlamp produces an electron concentration of $\sim 10^{11} \text{ cm}^{-3}$, which is in thermal, but not in chemical equilibrium. Electron concentration is monitored by a four electrode conductivity probe during the first 10 ms of relaxation. A detailed analysis of competing electron loss mechanisms (ion-molecule and recombination reactions are considered) indicates that electron concentration decay can be directly linked to recombination stabilized on the nitrogen.

*Work supported by the AFOSR, Grant 83-0108.

CA-2 The Electron-Temperature Dependence of the Recombination of Electrons with NO^+ Ions*, J. L. DULANEY, M. A. BIONDI, AND R. JOHNSEN, University of Pittsburgh - The electron-temperature (T_e) dependence of the dissociative recombination of NO^+ ions with electrons has been determined using a microwave-afterglow/mass-spectrometer apparatus employing microwave heating of electrons. It is shown that the discrepancy between the earlier microwave afterglow measurements of Huang et al.¹ ($\alpha(NO^+) \sim T_e^{-.37}$) and the trapped-ion results of Walls and Dunn² ($\alpha(NO^+) \sim T_e^{-.85}$) was caused by the reduction of the electron temperature due to inelastic collisions of electrons with neutral NO. We also found that the assumption of spatially uniform electron temperatures was not warranted. If these effects are properly taken into account in the analysis of afterglow data, the recombination coefficient is found to vary with electron temperature as $\alpha(NO^+) \sim T_e^{-.75}$, in good agreement with the trapped-ion data.

*Research supported by ARO, DNA, and NASA.

¹C. M. Huang et al., Phys. Rev. A 11, 901 (1975).

²F. L. Walls and G. H. Dunn, J. Geophys. Res. 79, 1911 (1974).

CA-3 Dissociative Recombination of Electrons with Hydronium Cluster Ions,* B. M. Penetrante, Weber Research Institute, Polytechnic U., and J. N. Bardsley, Physics Dept., U. of Pittsburgh --Afterglow experiments[1] show that the dissociative recombination rates for hydronium cluster ions vary very little when the electrons are heated through the application of microwave fields. This feature has puzzled theorists for many years. Before a new electron-capture process can be postulated, it is important to reassess the microwave power-electron temperature scale in order to see if the reported electron temperatures were indeed attained in the afterglow plasma. We have obtained numerical solutions of the Boltzmann equation to assess the effect of inelastic rotational and vibrational collisions on the electron temperature. The implication of the new electron temperature scale on the recombination process of hydronium cluster ions will be discussed.

*Work supported in part by ONR and NSF.

[1] C. M. Huang, M. Whitaker, M. A. Biondi and R. Johnsen, Phys. Rev. A 18, 64 (1978).

CA-4 Photoenhanced Electron Attachment to Electronically Excited Metastable Molecules,* MICHEL J. ROSSI, HANSPETER H. HELM, and DONALD C. LORENTS, SRI International, Menlo Park, CA 94025--Electron attachment coefficients for laser-excited molecules in 500 Torr of He were measured in a drift tube, where E/N varied from 8.3×10^{-19} to 4.13×10^{-17} V cm². The first molecular system, for which we observed photoenhanced electron attachment, was Chloranil (tetrachloro-p-benzoquinone, C₆Cl₄O₂, CA) excited at 350 nm. This excitation mode affords quantitative intersystem crossing to the lowest triplet state of CA. The ground state of CA did not attach electrons at the above values of E/N, and in view of the low vapor pressure of CA, all attachment experiments were conducted at high temperature (390 K). The laser flux was modest in the mJ/cm² range corresponding to 3 to 10% excitation of CA. We will report on electron attachment properties of electron-donor-acceptor complexes in electronically excited states (exciplexes) also involving electronically excited CA and triplet excited hexafluorobenzene (C₆F₆) generated through excitation of the ground state at 248 nm.

*Work supported by the Army Research Office.

CA-5 Optically Enhanced Electron Attachment from Electronically Excited Molecules,* S. R. HUNTER, L. G. CHRISTOPHOROU, and L. A. PINNADUWAGE, Oak Ridge National Laboratory --Optically enhanced electron attachment involving long-lived excited electronic states has been observed in thiophenol (C_6H_5SH) and thioanisole ($C_6H_5SCH_3$) in a swarm experiment using N_2 as a buffer gas. Ground state C_6H_5SH and $C_6H_5SCH_3$ molecules capture electrons weakly (electron attachment rate constants $k_a < 10^{-14} \text{ cm}^3 \text{ s}^{-1}$) below $\epsilon \approx 0.5 \text{ eV}$ but show a large photoenhancement (10^5 to 10^6) in k_a at thermal electron energies. The optically enhanced electron attachment mechanisms have been probed by performing the measurements over a wide range of partial attaching gas and N_2 pressures and over the mean electron energy, $\langle \epsilon \rangle$, range $0.04 \leq \langle \epsilon \rangle < 3 \text{ eV}$ using excimer laser light between 193 and 308 nm. Both fast ($< 100 \text{ ns}$) and slow ($> 10 \mu\text{s}$) formation time photoenhanced attachment processes have been observed over a wide range of laser intensities. Possible mechanisms leading to these photoenhanced attachment processes will be discussed.

*Research sponsored by AFOSR under DOE No. 40-1523-84 and by OHER, USDOE, under DE-AC05-84OR21400 with MMES.

CA-6 Electron Attachment to NF_3 Revisited,* S. R. HUNTER, Oak Ridge National Laboratory --The electron attachment rate constant, $k_a(\langle \epsilon \rangle)$, and total electron attachment cross section, $\sigma_a(\epsilon)$ have been measured in NF_3 using a high pressure swarm technique with N_2 and Ar buffer gases over the mean electron energy range $0.04 \leq \langle \epsilon \rangle \leq 4.8 \text{ eV}$. The $(k_a)_{th}$ ($T = 300 \text{ K}$) value is $5 \times 10^{-12} \text{ cm}^3 \text{ s}^{-1}$ which is at least four times smaller than the previous lowest literature value for $(k_a)_{th}$ for this gas.¹ The peak k_a value is $1.2 \times 10^{-8} \text{ cm}^3 \text{ s}^{-1}$ at $\langle \epsilon \rangle \approx 2 \text{ eV}$ which is approximately twice that estimated by Chantry¹ from a beam cross section measurement. The swarm unfolded $\sigma_a(\epsilon)$ has an appearance threshold at $\epsilon \approx 0.6 \text{ eV}$ in agreement with the measurements of Harland and Franklin.² Possible sources of error in the previous measurements are discussed.

¹P. J. Chantry, in *Applied Atomic Collision Physics - Gas Lasers* (E. W. McDaniel and W. L. Nighan, eds.), Vol. 3, Academic Press, New York, 1982, pp. 35-70.

²P. W. Harland and J. L. Franklin, *J. Chem. Phys.* **61**, 1621 (1974).

*Research sponsored by ONR under DOE No. 40-1246-82 and by OHER, USDOE, under DE-AC05-84OR21400 with MMES.

CA-7 Variation with Temperature of the Dissociative and Nondissociative Electron Attachment to n-C₄F₁₀.*
P. G. DATSKOS and L. G. CHRISTOPHOROU, Oak Ridge National Laboratory --The total electron attachment rate constant k_a for n-C₄F₁₀ in Ar as a function of mean electron energy, $\langle \epsilon \rangle$ (0.76 to 4.81 eV) and temperature, T (300 to 750 K) will be reported. A large variation of k_a with T was observed which depends on $\langle \epsilon \rangle$. In general, $k_a(\langle \epsilon \rangle)$ decreases slowly with T between 300 and 400 K, decreases precipitously between 400 and ~500 K, and increases for T > 500 K. The decrease of k_a with T is due to nondissociative and the increase due to dissociative electron attachment. The ratio $R_{d/t}$ of the dissociative to the total k_a is small at low $\langle \epsilon \rangle$ and T, but it increases with both $\langle \epsilon \rangle$ and T and reaches unity for T > 500 K and $\langle \epsilon \rangle > 1.5$ eV. These findings will be presented and discussed in relation to our earlier similar work on C₂F₆ and C₃F₈.
*Research sponsored in part by ONR under Interagency Agreement DOE No. 40-1246-82 and in part by OHER, USDOE, under contract DE-AC05-84OR21400 with Martin Marietta Energy Systems, Inc.

CA-8 Electron-Ion Recombination of Benzene Ions,*
D. J. ECKSTROM, J. S. DICKINSON, and M. N. SPENCER[‡] SRI International --In a separate paper, we report results of multiphoton ionization of benzene in high pressure buffer gases. The ionization yields and the subsequent plasma density decay were measured using the microwave cavity perturbation technique. Since we measure both the real and imaginary conductivities during the decays, we are able to deduce both the electron density and electron temperature histories. Analyses of the electron density histories indicate that the decays are dominated by electron-ion recombination. We believe that the primary ion is the parent C₆H₆⁺. The recombination rates are fast, with maximum values near 10⁻⁵ cm³sec⁻¹. The rate appears to vary with electron temperature approximately as T_e⁻¹. Insofar as we can determine, this is the first measurement of the recombination rate for a large organic molecule.

*Work supported by the Defense Advanced Research Projects Agency under Naval Surface Weapons Center Contract N60921-85-C-0210.

[‡]Current address: Physical Sciences, Inc., Andover, MA

CA-9 Two-Photon Ionization of Benzene at 248 nm at High Buffer Gas Pressures,* J. S. DICKINSON, M. N. SPENCER,† and D. J. ECKSTROM, SRI International --We have extended our study of benzene multiphoton ionization by KrF laser radiation to high buffer gas pressures. We used the microwave cavity perturbation method to measure the photoelectron densities and their time decays. Buffer gases included N₂, He, Ar, and Xe at pressures up to 700 torr. Collisions cause vibrational relaxation or quenching of the intermediate electronic state ¹B_{2u} of benzene populated in the two-photon process. The first three gases cause a gradual reduction of the ionization yield (due to vibrational relaxation) to a new asymptotic level that is about 50% of the collisionless value, while Xe reduces the yield drastically at high pressures due to quenching. However, the vibrational relaxation rates and quenching rate are apparently smaller than deduced from earlier fluorescence measurements.

*Work supported by the Defense Advanced Research Projects Agency through Naval Surface Weapons Center Contract N60921-85-C-0210.

†Current address: Physical Sciences, Inc., Andover, MA

SESSION CB

1:00 PM - 2:50 PM, Tuesday, October 7

Room 313 - Wisconsin Center

DC GLOWS

Chairperson: G. L. Rogoff, GTE Laboratories

CB-1 Kinetic Formalism for the Role of Vibrational and Electronic Processes in Particle-Beam Sustained Plasmas Discharges, N. PEYRAUD, OBSERVATORY, Nice, France -

We derive a general realistic formalism for the inversion of the Boltzmann high-energy operator in any particle-beam sustained molecular, or atomic plasma discharge, including all excitations transitions : ionization, electronic, vibrational, rotational, and eventually de-excitation from molecules excited in the first vibrational state. This theory predicts highly non-maxwellian electron-distribution function's "tail", from which we enhance some possible investigation tests for vibrational processes. Essential scaling-laws are also derived from this formalism. Applications are made in the case of low pressure molecular nitrogen lasers and to long distance energy transport in nitrogen atmosphere.

CB-2 Generation of Intense Large Area Electron Beams by Glow Discharges,* H. F. RANEA-SANDOVAL¹, N. REESOR, B. SZAPIRO, B. WERNSMAN and J. J. ROCCA, COLORADO STATE UNIVERSITY --High current density electron beams were generated by a helium glow discharge using a 3-inch diameter oxidized aluminum cathode. Beam generation at He pressures between 0.05 and 0.8 Torr and applied voltages up to 100 kV were studied. A small (0.005-0.01 Torr) amount of O₂ was added to the discharge to maintain the cathode surface oxidized, allowing high secondary electron emissivity following the bombardment by energetic ions and atoms. Electron beam current densities up to 40 A/cm² were measured. The pulse duration of 0.2 to 15 μ s FWHM was limited by the stored energy of the 100J pulse generator. A model of the discharge that includes both the cathode fall region and the negative glow was developed. Model predictions of electron beam current density as a function of gas pressure and applied voltage show good agreement with experimental results.

*Work supported by the U.S. Air Force.

¹On leave from C10p, Argentina.

CB-3 Abnormal Glow Discharge Electron Beam Spatial Profile and Electron Energy Distribution Studies,*

Z. YANG, L. LI, J. MEYER, Z. YU and G. COLLINS, Colorado State U.

--In soft vacuum, it is possible to create an abnormal glow discharge electron beam with typically a 3-10 keV energy beam at current levels of 0.1-1 A. Total beam power in excess of 6 kW is also possible. Point source, line shape and wide area electron beams have been constructed. We have measured the spatial beam profiles, $I(x,y)$, under varying plasma conditions as the beam propagates from the cathode sheath. In addition, the transmitted beam electron energy distribution, $I(E)$, has also been measured and compared to theoretical calculations.

*Work supported by ONR, RADC, Navalex, NSF and Applied Electron.

CB-4 A Novel Low Pressure Discharge with Partitions Containing an Orifice, V. GODYAK, R. LAGUSHENKO, J. MAYA and R. PAI, GTE Electrical Products Group -Experimental and Calculational results on the performance of a novel low pressure discharge containing partitions with an orifice perpendicular to the E field are reported. In particular the effect of the orifice diameter and distance between partitions on E field, electrical energy to radiation conversion efficiency and spatial separation of power input and power dissipation are discussed. Measurements of the absolute value of the electron energy distribution function (EEDF) and its spatial variation along the axis of a dc Hg-Ne discharge containing a partition with an orifice are reported. These measurements have been accomplished using a fast pulse Langmuir probe technique with a noise suppression circuit. The measurements reveal a substantial increase in the number of fast electrons on the cathode side close to the orifice, while on the anode side plasma density and mean electron energy drops to levels lower than in an undisturbed plasma. A volume averaged preliminary model is outlined and calculations for Hg-Ar and Hg-Ne are presented. These calculations are in reasonably good agreement with experiments.

CB-5 The Radial Distributions of Charged Particle Densities and Electric Field Strength in the Positive Column,* D. W. ERNIE and H. J. OSKAM, Univ. of Minnesota and A. METZE, Honeywell Systems and Research Center, Minneapolis, MN -- A model has been developed for the radial distributions of electron and ion densities and electric field strength in the positive column of a dc discharge for a monatomic electropositive gas. The set of equations involved consists of the momentum and particle conservation equations for the ions and the electrons and Poisson's equation. Utilizing this single set of equations and appropriate assumptions, this model has been solved, through suitable numerical techniques, for various discharge tube radii, r_0 , and gas pressures, p_0 . These calculations show the development of both the ambipolar electric field in the "bulk" of the positive column and the sheath field "near" the discharge wall. The results also demonstrate the existence of a nonzero difference between the ion and electron densities at the discharge axis and the increase in this difference for decreasing $p_0 r_0$. A comparison will be made between these results and previous models.

* Work supported by IBM and by NSF under Grant No. CBT-8411898.

CB-6 Moving and Standing Striations in Helium-Neon Laser,* R.J. BLAIR and J.P. HAUCK, Northrop Corp., Electronics Div.--Wavelength and dispersion of moving and standing striations were measured in Helium-Neon laser tube of 2.5 mm diameter at 3.75 Torr pressure, 7:1 HeNe mixture, 0.6 - 1.3 mA current. Damped, quasi-sinusoidal standing striations were observed to exist in the absence of moving striations. Moving striations were found to have slightly longer wavelength than the standing striations. The backward wave phase velocity was found to be directed toward the cathode. Standing striation wavelength was found to increase with current, contrary to present theories of striations while the wavelength of the moving striations decreased with current. Moving striation dispersion curves will be presented.

*This work supported with Northrop IR&D funding

SESSION DA

3:10 PM - 5:00 PM, Tuesday, October 7

Lakeshore Room - Wisconsin Center

HEAVY-PARTICLE COLLISIONS AND CLUSTERS

Chairperson: J. P. Doering, Johns Hopkins University

DA-1 Reactions of Electronic State-Selected Transition Metal Cations Created by Multiphoton Ionization, L. SANDERS, R. TONKYN, and J.C. WEISSHAAR, Dept. of Chemistry, U. of Wisconsin-Madison -- Effective bimolecular rate constants for reactions of first transition series metal cations M^+ with small alkanes have been measured in 0.75 torr of He buffer gas in a fast flow reactor. Packets of M^+ are created by pulsed laser vaporization of a metal target. Collisionally stabilized adduct ions $M(\text{alkane})^+$ dominate product mass spectra. For a given M^+ , the rates increase in the order $k(\text{CH}_4) < k(\text{C}_2\text{H}_6) < k(\text{C}_3\text{H}_8)$. The pattern of rates across the metal series is similar for the three alkanes. M^+ ions having ground or low-lying terms derived from the $3d^n$ configuration (e.g., Fe^+ , Co^+ , Ni^+ , and Cu^+) react 5 to 100 times faster than those having well isolated $3d^{n-1}4s$ ground terms (Sc^+ , Mn^+ , Zn^+). We have used time-of-flight photoelectron spectroscopy to show that one color resonance enhanced multiphoton ionization can selectively create the first excited term of Fe^+ , Ti^+ , and V^+ . We will present insights into the nature of the excited neutral resonant states and our initial results on the effects of electronic state on M^+ reactivity.

DA-2 Collisional Destruction of $\text{H}_2(c^3\Pi_u)$ Metastables by H_2 ,* A. B. Wedding and A. V. Phelps, JILA, Univ. of Colo. and NBS. -- Measurements¹ of rate coefficients for the collisional destruction of the $c^3\Pi_u$ metastable states of H_2 have been extended to a range of vibrational states v and rotational levels N , i.e., $v = 0 - 3$ for $N = 1$ and $N = 1 - 3$ for $v = 1$. Metastable destruction coefficients were determined from the time constants of recovery of density after depletion by a pulsed laser which excites the metastables to levels which radiate to a dissociating state. The metastable density was monitored by observing absorption of a cw laser. The data was fitted to linear dependences on H_2 density for 1 to $3 \times 10^{22} \text{ m}^{-3}$ and discharge current for 0.5 to 3.5 A. The rate coefficients for destruction by H_2 are 1.70 to $1.98 \times 10^{-15} \text{ m}^3/\text{s}$ with typical statistical uncertainties of $\pm 5\%$. No collisional transfer among levels of the $c^3\Pi_u$ state was detected.

*Supported in part by the Air Force Wright Aeronautical Laboratories.

¹H. Tischer and A. V. Phelps, Chem. Phys. Letters 117, 550 (1985).

DA-3 Argon Metastable Atom Interactions with the Cadmium Halides, C. L. BOHLER, L. D. SCHEARER, I. M. LITTLEWOOD, and S. ABAYARATHNA, U. of Missouri-Rolla--

We observe the fluorescent emission which results from the dissociative excitation of Cd halides by Ar metastable atoms in a flowing afterglow apparatus. From the observation of the fluorescence we conclude that the dissociative excitation yields neutrally excited Cd via the process $Ar^m + CdX_2 \rightarrow Ar + Cd^* + X + X$, where X indicates the halogen atom. We also observe that the Cd triplet is more efficiently excited than the singlet levels suggesting the presence of selection rules on total spin. In addition, truncation of the emission spectra allows us to determine the dissociation energy of the Cd-halogen molecules.

DA-4 Transport, Exchange and Quenching of Resonance Excitation in Cesium Vapor.* C.L.CHEN, C.S.LIU and P.J.CHANTRY, Westinghouse R&D Center -- With excitation by 852 or 894 nm radiation from a 9 ns tunable dye laser pulse, the time dependent fluorescence from both the $6P_{1/2}$ and $6P_{3/2}$ states has been measured for Cs densities from 10^{11} to 10^{14} cm^{-3} . At each density a slow and a fast time constant are derived by fitting the digitized data. At low densities these increase linearly with density, due to radiation trapping, but at the highest densities the inverse prevails, ascribed to collisional quenching. A quantitative fit to all the data is given by a kinetic model which includes (i) collisional exchange of energy between the two levels, with cross sections related by detailed balancing, (ii) the effects on the escape factor from hyperfine splitting of the lines, and from changes in the lineshape with density,¹ and (iii) equal quenching of both levels by ground state Cs. The derived cross section for exothermic energy exchange, assumed temperature independent, is 1.5×10^{-13} cm^2 , while that for quenching is 2.1×10^{-14} cm^2 .

*Supported in part by ONR Contract N00014-85-C-0035.

1. P. J. Walsh, Phys. Rev. 116, 511 (1959).

DA-5 Rate Coefficients for Reactions of Nitrogen Metastables with Silane, L. G. PIPER and G.E. CALEDONIA, Physical Sciences Inc., -We have studied the

reactions of a number of metastable nitrogen species with silane in a discharge-flow reactor. By monitoring the decays in the metastable number densities both as a function of time as well as a function of silane number densities, we have determined reaction rate coefficients, in units of $10^{-11} \text{ cm}^3 \text{ molecule}^{-1} \text{ s}^{-1}$, for the following species: $\text{N}_2(\text{A}^3\Sigma_u^+, v'=0)$, 0.59 ± 0.07 ; $\text{N}_2(\text{A}^3\Sigma_u^+, v'=1)$, 0.78 ± 0.21 ; $\text{N}_2(\text{a}^1\Sigma_u^-, v'=0)$, 14.5 ± 3.4 ; $\text{N}(^2\text{D})$, 4.0 ± 1.3 ; $\text{N}(^2\text{P})$, 0.06 ± 0.02 ; and N^4S , < 0.006 . We observe no spectral features of any kind, between 220 and 850 nm, when silane is added to a flow containing only $\text{N}_2(\text{A}^3\Sigma_u^+)$. Adding silane to a flow of atomic nitrogen excites several atomic lines of silicon, the SiN and SiH bands between 400 and 430 nm, and a continuum extending between 270 and 450 nm, all very weakly. Adding $\text{N}_2(\text{A})$ to the flow of atoms upstream from the silane addition inlet produces primarily $\text{N}(^2\text{P})$ and enhances the uv emissions. The uv spectral features are greatly enhanced when silane is added to active nitrogen, which is a mix of all the metastables studied, and in addition, vibrationally excited, ground-electronic-state nitrogen.

DA-6 Ion/Molecule Reactions of Carbon Cluster Ions Using Fourier Transform Mass Spectrometry, S. W. McELVANY* and A. O'KEEFE+, Naval Research Laboratory-

-This study utilizes the MS/MS capability and the long ion residence times allowed with a FTMS to study the ion/molecule chemistry of mass selected carbon cluster ions. Both positive and negative carbon cluster ions are formed by direct laser vaporization of graphite within the low pressure FTMS cell. The ion/molecule reactions of mass selected positive carbon cluster ions (C_n^+ ; $n=3-25$) with D_2 , O_2 , and small hydrocarbons have been studied. Several conclusions can be drawn concerning the carbon cluster ions from the differences in the observed chemical reactivity as a function of cluster size: 1) A conversion from linear to cyclic ion structures apparently occurs at $n=10$. 2) Evidence has also been observed for the presence of two structural isomers (linear and cyclic) for the $n=7$ cluster ion. 3) Differences are observed in the reactivity of odd and even carbon cluster ions ($n=3-9$) which probably result from thermochemical rather than structural differences.

*NRC/NRL Postdoctoral Research Associate

†current address: Western Research Corporation

DA-7 Reactions of Silicon Cluster Ions and Silicon Surfaces studied using Fourier Transform Mass Spectrometry, by W. R. CREASY* and A. O'KEEFE⁺, Naval Research Laboratory--The reactions of both silicon cluster ions, Si_n^+ for $n=1$ to 6, and silicon surfaces were studied using laser vaporization of ions from a piece of single crystal silicon into a Fourier Transform Mass Spectrometer, using a frequency-doubled Nd:YAG laser. For the gas phase reactions, one ion was isolated and allowed to react with a background gas such as CH_3OH , O_2 , NH_3 , H_2O , and N_2O . The relative rates for these reactions are compared, and the rate constants and branching ratios of the reactions of CH_3OH and O_2 are discussed in detail. The silicon surface reactions are observed due to the vaporization of ions other than the Si_n^+ distribution from the surface, which are not due to gas phase reactions. For example, exposure of the surface to H_2O produces the ion SiOH^+ , and to C_2H_2 produces $\text{Si}_n\text{C}_2\text{H}^+$ and Si_nC_n^+ , for $n=1$ to 3. The detailed dependence of the formation of Si_2N^+ from exposure of the surface to NH_3 is discussed.

- * NRC/NRL Postdoctoral Research Associate
- + current address: Western Research Corp.

SESSION DB

3:10 PM - 5:00 PM, Tuesday, October 7

Room 313 - Wisconsin Center

RF GLOWS

Chairperson: D. Graves, University of California-Berkeley

DB-1 Equivalent Circuits of Arbitrary Geometry Rf Gas Discharges, C.B. ZAROWIN, Perkin-Elmer Research--The electrical behavior of rf excited gas discharges can be characterized in terms of a unique equivalent circuit. Because of the vector nature of Maxwell's field equations, it can be derived from electromagnetic theory only for the simplest discharge geometries. In contrast, when the same vector equations are combined into a scalar (energy) equation through the use of the Poynting theorem, a general apparent impedance can be obtained for a discharge of arbitrary geometry. For a given frequency, we will obtain the rf power and other plasma parameter behavior of direct, capacitive and inductive coupled gas discharges, for geometries applicable to plasma etch/deposit reactors, ICP spectral and MS sources and "downstream" free radical generators.

DB-2 Comparison Between a Simple Circuit Model and the Electrical Characteristics of a RF Parallel Plate Discharge, P. BLETZINGER and MARK J. FLEMMING, WPAFB, Ohio. -- The detailed modelling of rf-parallel plate discharges can become very complex, especially when the electrode sheaths are included. In contrast, we have used a very simple electrical circuit model which simulates detailed measurements of electrical discharge characteristics as a function of gas pressure and operating frequency surprisingly well. It exhibits the relatively large change in phase between current and voltage as a function of pressure measured in a discharge parameter range where the operating frequency is above the ion plasma frequency and far below the electron plasma frequency. A constant stray capacitance, a constant resistive component (plasma volume) and a series capacitance which increases linearly with pressure (sheaths, assumed to be collisionless, thickness inverse function of pressure) are used. At higher pressures, a better fit results from increasing the resistance with pressure. The effective thickness of the electrode sheaths under different operating parameters can be estimated from the model. With the measured non-sinusoidal current waveforms, the variation of the effective sheath thickness during an rf cycle can be obtained.

DB-3 A Calculation of Self-Bias Voltage as a Function of Electrode Area Ratio in the Ion Fluid Model.

S. E. SAVAS, Lawrence Berkeley Laboratory

The relationship of the self-bias voltage to the area ratio of electrodes in an rf discharge is derived using an ion fluid model in spherical geometry. The results are found in two cases: the high frequency case in which the sheath impedance is assumed capacitive and the driver frequency, ω , is greater than the electron collision frequency, ν_e ; the low frequency case in which sheaths are resistive and $\omega \ll \nu_e$. Ion-neutral collisions are assumed to dominate, keeping the ions at low temperatures and allowing the use of the drift-diffusion model for the ion fluid in the time averaged E field. Electrons are assumed Maxwellian and carry the rf current, ionizing locally at a rate $\propto j \cdot E$, where j is the current density. The resulting ion equations are massaged to give stable diff. eqns. for flow speed and density which are numerically integrated giving relations between j and electrode area. These are combined with equations such as $(\Delta V_p)^{1/2} A_w = V_{rf} j^{1/2} A_t$ to yield relations between $V_{dc} = V_{rf} - 2(\Delta V_p)$ (Coburn's notation) and the area ratio such as $(\Delta V_p)^2 A_w^2 = V_{rf}^2 A_t^2$. Results are compared with ours and others' experiments.

DB-4 The Electric Field in a RF Discharge,* G. A. HEBNER and J. T. VERDEYEN, University of Illinois at Urbana-Champaign -- Since the electric field distribution in the parallel plate RF discharge is unknown except for a few cases, it is not possible to identify the means by which the RF power enters the plasma. By measuring the macroscopic parameters; RF voltage, current and average power, and the spatially averaged bulk electron density by microwave interferometry, one can establish limits on the value of the RF electric field in the bulk of the discharge (exclusive of the sheath). For the gases studied (He, Ar, N₂, H₂) and the macroscopic parameters that are used, power or current, the inferred values of the RF electric field in the bulk of the plasma can be as low as ~20 mV/cm to a high of ~7 V/cm in the experiments considered. In either case, the plasma voltage drop is negligible when compared to the applied RF value, and thus most of the applied voltage should be assigned to the sheath.

*Work supported by ARO (DAAG-29-83-K-0108).

DB-5 Effect of RF fields on the dynamics of an isolated plasma,* R. G. Beeler, H. L. Chen, P. Gabriele, E. Fehring, J. Beard, J. Wooldridge, Lawrence Livermore National Laboratory and J. DeGroot, University of California, Davis.--A Nd-Yag pumped dye laser tuned to about 4247\AA was used in a two step photoionization scheme to ionize cerium vapor. The photoplasma was then subjected to externally applied RF fields in the 5-10 MHz regime. The time histories of electron and ion fluxes to a set of current probes was measured. The current waveforms were then used to follow the kinetics of the isolated plasma. Recent experimental findings and proposed heating mechanisms will be discussed.

* Work performed under the auspices of the U. S. Dept. of Energy by Lawrence Livermore National Laboratory under Contract No. W-7405-ENG-48.

DB-6 Measured and Predicted Light Emission from RF Discharges in CH_4 , L. E. KLINE, W. D. PARTLOW and W. E. BIES, Westinghouse R&D Center -- Survey spectra in a 2 Mhz discharge between parallel plane electrodes show that the dominant visible light emissions are the CH(A-X) band at 430 nm and the H Balmer lines. The measured absolute photon fluxes (s^{-1}) from a 124 cm^3 discharge at 20 W are 7.5×10^{15} for CH and 1.9×10^{15} for H β . The total light output power is less than 0.5% of the input power. Photon fluxes predicted by using measured cross sections for dissociative excitation of CH_4 and the time and space averaged value of E/n in the discharge are several times higher than the measured fluxes. Spatial scans of the time averaged luminosity show a dark space near the powered electrode followed by a bright region and relatively uniform luminosity in the rest of the gap. The powered electrode area is much smaller than the grounded electrode area. A simple model which assumes values of field and electron density vs. position and time and equilibrium local excitation rates predicts a much less uniform luminosity profile.

Supported in part by USAFOSR Contract F49260-84-C-0063DEF.

DE-7 α and γ RF Discharges in N_2 at Intermediate Pressures, P. VIDAUD, S.M.A. DURRANI and D.R. HALL, U. of Hull, Hull, UK — Measurements have been made on the current/voltage characteristics and time resolved/averaged visible emission of α and γ type RF discharges at frequencies between 10 and 30 MHz in N_2 over the pressure range 10 to 100 torr. A model is proposed for the internal charge and potential distribution of α discharges and the transition α to γ .

SESSION EA

8:00 AM - 10:00 AM, Wednesday, October 8

Lakeshore Room - Wisconsin Center

RADIATION TRANSPORT IN ARCS

Chairperson: P. A. Vicharelli, GTE Laboratories

EA-1 Departures from LTE of Free-burning Arcs in Argon
 G N HADDAD, A J D FARMER, L E CRAM, and J J LOWKE, CSIRO
 Division of Applied Physics, Sydney, NSW 2070 - Measure-
 ments¹ of arc temperatures using the Fowler-Milne
 method and predictions² of temperature profiles assuming
 local thermodynamic equilibrium are in fair agreement
 over most of the arc volume for argon arcs at a pressure
 of 1 atmosphere and currents of the order of 100 A.
 However, measurements and calculations indicate that
 significant departures from equilibrium may occur near
 the cathode³ and in the outer regions of the arc. In
 the arc mantle for temperatures of less than 10 000 K
 new measurements of temperature using Rayleigh scatter-
 ing from an argon ion laser give temperatures up to
 5000 K lower than temperatures from the Fowler-Milne
 method, but which are in agreement with theoretical pro-
 files derived assuming LTE. Furthermore, profiles of
 the 763.5 nm ArI line show self-absorption which cannot
 be explained assuming LTE but which indicates overpopula-
 tion of the lower level of the 763.5 line by the absorp-
 tion of resonance radiation in the outer mantle.

1 G N Haddad & A J D Farmer, J.Phys.D 17,1189 (1984)

2 P Kovitya & J J Lowke, J.Phys.D 18,53 (1985)

3 A J D Farmer & G N Haddad, Appl.Phys.Lett.45,24 (1984)

EA-2 Generalized Multithermal Equilibrium Diagnostics
of Argon and Hydrogen Arcs,* T. L. EDDY, Georgia Tech --
 The multithermal equilibrium (MTE) model¹ has been Modi-
 fied to correct the simplification that the various
 ensemble temperatures are equivalent. The new general
 multithermal equilibrium (GMTE), LTE, PLTE, and MTE
 models are applied to 0.1 hydrogen and 1 atm argon arcs
 to determine T_e and compare values found. N_e is deter-
 mined from Stark broadening corrected to the $2-\lambda$ inter-
 ferometer based scale. Independent calculations found T_e
 $= T_e$, due to the high pressures and low field strengths.
 The PLTE method yields a contradiction between $T_e = T_e$
 from upper levels and T_e from the method of extrapolation²
 of the upper level² Saha equation to E_e . The latter
 method with MTE yields $T_e \sim 2T_e$, which many consider to
 be too large. The GMTE solution gives $T_e \sim 1.1 T_e$ and
 $T_e \sim 1.1 T_e$, which is reasonable. The GMTE ionization
 equation (equivalent to that of Potapov² except for
 additional temperatures dictated by experiment) can cre-
 ate large deviations in density from the LTE or PLTE con-
 dition with the small temperature differences so found.

*Work supported in part by NSF Grant CPE-8311325.

¹ T.L.Eddy, et al., IEEE Trans. Plas. Sci. 1, 31 (1973).

² A.V.Potapov, High Temperature 4, 48 (1966).

EA-3 GMTE Analysis of Argon Arc Plasma at various pressures. A. Sedghinasab and T.L. Eddy, Georgia Institute of Technology --Argon wall-stabilized arc plasma experiments at various pressures (.5-10 bar) and 30 amp are reported and data is analyzed via the Generalized Multi-thermal Equilibrium (GMTE) model to determine the extent of non-LTE in similar plasmas. The model relaxes many of the assumptions of LTE and two-temperature models. Due to large particle densities ($n \sim 10^{18} \text{ cm}^{-3}$) and low electric field strengths ($E \sim 10 \text{ V/cm}$), kinetic equilibrium has been assumed, although none of the excitation modes have been assumed to be in equilibrium with kinetic (translational) energy modes. Electron density is independently determined from the hydrogen $H\beta$ line profile, using the broadening theory of Ref.[1]. n_e is found in general to be larger than LTE n_e calculated using absolute line emission coefficients. Final results regarding the variation of the electron temperature and the various excitation temperatures as a function of pressure are being evaluated and will be reported at the conference.

* Work supported by NSF Grant CPE-8311325

¹ C.R.Vidal, J.Cooper, and E.W.Smith, *Astrophys. Journal Suppl. Series*, no.214, vol.25, p. 37, 1973

EA-4 Generalized Multi-Temperature Relations for Hydrogen Plasma. K.Y. Cho and T.L. Eddy, Georgia Institute of Technology --For a partially ionized plasma, diagnostic methods based on complete (CLTE) or partial (PLTE) local thermal equilibrium or multithermal equilibrium¹ (MTE) have a limited range of applicability. This work extends the applicable region for non-LTE diagnostics by a general multithermal equilibrium (GMTE) model derived by minimizing the free energy. The resulting ionization equation is similar to that of Potapov,² but extended to include additional temperatures found necessary for non-LTE diagnostics. The GMTE results differ from MTE, which assumed equivalence of ensemble temperatures based on different properties, and which is found to be valid only for near-LTE conditions, as is PLTE. Significant results of the GMTE model applied to hydrogen plasma are presented. For diagnostics it is found that as in MTE, $T_{\text{exa}} \approx T_{\text{LTE}} \neq T_e$ when $T_{\text{LTE}} < T_{\text{Norm}}$; but that the non-LTE state diagram is much different. Since transport properties are strongly dependent on densities, it is very important to use the proper ionization relation and temperatures in modeling.

*Work supported by NSF Grant CPE-8311325.

¹T.L. Eddy, E. Pfender, E.R.G. Eckert, *IEEE Trans. Plas. Sci.* **1**, 31 (1973).

²A.V. Potapov, *High Temperature* **4**, 48 (1966).

EA-5 Determination of the Cd $5^1D_2 \rightarrow 5^1P_1$ ($\lambda=643.8\text{nm}$) Transition Probability from a Cadmium-doped High Pressure Mercury Arc, T.P. BENSON and A.K. BHATTACHARYA, GENERAL ELECTRIC COMPANY, Cleveland, Ohio--The transition probability of the cadmium 643.8nm line was determined from the spatially resolved arc temperature profile and mercury/cadmium density measurements from a cadmium doped high pressure mercury arc. Absolute intensities of the optically-thick Hg 546.1nm line were used to determine the arc temperature. The optically-thin Hg 577.0nm and Cd 643.8nm lines were Abel-inverted to determine the Hg and Cd densities. Using the literature transition probability¹ good agreement between the measured density and that expected from full vaporization of the dose amount was found for Hg, but agreement for Cd required a value for the transition probability half its literature value ($5.9 \times 10^7 \text{ sec}^{-1}$).²

1. P. van de Weijer and R.M.M. Cremers, J. Appl. Phys 54, 2835 (1983).
2. B. Chevon, J. Jardsz, and P. Verisch, J. Phys. B. Atom. Molec. Phys. 13, 2413 (1980).

EA-6 Spectroscopic Investigation of a Flow Stabilized DC-Arc with a Metal Vapor Core, R. SIELKER, J. MENDEL, Ruhr-University Bochum, FRG -- A high current arc is operated in a water cooled discharge vessel between a tubular graphite cathode (6.8 mm diam.) and a nozzle shaped copper anode (7.7 mm inner diam.) which are enclosed in a double walled quartz tube (40 mm inner diam.). Cadmium is fed into the arc core from a furnace through a bore of the cathode. An argon flow is injected tangentially at the cathode side forming a plasma envelope of the metal vapor plasma. By vortex- and anode nozzle-flow a cylindrical arc is formed which emits non self-reversed atomic and ionic cadmium lines with high intensity. Peak intensities of 20 resp. 34 $\text{W cm}^{-2} \text{ nm}^{-1} \text{ sr}^{-1}$ are measured for Cd I lines (228.2 nm, 361 nm) and Cd II-lines (214.4 nm, 226.5 nm). Typical operation conditions are: current strength 600 A, mass flow 300 Nl min^{-1} , pressure $4 \times 10^5 \text{ Pa}$, arc length 40 mm, furnace temperature 1300 K. Work supported by Deutsche Forschungsgemeinschaft and Minister fuer Wissenschaft und Forschung des Landes NRW.

EA-7 K-Shell Aluminum Resonance Line Ratios for Plasma Diagnosis Using Spot Spectroscopy*, J. P. APRUZESE, J. DAVIS and D. DUSTON**, Naval Research Laboratory--We have calculated four resonance line ratios as a function of temperature and density for cylindrical aluminum tracer dot plasmas. The conditions are applicable to experiments using the spot spectroscopy technique for plasma diagnosis. In many instances, the resonance lines are optically thick despite the relatively small ($\sim 100 \mu\text{m}$) size of the plasma. Total aluminum ion densities considered range from 10^{19} cm^{-3} to 10^{21} cm^{-3} , and the plasma temperatures vary from 200 eV to 700 eV. Presentation of the ratios as contour plots clearly exhibits the physical influences of plasma size and density as well as temperature.

* Work Supported by the Defense Nuclear Agency

** Strategic Defense Initiative Organization/IST, Washington, D.C.

EA-8 Recovery Phenomena of High-current Vacuum Arcs, E. SCHADE, E. DULLNI, B. GELLERT, BBC Research Center, CH-5405 Baden, Switzerland -- Diffuse and constricted high-current vacuum arcs (OFHC-Cu, $D=25\text{mm}$, $d=7.5\text{mm}$, 5ms-rectangular current pulse up to 9kA) are investigated. In situ observation of the liquefied contact surfaces by a laser shadow-technique shows particle emission from the molten surfaces shortly before and after $I=0$. Particles are responsible for the slow decay of vapour measured by laser-induced fluorescence (LIF). Radiative transfer had to be considered in the evaluation of the vapour densities. Measured post-arc currents are theoretically described. Secondary electron emission due to ion bombardment of the cathode results in an essential contribution to the post-arc current at voltages above 10kV. The residual plasma contains ions with low energies which correspond to temperatures of 5000K after diffuse arc, and even lower temperatures after anode spot formation. Effects of residual charge carriers determine dielectric recovery decisively. Up to 9kA the vapour by itself does not initiate breakdown despite of strong anode activity. At high currents breakdown strength is reduced during a short time interval (appr. 40 μs at 9kA). Subsequently, it quickly reaches 90% of the value which is approached after a long time.

SESSION EB

8:00 AM - 10:00 AM, Wednesday, October 8

Room 313 - Wisconsin Center

LASER DIAGNOSTIC TECHNIQUES

Chairperson: B. N. Ganguly, Wright Patterson Air Force Base

EB-1 Optical Diagnostics of RF Plasmas,
TERRY A. MILLER, DEPT. OF CHEM., OHIO STATE U.
-- An overview of optical diagnostic techniques for low pressure cold plasmas, such as those used in the electronics industry, is presented. Two techniques are considered in detail: optical emission and laser induced fluorescence. The use of optical emission to determine species concentrations and energies is described. Laser induced fluorescence detection of ions, radicals, and atoms is discussed.

EB-2
A STUDY OF MOLECULAR ION DISTRIBUTION IN THE POSITIVE COLUMN OF D.C. GLOW DISCHARGES BY DIODE LASER SPECTROSCOPY

Fu-Shih Pan and Takeshi Oka

The high spatial resolution of laser infrared ion spectroscopy enables us to monitor the distribution of molecular ions in situ in the discharges. We observed the radial distribution of ion densities in the positive column of glow discharges using strong absorption lines of ArH^+ and H_3^+ . The results show a remarkable depletion of ion densities in the center of plasma for the high current density (400 mA/cm^2) and/or high pressure (10 torr) regime. The very high abundance of ArH^+ allows us to measure also the translational, rotational and vibrational temperatures. Together with our previous study of ion mobility,¹ this method provides us with a powerful means of plasma diagnostics which is sensitive to quantum state.

¹N.N. Haese, F.S. Pan, and T. Oka, Phys. Rev. Lett., 50, 1575 (1983).

EB-3 Observation of the Reversal of the Optogalvanic Signal Using Counterpropagating Beams, WAYNE RICHARDSON and L. MALEKI, JPL--The optogalvanic effect has the potential for application in the area of pulsed power switching. We have observed for the first time a controlled reversal of the impedance change, induced in a mercury-argon discharge by a weak probe. Counterpropagating beams from a CW frequency stabilized ring dye laser are tuned to the 6 P --7 S transition of mercury. A Lamb dip is observed in the impedance change due to the weak probe (0.3 mW) as the laser frequency is scanned through the transition. As the backward pump power--typically tens of milliwatts and far above saturation, is increased, the optogalvanic Lamb dip also increases. Eventually, the dip becomes larger than the off line center signal, indicating a reversal of the impedance change when the laser frequency is exactly on resonance. The reversal of the impedance change is believed to be due to the competition between different ionization processes that contributes to the signal.

LBL-21923a

EB-4 Measurement of H-atom Density in a Hydrogen Discharge,* A.S. SCHLACHTER, G. STUTZIN, K.N. LEUNG, J.W. STEARNS, W.B. KUNKEL, LBL; R. STEVENS, G. WORTH, LANL; E.M. BERNSTEIN, Western Michigan Univ.; P. GOHIL, GA Tech.; W.G. GRAHAM, Univ. Ulster--Hydrogen atoms are believed to play an important role in H⁻ ion-source discharges, both in destruction of H⁻ ions and in modification of H⁻ energies through charge-exchange collisions. Experiments are now underway to measure the density of H-atoms in the ground state in two types of H⁻ ion sources: a filter multicusp source and a Dudnikov-type Penning discharge. Measurement will be made of absorption of Lyman-beta radiation produced by frequency tripling of light from a dye laser; attenuation of the Lyman-beta radiation provides a measurement of the integrated H-atom density in the discharge. Future plans are to correlate extracted H⁻ current with the discharge parameters.

*Supported by AFOSR, Los Alamos Natl. Lab., and U.S. DOE contract No. DE-AC03-76SF0098.

EB-5 Applications of Laser Spectroscopy in Gaseous Electronics,* P.J. HARGIS, JR., Sandia National Laboratories, Albuquerque, New Mexico —The high spatial, spectral and temporal resolution associated with gas-phase laser spectroscopy have established it as the method of choice for understanding the fundamental processes that occur in electrical discharges. Despite the advances made in understanding technologically important systems such as rf-discharges, laser diagnostic techniques are rarely used in other areas of gaseous electronics. The complex physical and chemical processes that frequently occur in gaseous electronic applications make it imperative to use simple-to-interpret diagnostic techniques such as laser-induced fluorescence and Raman spectroscopy. Laser spectroscopic measurements in diagnostic studies of pulsed-vacuum arcs, gas breakdown, ion-diode sources, and dc- and rf-discharges will be illustrated. Emphasis will be placed on the use of pulsed-ultraviolet laser Raman spectroscopy for absolute number density measurements and on the use of dipole-forbidden transitions to measure atomic number densities between 10^{14} and 10^{16} atoms/cm³.

*This work performed at Sandia National Laboratories, supported by the U. S. Department of Energy under contract no. DE-AC04-76DP00789.

EB-6 Novel Intersecting Laser Beam Technique for Fluorescent Lamp Diagnostics*, P. MOSKOWITZ, GTE Electrical Products, Danvers, MA -Knowledge of the Hg(6^3P_1) spatial distribution in Hg-rare gas low pressure discharges is important for understanding radiation transport, and aids in the formulation of discharge models⁽¹⁾ for fluorescent lamps. There is a need to perform measurements of this distribution with high accuracy, as small differences in the spatial profile may indicate relatively large effects on the transport of radiation from the center to the walls of the discharge. In this paper we report on a novel intersecting two laser beam technique which circumvents many of the problems with conventional laser absorption techniques. The experiment makes use of a weak "probe" and a strong, modulated "pump" beam originating from the same CW ring dye laser operating at 435nm, to yield localized Hg(6^3P_1) population density information across a cylindrical discharge tube.

*Partially supported by the US Department of Energy through a subcontract from Lawrence Berkeley Laboratory.

¹R. Lagushenko and J. Maya, Journal of IES, p. 306-314 Oct. 1984; *ibid* Bull. of Am. Phys. Soc. 30, 139 (1985).

EB-7 Laser Absorption Measurement of Sodium Density in a Metal-Halide Discharge Lamp*, G. ALLEN, R. LAGUSHENKO, W. KEEFFE and J. MAYA, GTE Electrical Products, Danvers, MA -In the sodium-scandium-iodide formulation of the metal-halide lamp, the sodium additive strongly influences the stability, conductivity, efficacy, color rendering, and lifetime of the lamp. We have developed a laser absorption technique to measure the density of ground-state sodium atoms in the discharge. We tune the output of a pulsed (synchronized with the lamp), nitrogen-pumped dye laser to within 2 to 4Å of the sodium D-2 resonance line, and measure the laser transmission vs. lateral displacement of the laser beam from the discharge axis. The radial profile of sodium density is obtained by Abel inversion of the data, and by invoking a previously measured temperature profile and absorption cross-section. Sodium density is observed out to 95% of the arc tube wall radius. Density profiles taken at several axial positions along the vertically burning arc demonstrate the effects of ionization depletion and axial segregation of the sodium. A crossed-beam laser absorption technique is being implemented in order to eliminate the need for Abel inversion of the data.

*Partially supported by the D.O.E. through a subcontract from Lawrence Berkeley Laboratory.

SESSION FA

10:30 AM - 3:45 PM, Wednesday, October 8

Robert P. Lee Lounge - Wisconsin Center

POSTERS; PROCESSING

Chairperson: J. Ingold, General Electric Company

FA-1 Novel Heat Pipe Device Producing Stable Discharge in Corrosive Metal Vapors*, S. B. HUTCHISON, XMR Inc., Santa Clara, CA 95054 --Research on certain corrosive vapors using discharge excitation has been hindered by the lack of suitable means of maintaining a stable discharge without severe corrosion of and contamination by the electrode material. This paper presents results of experiments in which stable discharges have been produced in a heat pipe device having long-life non-metallic electrodes which also serve as the wick material. In a small device (~40 cm active length), pulse input energies of as low as 50 mJ produce sufficient excitation for discharge and afterglow fluorescence and absorption/gain experiments. This device has also been used to produce multiline lasing in diatomic sulfur (B-->X) at oven temperatures of under 350°C. Moderate resolution spectral data from afterglow experiments in sulfur and selenium are presented, demonstrating afterglow kinetics.

* This work is supported by an SBIR contract from the National Science Foundation.

FA-2 Tunable Diode Laser Detection of Atoms and Molecules in Process Plasmas,* J. WORMHOUDT, Aerodyne Research, Inc. -- Infrared tunable diode lasers allow quantitative measurement of the concentrations of both stable and transient species in the glow discharges used in plasma etching and deposition of semiconductor materials. Temperature measurements can be made using Doppler line widths or line intensity ratios. These quantitative diagnostics are only possible if line strengths and positions have already been measured in laboratory experiments. Results of such experiments for chlorine atoms and CF_x , SiF_x , and SiH_x radicals are presented, and applications to discharge diagnostics are described.

*Supported by AFOSR Contract F49620-84-C-0036

FA-3 Excited states in N₂ reactive plasmas for steel surface nitriding, A. RICARD, Plasmas Phys. Lab., Paris-Sud Univ., 91405 ORSAY (FRANCE) --Vibrational state densities of ground state N₂(X,V) molecules in glow discharges have been measured by the CARS method¹. Populations up to V = 14 have been detected for residence times 10⁻² sec in the N₂ discharge (p = 5 Torr, T₀ = 500 K, E/n₀ = 6 × 10⁻¹⁶ V cm², n_e = 5 × 10¹⁰ cm⁻³). The experimental results can be interpreted by a Treanor-type distribution². The N₂(X,V) vibrational excitation has been found to increase with residence time (10⁻⁶ - 10⁻² sec.) in discharge and post-discharge conditions. A correlation was established between the vibrational excitation of N₂(X,V) in the gas phase and the chemical composition and depth of the nitride layer on the steel surface.

¹B. Attal et al., Rev. Phys. Appl. 18 (1983) 39.

²M. Capitelli et al., J. Chem. Phys. 80 (1984) 149, 82 (1985) 1900 and 84 (1986) 4717.

FA-4 Ultraviolet and Visible Chemiluminescence Observed from Fluorine and Xenon Difluoride Etching of Silicon,* M. J. MITCHELL, M. SUTO, L. C. LEE, San Diego State U. and T. J. CHUANG, IBM, San Jose--Ultraviolet and visible chemiluminescence, resulting from the etching of Si(1-1-1) by microwave discharge generated fluorine and gaseous xenon difluoride, has been dispersed. The previously reported visible wavelength chemiluminescence was observed along with new and unreported ultraviolet emissions in the 220-250 nm region. The spectra obtained from the two reactions are quite similar leading to the conclusion that the etching process is independent of the nature of the source of fluorine radical. Photochemical excitation of CF₃Cl, CF₃Br, CF₃H and CF₄, gives fluorescence spectrum similar to that observed from the etching process. The gas phase fluorescence has been attributed to CF₃ excited state species and suggests that the source of the observed chemiluminescence in the etching reactions is excited SiF₃. XeF(B-X) fluorescence is observed in the Si and XeF₂ etching. The chemical process for producing the observed fluorescence will be discussed.

*Work supported by NSF under Grant No. CBT-8518555.

FA-5 Plasma Source Ion Implantation,* J.R. CONRAD AND T. CASTAGNA, University of Wisconsin-Madison -- In conventional ion implantation an ion beam is extracted from a plasma source, accelerated to the desired energy, and then transported to the target. To process large-scale targets, and to avoid shadowing of non-planar targets, beam rastering and target rotation during the implantation is required. We are developing a simpler technique in which the target is placed directly in the plasma and is pulse-biased to a large negative potential so that plasma ions gain energy as they accelerate through the potential drop across the sheath. Because the sheath surrounds the target on all sides, all surfaces of the target are implanted without beam rastering or target rotation. We have implanted nitrogen ions from a multi-dipole source at energies up to 40 keV and fluences up to 10^{17} cm⁻² in tool steel, invar, carbide, and other targets. The implantation process has produced significant improvements in surface microhardness and wear properties.

*Supported by NSF Grant ECS-8314488.

FA-6 Particle Simulation of Plasma in a Dense Neutral Background, W. N. G. HITCHON, Electrical and Computer Engineering, University of Wisconsin-Madison, Madison, Wisconsin 53706 -- A fast numerical 'particle' simulation of a dense, partially ionized plasma has been developed and applied to modeling a plasma-optical system used in thin-film deposition.

The calculation of the electron 'step' is performed efficiently by sampling from the distribution of distances travelled by electrons during many elastic collisions, between inelastic collisions. The distribution is valid provided the change in the electron potential energy is small, so, for instance, electrons in the sheaths are integrated separately. Application of the calculation to plasma etching requires the inclusion of several different species and excitation states and processes which change the species of the particles and create new particles. Initial applications to etching will be described.

FA-7 Production of Gold Oxide Ions During Sputter Deposition of Gold Films in Argon-Oxygen Discharges,* Carolyn Rubin Aita, Materials Department and Laboratory for Surface Studies, U. Wisconsin-Milwaukee, P.O. Box 784, Milwaukee, WI 53201: The addition of O_2 into an Ar glow discharge during the sputter deposition of Au is known to increase film adhesion. The traditional reasoning is that oxygen is adsorbed at the substrate and lowers the nucleation barrier of Au. The resulting structure, smaller, less well-ordered nuclei, form a continuous film at a lower thickness and this film contains less internal stress. This analysis assumes that Au is the only target species that arrives at the substrate. However, in the present paper we use glow discharge mass spectrometry to show that AuO and AuO₂ species are formed at and sputtered from the target surface. These species, in addition to Au, arrive at the substrate and contribute to the growing film.

*Work partially supported under U.S. ARO Grant No. DAAG29-84-0126.

SESSION FB

10:30 AM - 3:45 PM, Wednesday, October 8

Alumni Lounge - Wisconsin Center

POSTERS; DIAGNOSTICS

Chairperson: S. Chung, University of Wisconsin Madison

FB-1 Influence of Electrical Resonance upon Interpretation of Optogalvanic Data,* SEONG-PONG LEE, ERHARD W. ROTHE, and GENE P. RECK, Wayne State University, Detroit --Resonant laser light and electrical pulses are used to induce time-dependent optogalvanic signals from commercial hollow-cathode lamps. Previous workers have observed such signals induced by a laser and interpreted them in terms of specific molecular processes. Electrical resonance in the lamp and its associated circuit, when combined with the negative resistance characteristic in the lamp, create a circuit which is capable of oscillation. This circuit, under some conditions, oscillates spontaneously. Alternatively it may be stimulated to yield damped oscillations through the action of an electrical pulse or by a resonant laser pulse. Such effects must be considered in interpreting time-dependent optogalvanic data in addition to any specific molecular processes occurring in the discharge.

*Supported by NSF and PRF

FB-2 Effect of Photodetachment on a Radio Frequency Discharge through BCl_3 , CARL E. GAEBE, TODD R. HAYES, and RICHARD A. GOTTSCHO, AT&T Bell Laboratories -- We present a novel spectroscopic diagnostic which provides a detailed picture of the plasma's response to photodetachment of electrons from negative ions in a 50 kHz discharge through BCl_3 . Spatially- and temporally-resolved changes in the local electric field are monitored using Stark mixing spectroscopy and are compared to current transients which appear simultaneously in the external circuit (optogalvanic effect). Both the external current and the local field exhibit oscillations at frequencies characteristic of ion motion; however, the local measurements provide a more detailed picture of the changes in sheath structure. Near the momentary anode, the sudden increase in negative charge mobility causes a reduction in the sheath field magnitude but an overall increase in sheath thickness. Initially, the plasma potential floats up toward the anode potential because of the loss of negative charge but subsequently decreases below the initial level as the system relaxes back to steady state in an oscillatory manner.

FB-3 Study of the Direct Electron Impact Ionization process in Ne/Hg HCD tube by the Pulsed Optogalvanic Technique. M. HAKHAM-ITZHAQ and R. SHUKER. Ben-Gurion University of the Negev Beer-Sheva ISRAEL. --The Direct Electron Impact Ionization (DEII) and the Penning ionization processes of the cathode metal vapor atoms are responsible for the existence of the discharge in hollow cathode discharge (HCD) tubes. At low currents, the high density of the inert gas (Neon), which is about 10^{17} cm^{-3} controls the ionization of the metal vapor atoms, mainly through Penning ionization process while the sputtering process supplies the major part of the metal vapor atoms density. The DEII of the metal vapor atoms process has a high rate only when the metal vapor density is high. In most of the HCD tubes such as Ca/Ne, Cu/Ne etc, this occurs only at extremely high currents. In contrast, an Hg/Ne HCD tube has an exceptional behavior. Here a high density of mercury is obtained at low currents ($i > 1\text{mA}$). Thus a high DEII rate is attained. At this stage, the sputtering contribution to the discharge can be ignored and the DEII process of mercury dominates the discharge. These experimental results are detected through the pulsed resonant optogalvanic technique.

(1) R. Shuker et al. J. App. Phys. **54** (1983)

FB-4 Electronic Temperature Measurements of Helium Microwave Discharges*, J. HOPWOOD, M. KUBINEC, J. ASMUSSEN and M.L. BRAKE⁺, Michigan State U., East Lansing, MI 48824--The electronic temperatures of helium microwave (2.45 GHz) discharges were measured using spectroscopic techniques at discharge pressures from 1 to 1400 Torr and with input power levels of 40W to over 250W. The discharges were created within 7-29.5mm ID quartz tubes located in the central $\lambda/2$ axial portion of a cylindrical cavity excited in the TM_{012} mode. At low pressures (1-100 Torr) the discharge glow filled the center cross section of the tube and at higher pressures discharges separated from the tube walls and became a wall stabilized microwave arc. The electronic temperatures were determined from atomic Boltzmann plots of emitted line intensities for neutral helium. The temperatures decreased from 2500K at 1 Torr to 800K at 100 Torr with absorbed power of 35W. However, at 150W the temperatures were found to increase with pressure from 2200K at 200 Torr to 2700K at 700 Torr. These results will be discussed in terms of diffusion-dominated and constricted, wall stabilized arcs.

*Supported by NSF

⁺University of Michigan, Ann Arbor, MI 48109

FB-5 Determination of Two-Dimensional Temperature and Additive Density Distributions in an Arc. G.L. ROGOFF, A.E. FEUERSANGER, J.P. DRUMMEY, GTE Laboratories Inc., H.L. ROTHWELL, Jr., GTE Lighting Products--Segregation of additive species can lead to significant axial and radial nonuniformities in enclosed, vertical high-pressure arcs. A diagnostic method has been developed to determine two-dimensional distributions of temperature and additive density along with the pressure in a rotationally-symmetric LTE arc. Making use of the known vaporized quantity of the major component of the gas mixture, the method consists essentially of making several absolute intensity scans of emission from the major species and additive(s) at several axial locations, converting the intensities to radially-dependent emission coefficients, using the major-species emission coefficients and a volume integration to determine the temperature distribution and pressure, and using the additive coefficients to obtain the additive density distribution(s). Although the method can be applied to time-resolved studies with various (e.g., electronic) detection schemes, it has been used for a time-integrated analysis of a 175 W, 60 Hz lamp arc with mercury the major component and sodium the additive of interest, using photographs made through narrow band filters (Hg 577 nm and a region in the Na D line) and Abel inversions.

FB-6 Plasma Potential Diagnostic Based on Emitting Probes,* E.Y. WANG, N. HERSHKOWITZ, T. INTRATOR, M.H. CHO, C. FOREST, University of Wisconsin-Madison -- We describe a variety of emitting probes for plasma potential measurements that were developed in our laboratory. These are differential emitting, secondary emitting and capacitive probes. They have been used in basic and fusion plasma experiments successfully. The emitting probes are adaptable to measurements in strong RF environments such as exist in many gaseous-discharged experiments. Investigations of the effects of RF on plasma potential measurements with electron emitting probes and methods for interpreting data are also presented. Three time-averaged techniques are given the floating and inflection point methods of single emitting probe and differential emitting probes. A simple method of measurement of plasma potential fluctuations is given which makes use of time-averaged emitting probe I-V characteristics.
This work was supported by U.S. NSF Grant ECS-8314488 and NASA Grant NAGW-275.

PB-7 Measurement of Discharge Plasma Conductivity with RF external coil Probe, A.M. POINTU and P. ZELLER, Lab. Phys. Gaz & Plasmas, Orsay, France. -- Several experimental methods to determine the RF electrical conductivity, σ , of weakly ionized plasmas are known. They consist in measuring the impedance variation DZ/Z , of a coil when a plasma is set in its vicinity. Due to the frequency range, they are very sensitive to the e-n collision frequency, ν_{e-n} , allowing to get the electron temperature. Contrarily to usual crude approximations leading to analytical but very imprecise solutions, we solve numerically 3D Maxwell's equations to get more accurate DZ/Z (σ) values. Furthermore this makes measurement calibration not necessary. We also study the stray capacitive effect between the coil and the plasma and we present a device to eliminate it. Application has been performed on a negative glow (about 10^{11} cm⁻³, 0.2 eV, 0.2 torr). The variation of the coil impedance is determined from the shifts of the frequency, f , and the quality factor, Q , of a LC oscillator containing the coil. As the relative shift, Df/f is much easier to measure, a method based on the variation law $Df/f(f)$ allows to determine the electron density and ν_{e-n} , provided that e.d.f and velocity dependence of e-n cross section are known.

SESSION FC

10:30 AM - 3:45 PM, Wednesday, October 8

Robert P. Lee Lounge - Wisconsin Center

POSTERS; SPECTROSCOPY

Chairperson: J. Ingold, General Electric Company

FC-1 Prompt and Delayed Photolysis of Simple Molecules,*
F. Davanloo, C. B. Collins, U. of Texas at Dallas.
In recent years series of experiments concerned with the correlation of photolysis bands with the dissociation products have been carried out in our laboratory. In these studies a time-delayed, double resonance technique¹ was used for the study of state selective photolysis of Cs₂ and CsKr. Particular attention was placed on the production of the fine structure components of the 5²D and 6²P states of Cs. Quantitative models were constructed to fit the data obtained at several wavelengths of photolysis over the visible spectrum. Not only were the prompt sources from dissociation and predissociation of excited states of Cs₂ and CsKr confirmed, but new kinetic channels for delayed photolysis were found. Here we review the various aspects of these studies. Some new results concerning the delayed sources for the production of Cs(5²D_{5/2}) and Cs(6²P) atoms with the blue wavelengths of photolysis are presented.

*Supported by NSF Grant PHY8214273.

¹F. Davanloo, C. B. Collins, A. S. Inamdar, N. Y. Mehendale and A. S. Naqvi, *J. Chem. Phys.*, 82, 4965 (1985).

FC-2 ArZn Excimer. Y. TAMIR and R. SHUKER, Ben-Gurion U. of the Negev, Israel -- Emission spectra of ArZn mixture in pulsed and C.W. discharges are studied. Whenever Ar density has been raised above 10¹⁵ cm⁻³, the line shape of the ZnI 213.9 nm resonant emission line shows a resemblance to the HgAr one¹. The line is broadened asymmetrically with a red wing of about 50 nm. The maximum of the emission line is shifted to long wavelengths by about 0.6 nm and diffused maxima appear on the red wing. We assume that the ZnAr and HgAr ground and first few excited states are behaving relatively in the same way as it appears in the KAr and CsAr systems². A potential well depth of about 850 cm⁻¹ is estimated for the ArZn excimer ¹1 bound-state from the maximum shift and from HgAr ¹0⁺ ground-state data¹. The blue wing of the line ends in a cut off at about 208.7 nm assumingly caused by a hump in the repulsive part of the excited ¹0⁺ potential curve.

¹C. Bousquet, N. Bras and Y. Majdi. *J. Phys. B: At. Mol. Phys.*, 17, 1831, (1984).

²J. Pascale and J. Vandeplanque. *J. Chem. Phys.* 60, 2278, (1974).

FC-3 The UV-Visible Spectroscopy of Laser Produced Aluminum Plasmas,* J.T. KNUDTSON, W.B. GREEN and D.G. SUTTON, The Aerospace Corporation --The optical emission spectra (180 nm to 760 nm) of plasmas produced by a flashlamp pumped dye laser focused on a aluminum target have been recorded and analyzed. In the incident intensity range from near plasma threshold to 5×10^7 w/cm² the electron temperature was calculated from the relative emission intensity of Al (II) states ($T_e = 8.0 \times 10^3$ K). The electron density was determined from Stark broadened line-widths of four Al(II) lines. Both the spatial and temporal dependence of the emission spectra were obtained providing a map of the electron density and temperature.

*Work conducted under Air Force Contract FO-4701-85-C-0086.

FC-4 Measurement of Barium Ion Density in the Vicinity of Fluorescent Lamp Electrodes by Laser Induced Fluorescence, P.G. HLAHOL and A.K. BHATTACHARYA, LIGHTING BUSINESS GROUP, GENERAL ELECTRIC CO., NELA PARK, Cleveland, OH 44112--A Laser Induced Fluorescence technique was developed to monitor the ionic barium density near the vicinity of an operating fluorescent lamp electrode. A collimated beam of 455.4nm radiation from a pulsed dye laser was used to excite Ba(II) ions present near the electrode of an operating lamp. The subsequent fluorescence signal at 614.2nm was detected using a monochromator-boxcar data acquisition system. Results of such measurements on F-lamps operating on electromagnetic ballasts will be presented. It will be shown that significant amounts of Ba(II) ions are detected near the electrode during the anode half-cycle rather than the cathode half-cycle. The number density of Ba(II) ions detected in the vicinity of electrodes depends upon the volt-ampere characteristics of the lamp-ballast system.

FC-5 Temporal Behavior of an RF Discharge in Silane, L. OVERZET and J. VERDEYEN, U. of Illinois -- The time evolution of the electron density and the plasma fluorescence in response to a square wave modulated RF excitation of helium-silane mixtures has been studied and compared to the more conventional CW discharge. The bulk electron density in the modulated discharge undergoes a complex temporal variation and can be significantly larger than that in the CW glow, despite the same peak RF powers. The helium fluorescence in the modulated discharge does not exhibit such a complex temporal behavior nor is it significantly brighter than in the CW glow. The deposition rate of a-Si:H also increased (in 1% silane glows modulated at frequencies below ~1000 Hz) despite the decrease in the average power and appeared to follow the magnitude of the electron density.

This work was supported by the Joint Services Electronics Program (U.S. Army, U.S. Navy, and U.S. Air Force under contract No. N00014-84-C-0149).

FC-6 Study of an Oxygen D.C. Glow Discharge by V.U.V. Absorption Spectroscopy. G. GOUSSET, P. PANAFIEU, M. TOUZEAU, M. VIALLE, Plasmas Lab. U. of ORSAY FRANCE -- Simultaneous measurements of atom, metastable $O_2(1\Delta)$ and ozone concentrations by V.U.V. absorption in a d.c. glow discharge are presented. The discharge is created in a pyrex tube (length: 50 cm; ϕ : 16 mm), for currents up to 80 mA and pressures between 0.1 and 5 torrs. $O_2(1\Delta)$ concentrations of the order of 10% have been measured by absorption of the light emitted by an hydrogen lamp at 128.5 nm. The atomic concentration has been measured by the absorption of the 130 nm $O(3S-3P)$ resonance line. Weak ozone concentrations are measured by absorption of the 254 nm Hg line. Experimental results are reported as a function of the reduced electric field E/N (measured by electrostatic probes) and of the electronic density (measured by R.F. cavity method). These results are compared to the results of a kinetic model including O , O_2 , $O_2(1\Delta)$, O_3 , e, O_2^+ , O^- .

Work supported by the CNRS-PIRSEM.

FC-7 Absorption in Long-Pulsed, Electron-Beam
Generated Helium Plasmas, L. W. Downes, S. D. Marcum
and W. E. Wells, Department of Physics, Miami
University 45056. In addition to the emission that we
have observed at 431 nm in helium plasmas generated by
long-pulsed, electron-beam discharges (250 kV, 10
A/cm⁻², 900 ns pulse length) at multiple
pressures[1], we have now measured their absorption
spectra over the range 380-750 nm. As expected, large
absorptions occurred at the 465.0 nm band (He₂(2³)
molecular metastable) and the 388.9 nm line (He(2³S)
atomic metastable). In addition, a smaller, broadband
(350-550 nm) and featureless absorption of
undetermined origin has been measured. The afterglow
destruction frequency of the molecular metastable was
less than that of the atomic metastable and peaked in
the afterglow. The absorption results and their
relation to the as yet unidentified source of the 431
nm emission band will be presented and discussed.
1. L.W. Downes, S.D. Marcum and W.E. Wells, Phys. Rev.
A 34, 401(1986).

FC-8 Possible Origin of High Tem-
perature Solar Coronas. J. G. Winans
State University of New York, Amherst
New York. The high temperature, over
10⁶ °K, in the atmosphere of the sun,
differs greatly from the surface tem-
perature of 5,500 °K. X ray photos of
the solar surface, obtained from earth
orbiting satellites, show solar areas
where X rays are emitted. X ray en-
ergy corresponds to over 10⁶ °K. Solar
spectra show lines emitted from mul-
tiple ionized atoms in the solar atmo-
sphere. These atoms collide with atoms,
in their ground states, to produce two
multiply ionized atoms close together.
The force of repulsion produces high
temperature atoms in the solar atmo-
sphere. Multiply ionized atoms trans-
fer high potential energy into high
kinetic energy through collisions.
This balances the production of multi-
ply ionized ions, by X ray absorption.

FC-9 Decay of Cd(II) 441.6nm Line Intensity in a Hollow Cathode He-Cd⁺ Laser Discharge, T. ARAI, Ikutoku Tech. U., K. NIHIRA, Meiji U., T. IIJIMA, Tokyo Voca. Train. Col., and T. GOTO, Nagoya U. --The decays of the He 2³S metastable state density and the endlight intensity of Cd(II) 441.6nm line were measured under the quasi-cw excitation, in the hollow cathode He-Cd⁺ laser discharge. The measurement was made under the near-optimum conditions for laser action. The cathode was 6cm in length and 4mm in inner diameter. In the pulsed discharge current region of more than 100mA, the endlight intensity of Cd(II) 441.6nm line falls quickly after the cut-off of quasi-cw excitation and then decreases slowly. The time constant of slow decay of the endlight intensity of the Cd(II) 441.6nm line agrees well with that of the decay of the He 2³S metastable state density. The result shows that the upper level of the Cd(II) 441.6nm laser line is populated not only by the Penning excitation process but also by other processes, probably electron excitation processes.

FC-10 Measurements of the Balmer Line Ratios Emitted from a Discharge in a Hydrogen Thyatron at High Current Densities, J. Fuhr, Th. Aschwanden, B. M. Penetrante, S. Kuo and E. E. Kunhardt, Weber Research Institute, Polytechnic University -- A high resolution monochromator/photomultiplier system was used to determine the intensity ratios of the Balmer lines H_α, H_β and H_γ emitted by atomic hydrogen in a thyatron discharge. Current densities up to 3000A/cm² have been investigated. The line ratios H_α/H_β, H_β/H_γ and H_α/H_γ do not show a significant dependence on current density. This is in agreement with a theoretical calculation of the relative line ratios [1]. However, the absolute values of the measured ratios are generally higher than the calculated ones. Time resolved measurements of the light emitted at the wavelength of the corresponding atomic states have been carried out and comparison was made with the time dependent current density in the discharge.

* Work supported by the Defense Nuclear Agency.

[1] B. M. Penetrante and E. E. Kunhardt, J. Appl. Phys. 59, 3383 (1986).

SESSION GA

10:30 AM - 3:45 PM, Wednesday, October 8

Alumni Lounge - Wisconsin Center

POSTERS; ELECTRON-ATOM/MOLECULE COLLISIONS

Chairperson: S. Chung, University of Wisconsin-Madison

GA-1 Vacuum Ultraviolet Studies of Electron Impact Cross Sections for H₂ in the Threshold Energy Region, J. M. AJELLO and D. E. SHEMANSKY, Jet Propulsion Laboratory and University of Arizona -- We have completed a study of H₂ in the vacuum ultraviolet (VUV) in the threshold energy region (10 to 20 eV). Electron impact induced VUV fluorescence spectra and cross sections have been measured for the $X^1\Sigma_g^+ \rightarrow a^3\Sigma_g^+$, $1^1\Sigma_u^+ n p \sigma$ and $1^1\Pi_u n p \pi$ ($n = 2, 3, 4$) molecular transitions and Lyman- α . In the threshold energy region the VUV emission spectra are dominated by dipole forbidden transitions viz $X^1\Sigma_g^+ \rightarrow a^3\Sigma_g^+$ and $X^1\Sigma_g^+ \rightarrow E, F^1\Sigma_g^+$. In addition thresholds effects¹ are shown to distort the relative band intensities for all electronic transitions, leading to enhanced relative excitation cross sections of low v' . The excitation cross section of the Lyman- α transition has been studied at 0.2 eV energy resolution. The threshold behavior of transitions of other molecules O₂, N₂, C₂H₂ and CH₄ will be discussed. The instrumentation used in this experiment has been described in a previous paper.²

1. J.M. Ajello and D.E. Shemansky, J. Geophys. Res. 90, 9845 (1985).
2. J.M. Ajello, D.E. Shemansky, T.L. Kwok and Y.L. Yung, Phys. Rev. A 29, 636 (1984).

GA-2 VUV Polarization Studies of the Excitation of the Rare Gas Atoms by Electron Impact, P. HAMMOND^{*}, A.G. McCONKEY and J.W. McCONKEY^{††}, U. of Windsor, Ontario, Canada -- VUV polarization measurements have been made for the electron impact excitation of the light rare gas atoms in the energy range from threshold to 400 eV using a single gold mirror analyzer. In helium the polarization is found to increase sharply in the vicinity of the short-lived, negative ion states that lie near the threshold of the 2¹P state. The first measurements of the optical excitation function and polarization of the 1215 Å line of He⁺ ($n = 4 \rightarrow 2$) have been performed by coupling the polarizer with a LiF window.

* Research supported by the Natural Sciences and Engineering Research Council of Canada.

† U.K. S.E.R.C. Fellow.

†† Canada Council Killam Fellow.

GA-3 Cross Sections for Excitation of Long-Wave Infrared Emission of Nitrogen Atoms by Electron Impact on Nitrogen Molecules,* SUNGGI CHUNG, CHUN C. LIN, U. of Wisconsin, and EDWARD T. P. LEE, Air Force Geophysics Lab.--- Direct measurement of the cross sections for long-wave infrared (LWIR) emission of the N atoms excited by electron impact on N_2 molecules is difficult because of the problems with high-sensitivity photon detection in that region. An alternative procedure is to measure the cross section of a transition $i \rightarrow k$ at a lower wavelength that shares the same upper level as the LWIR line ($i \rightarrow j$) and obtain the LWIR cross section as the product of the measured $i \rightarrow k$ emission cross section times the ratio of the appropriate transition probabilities. We have calculated the transition probabilities for the $2p^2n\ell \rightarrow 2p^2n'\ell'$ series for the N atoms with n from 3 to 10 by a Hartree-Fock procedure with configuration interactions. These values are used to determine the cross sections for several groups of LWIR emission of atomic N produced by electron impact dissociation of N_2 .

* Supported by the AFGL.

GA-4 Electron-Excitation Cross Sections of the $5p^56p$ States of Xenon and Their Pressure Dependence,* JOHN E. GASTINEAU,† CHUN C. LIN, L. W. ANDERSON, U. of Wisconsin, and KEITH G. WALKER, Point Loma Nazarene College---The electron excitation functions of the ten $5p^56p$ levels ($2p$ in Paschen's notation) have been measured between threshold and 100 eV. The results exhibit significant pressure dependence in the range of 0.05 to 2 mTorr. This is a much lower pressure range for non-linear behaviors than is seen in other gases. Pressure dependence becomes noticeable at electron energies above 30 eV. Below 15 eV the optical emission cross sections are constant with pressure. The $2p_1$, $2p_3$, $2p_8$, and $2p_9$ excitation functions reach their low-pressure limits by 0.1 mTorr, and the absolute apparent excitation cross sections have been measured. The excitation functions for the remaining $2p$ levels do not reach a limiting form by 0.1 mTorr; only estimates for the absolute cross sections are obtained.

* Supported by the AFOSR

† Present address: Department of Physics, Lawrence University, Appleton, Wisconsin 54911

GA-5 Electron Excitation of the Second Negative Band System of the Oxygen Molecule,* R. SCOTT SCHAPPE, M. BRUCE SCHULMAN, FRANCIS A. SHARPTON, and CHUN C. LIN, U. of Wisconsin--Emission cross sections of the $A^2\Pi_u(v') \rightarrow X^2\Pi_g(v'')$ transitions of O_2^+ (the second negative band system) excited by electrons colliding with O_2 molecules have been measured. Optical measurements are made for the $v' \rightarrow v''$ bands that do not significantly overlap with other bands. The excitation functions show a broad peak characteristic of the simultaneous ionization and excitation process. Absolute emission cross sections have been obtained for v' from 0 to 12 and the magnitude ranges from $1 \times 10^{-20} \text{ cm}^2$ to $2 \times 10^{-19} \text{ cm}^2$ at 100 eV.

* Supported by the AFGL

GA-6 Emission of Atomic Nitrogen Spectral Lines Produced by Electron-Impact Dissociation,* DAVID L. A. RALL, ALBERT R. FILIPELLI,† FRANCIS A. SHARPTON, and CHUN C. LIN, U. of Wisconsin--Measurements have been made for the absolute optical emission cross sections for transitions of the N atoms in the range 3800-7000 Å originating from some forty terms of the $N(2p^2nl)$ configurations (n up to 9) produced by electron-impact dissociation of the N_2 molecule. In most cases the individual $J \rightarrow J'$ members of a multiplet are resolved, and the population of a J-level within a multiplet is found to be proportional to the statistical weight. Near the threshold energy the formation of the excited nitrogen atoms is believed to be largely due to dissociative excitation through the repulsive part of the Rydberg states of N_2 that converge to $N_2^+(D^2\Pi_g)$. An abrupt increase in the slope of the excitation functions at 5 eV above threshold suggests higher energy channels which may possibly be attributed to the Rydberg states of N_2 that converge to $N_2^+(C^2\Sigma_u^+)$.

* Supported by the AFOSR

† Present Address: National Bureau of Standards, Gaithersburg, MD 20899.

GA-7 Optical Excitation Functions: Study of Threshold Excitation of Helium Autoionizing States. P. J. M. VAN DER BURGT*, J. VAN ECK and H. G. M. HEIDEMAN, Fysisch Laboratorium, Rijksuniversiteit Utrecht, 3584 CC Utrecht, The Netherlands. --We have studied the threshold excitation of autoionizing states in electron-helium collisions. If the scattered electron is still close to the atom at the moment of autoionization, the post-collision interaction causes capture of the scattered electron into a singly-excited state. Thus the measurement of optical excitation functions in the autoionization region provides information on near-threshold electron-impact excitation of autoionizing states. We have measured optical excitation functions for $n=3,4,5$, $L=S,P,D$ states^{1,2}. It is found that only autoionizing states with particular correlation quantum numbers are strongly excited near threshold. The measurements show indications that these autoionizing states are strongly excited via shape resonances (or virtual states).

*Department of Physics, North Carolina State University, Raleigh, NC 27695-8202.

¹P. J. M. van der Burgt and H. G. M. Heideman, *J. Phys. B: At. Mol. Phys.* 18, L755 (1985).

²P. J. M. van der Burgt et al., *J. Phys. B:* (1986), to be published.

GA-8 Resonances in Low Energy Electron Impact on Magnesium. D. CHEN and G.A. GALLUP, Univ. of Nebraska-Lincoln --Resonance energies below the first ionization threshold have been calculated for electron-magnesium collisions. In the analysis, the correlation energy was divided into, A). The portion among the core (1s, 2s, 2p) electrons; B). The portion among the electrons most involved in the resonance (3s, 3p, 4s, 3d, ...); and C). The intershell portion (1s excluded). By assuming the difference of the correlation energies between Mg and Mg for parts A and C are relatively small, we were able to reduce the number of configurations to reasonable size, and thereby to treat the correlation of part B, without much sacrifice. The 11 core excited resonances calculated (including 1 shape resonance, $3s3p^2$, at 2.76 eV and 10 Feshback resonances) agree well with the measurements of Johnston and Burrow.¹ An analysis of the two-electron correlation in the resonances and other details of the calculation will be presented.

¹A. Johnston and P. Burrow; private communication.

GA-9 Electron Energy Loss Spectra of Disilane from 5-25 eV, M. A. DILLON, H. TANAKA,[†] and D. SPENCE, ARGONNE NATIONAL LABORATORY --Electron impact spectra of disilane as a function of scattering angle have been obtained using electrons of 200 eV incidence over an energy loss range that includes all single electron excitations from the valence shell. Below an energy loss of 12 eV the spectra reveal 4 broad bands with similar angular behavior and a spectral intensity approximating that of the HeI photoelectron (PE) spectrum.¹ These bands are tentatively identified as the first members of Rydberg series converging to the ionized orbital pattern depicted in the PE spectrum. Features at larger energy losses indicate the presence of transitions converging to the $(a_{2u})^{-1}$ ion state at 16.5 eV. Spectral intensities are presented as cross sections obtained by the relative flow method employing the 2^1P transition in He as the comparison peak.

*Supported by the U.S. Dept. of Energy, Office of Health & Environmental Research, Contract W-31-109-Eng-38.

[†]Sophia University, Tokyo, Japan.

¹H. Bock, W. Ensslin, F. Feher, and R. Freund, JACS 98, 668 (1976).

GA-10 Electronic and Vibrational Excitation of N₂ in a Glow Discharge, J. LOUREIRO and C.M. FERREIRA, Centro de Electrodinâmica, Lisbon Tec. U. --The electron rate coefficients for $X, v'' - Y, v'$ transitions ($Y=A; B; C; W; B'; a; a'; w$) in a N₂ discharge were calculated by solving the Boltzmann equation together with the rate balance equations for the fractional populations in the X, v'' levels, $\delta_{v''}$. The excitation cross sections employed were generated assuming the expression $\sigma_{x, v''}^{y, v'} = \sigma_x^y (u/u_{x, v''}^{y, v'}) q_{x, v''}^{y, v'} R_e^2$, where the functions σ_x^y were determined by requiring that $\sum_{v', x, 0} \sigma_{x, v''}^{y, v'}$ be identical to the cross sections proposed by Pitchford and Phelps¹. The total rate coefficients $\sum_{v''} \delta_{v''} \sum_{v'} C_{x, v''}^{y, v'}$ differ by a factor less than 2 at $E/N \sim 10Td$ and by less than 10% at $E/N \sim 100Td$ from those recently calculated² treating electronic excitation as single energy loss processes. The inclusion of $X, v'' - Y, v'$ transitions only introduces minor corrections in our previous calculations² of transport parameters, dissociation rate, power transfer to the molecular modes, and vibrational temperature as a function of E/N and n_e/N .

¹Pitchford and Phelps, Bull. Am. Phys. Soc. 27, 109 (1982).
²J. Loureiro and C.M. Ferreira, J. Phys. D 19, 17 (1986).

GA-11 Collision Cross Sections and Excitation Rate Coefficients in Argon, V. PUECH, U. Paris-Sud, and L. TORCHIN, Laboratoires de Marcoussis, France --Excitation rate coefficients of about 30 argon levels have been calculated by solving the Boltzmann equation for $10^{-19} < E/N < 2 \times 10^{-15}$ V.cm². The detailed set of collision cross sections previously used¹ to study the relativistic-electron-beam-produced argon plasma was used without any adjustment to fit among themselves the calculated and measured values of the transport parameters. Our predicted values of these parameters are in excellent agreement with the most recent experimental data. The fractional power deposited in each level is reported versus E/N. For each level, we give the excitation rate coefficients for the direct excitation from the ground state and for the cascades from upper levels. Our predicted rates agree with the experimental results when these latter are available.

¹J. Bretagne, G. Callède, M. Legentil and V. Puech, J. Phys. D : Appl. Phys. 19, 761 (1986).

GA-12 New Semi-Emperically Derived Absorption Potentials for e⁺ -Molecule(Atom) Collisions from Ps Threshold to up to 600 eV, A. JAIN, Phys. Dept., KSU, Manhattan, KS--We report first such calculations on the total (σ_t) cross sections of e⁺ - CH₄ system from the Positronium threshold (E_{ps}), where the σ_t are characterized by a sharp increase following a broad peak around 25-30 eV. Our semi-emperically derived (parameter-free) absorption potential fully describes this sharp increase at the E_{ps} and reproduces the bell-shaped structure of the σ_t at E_{ps} -600 eV in accord with experiments. The total complex-optical-potential (COP) is spherical and involves no free parameter except the mean excitation energy, which needs little adjustment. We test this model for e⁺ - He system also at E_{ps} -200 eV; again there is a qualitative agreement with experimental data. It is possible from this model to extract information on various cross sections such as the Ps formation, annihilation, elastic, momentum transfer and differential cross sections. The real part of the COP is generated accurately from near-Hartree-Fock wave target functions and the polarization is approximated via $-\alpha_0/2r^4$ joined smoothly with correlation potential at small distances.

¹A. Jain, Phys. Rev. A34, 1986 (in press).

SESSION GB

10:30 AM - 3:45 PM, Wednesday, October 8

Robert P. Lee Lounge - Wisconsin Center

POSTERS; BREAKDOWN AND TRANSPORT

Chairperson: J. Ingold, General Electric Company

GB-1 Theory of Runaway Electrons in Weakly Ionized Plasmas - K.U. RIEMANN, Ruhr-Universität Bochum, FRG.

The stationary electron Boltzmann equation is considered for the case of high E/N values. To account for the runaway effect the velocity space is separated into two regions: For "low" energies $u < u_R$ below the "runaway threshold" the usual two term spherical harmonic expansion is applied. The distribution of the runaway electrons ($u > u_R$) is constructed from a development in the angle with respect to the field axis and a subsequent matching to the range $u < u_R$. In the case of a ionization avalanche (exponentially growing electron density) the runaway effect is seemingly "hidden" because the runaways have a Maxwellian distribution. Nevertheless it has a strong influence on the ionization coefficient α . This is shown for the case of He where α decreases with E for high E/N .

GB-2 Transport Property of Electrons in Ramsauer Gas, K.Yamamoto and N.Ikuta, Shikoku Women's U., Tokushima U, Japan, --Effects of Ramsauer minimum on the transport of electrons in CH_4 and in model Ramsauer gases were studied by simulating the electron motion in detail with a Monte-Carlo procedure. Simulation was carried using the "direct method"¹ with "time serial" and "collision sequential" sampling.² For CH_4 , we adopted the cross sections presented by Kleban and Davis.³ Not only the drift velocity takes maximum value at about 3.9 Td, the diffusion coefficient D_V , the transverse diffusion coefficient D_T and also the mean flight time take similar characteristics with E/N . Excitation collision seems to play an important role to provide low energy electrons which form a stream as pointed out by Kleban and Davis. The values of D_V/μ and D_T/μ show large differences from the electron energy especially above 3.9 Td, where Einstein relation does not hold. Simulation was carried also for several types of model cross sections. The results show the effects of the bottom width, depth and of excitation collision distinctively.

1 I.D.Reid: Aust.J.Phys. 32,231(1979).

2 N.Ikuta et al: J.Phys.Soc.Jpn. 54,2485(1985)

3 P.Kleban and H.T.Davis: J.Chem.Phys. 68,2999(1978)

GB-3 Effect of Ramsauer Minimum for Transport of electrons, A.Takeda and N.Ikuta, Tokushima U., Japan,

Electron transport property in model Ramsauer gases were examined using a new procedure "flight time integral method". Cross sections used had variety in the bottom width and the depth of the Ramsauer minimum, while the acclivity of the higher energy side cliff was kept always constant. When only elastic collision occurs, the increase of the bottom width makes D_T large due to the long flight time but does not change the values of D_L and of the drift velocity W_V and W_R . The lowering of the bottom level does not change D_T due to unchanged flight time, but make D_V increase remarkably. This fact shows that D_V is inadequate to give the diffusion transport in configuration space. It is noticeable that the second term of the energy distribution $F_1(\epsilon)$ is almost zero within the bottom region due to bidirectional flight with few collisions. If an excitation collision is introduced, $F_1(\epsilon)$ rises up even in the bottom region and the drift velocity increases markedly. This is caused by the abundant supply of low energy electrons which make an unidirectional stream as pointed out by Kleban and Davis, where both of $\epsilon_{||}/\epsilon_{\perp}$ and $D_{V||}/D_{V\perp}$ also take larger values than unity.

P.Kleban and H.T.Davis: J.Chem.Phys. 68,2999(1978).

GB-4 Excitation mechanisms in argon at very high E/n,* D. A. Scott† and A. V. Phelps,‡ JILA, U. of Colo. and NBS. -- A pulsed drift tube was used to study excitation in argon at very high E/n. Pulsed laser irradiation at 266 nm of a semitransparent Au-Pd film on quartz was used to obtain current pulses of 1-10 mA and 10 ns width. The 811.5 nm ($2p_9-1s_5$) and 750.4 nm ($2p_1-1s_2$) emission was monitored using a photomultiplier, interference filters, and fast digitizer. E/n was varied from 300 to 20,000 Td (1 Td = 10^{-21} V m²) at Ar densities of about 2×10^{21} m⁻³. At $E/n \lesssim 4$ kTd the time of maximum emission (10-100 ns) is consistent with electron excitation of the argon. At 18 kTd the 811.5 nm emission consists of a peak caused by the initial electron avalanche followed by a broad peak at 10% to 70% of the ion transit time of ~ 4 μ s depending on the portion of the gap observed. The 750 nm emission at the later times is much weaker. These are consistent with excitation of argon by ions or fast atoms.

*Supported in part by Lawrence Livermore National Labs.

†Now at CSIRO Div. of Appl. Phys., Sydney, Australia.

‡Quantum Physics Division, NBS and Physics Dept., CU.

GB-5 Electrical Breakdown Induced in Spark Gaps by an X-ray Pulse, R. V. HODGES, L. E. McCOY and J. F. RILEY, Lockheed Palo Alto Research Laboratory - An X-ray pulse induces electrical breakdown in a spark gap if the applied voltage is greater than a critical value. We measured the current and voltage across N₂- and H₂-filled spark gaps during breakdown induced by a 20-ns X-ray pulse from a 2-MeV Febetron. Measurements were made as a function of X-ray dose rate, series resistance, and applied voltage. The spark gap was partially discharged during the pulse and recharged at a rate determined by the series resistance. The critical applied voltage for breakdown increased with the series resistance, because of the slower voltage recovery after the pulse. Above the critical voltage the gap voltage collapsed in two or three steps, the last one occurring about 1 μ s after the X-ray pulse. As the applied voltage increased, the first step became larger and occurred sooner after the X-ray pulse.

GB-6 Optical Switching of Glow Discharge with an Excimer Laser, M. SAPOROSCHENKO,* M. J. ROSSI, and H. HELM, Molecular Physics Department, SRI International -- The response of a glow discharge to illumination by an excimer laser pulse at 248 and 193 nm has been investigated. The experimental arrangement consists of a cylindrical hollow cathode and a wire-loop anode, with an external voltage applied between cathode and anode slightly below the breakdown voltage of the gas mixture (0.2 to 1 torr). Axial illumination of the device through cathode and anode by an apertured, unfocused excimer beam is observed to initiate a DC glow discharge in a variety of gases. When a gas mixture of 2% vinyl-chloride and helium is used it is observed that the second laser pulse extinguishes the glow discharge. Alternate laser pulses continue to initiate and extinguish the self-sustained discharge at rates between 0.01 and 10 Hz. In addition to the simple explanations of laser ionization and photo-induced electron attachment, we will also discuss discharge instabilities induced by the laser.

*Permanent Address: SIU, Carbondale, IL 62901

Research supported by ARO.

GB-7 The Effect of Humidity and Gas Density on
Switching-Impulse Breakdown of Air*, A.J.DAVIES,
J.DUTTON, R.TURRI and R.T.WATERS, Swansea University and
UWIST, Cardiff -- Breakdown measurements of sphere-plane
gaps subjected to switching impulses have been carried
out over the pressure range 0.7 - 1.4 bar and absolute
humidity levels from of order 2 to 15 g m⁻³. An all-
metal sealed metal ionization chamber was used and the
pressure and humidity levels could be closely monitored
and controlled. The measurements show that, for the
configuration studied, the breakdown voltage increases
linearly with pressure at a given humidity level with a
slope of approximately 1.5 kV per g m⁻³. The breakdown
probabilities satisfy a normal distribution. The
humidity correction factors differ appreciably from
those given in Standard Tables¹.

¹High-voltage test techniques. Part 2: Test procedures.
IEC 60-2: 1973.

* This work is supported by the Science & Engineering
Research Council.

SESSION GC

10:30 AM - 3:45 PM, Wednesday, October 8

Alumni Lounge - Wisconsin Center

POSTERS; SHEATHS

Chairperson: S. Chung, University of Wisconsin-Madison

GC-1 Plasma Pre-Sheath in a Collisional Plasma, J.T. SCHEUER, G.A. EMMERT, University of Wisconsin -- The problem of a collisional plasma flowing into a perfectly absorbing wall has been investigated using a kinetic approach. The plasma is assumed to have a nonzero ion temperature and a Boltzmann distribution of electrons. Ion collisions are included in the analysis through a Bhatnagar, Gross and Krook¹ collision term, which conserves particles and momentum. An equation describing the electrostatic potential variation in the pre-sheath region is derived. This equation is solved numerically for a range of collisionalities. In addition to the electrostatic potential in the pre-sheath, the ion distribution function, the wall potential, and the ion particle and energy fluxes to the wall are also calculated.

¹Bhatnagar, Gross and Krook, Phys. Rev. 94, 511 (1954).

GC-2 The Properties of Plasma Sheaths in the Presence of Negative Ions,* M. F. TOUPS, D. W. ERNIE, and H. J. OSKAM, Univ. of Minnesota -- A model has been developed which describes the effect of the presence of negative ions (in addition to positive ions and electrons) on the conductivity and capacitance of a plasma sheath. A Bohm criterium modified for the presence of negative ions has been determined. The resulting plasma sheath conduction current and capacitance have been incorporated into an equivalent circuit model characterization of a planar rf plasma reactor. The effect of negative ions on the voltage waveforms across the plasma sheaths adjacent to the reactor electrodes has been calculated for various negative ion to positive ion density ratios. These sheath voltage waveforms have been used to determine the resulting influence of the presence of negative ions on the energy distribution of positive ions bombarding the electrode surfaces. The implications of these results for plasma processing systems will be discussed.

* Work supported by Air Force Wright Aeronautical Laboratories, IBM, and the Center for Microelectronics and Information Sciences, Univ. of Minnesota.

GC-3 Plasma-Sheath Structure for an Electrode Contacting an Isothermal Plasma: III. Cathodes,* L. D. ESKIN and S. A. SELF, Mech. Engr. Dept., Stanford Univ. -- The electron and ion continuity and momentum equations are solved with Poisson's equation for the cathode boundary layer region of a collision dominated atmospheric pressure plasma. Electron impact ionization and three-body (electron) recombination processes are included. We have considered both non-emitting and electron emitting cathodes over a broad range of plasma conditions and net current density. The ionization non-equilibrium region is shown to play an important role in the plasma-sheath structure and resulting current-voltage characteristics. The net current density is limited by the sum of the total net generation rate of electron-ion pairs in the layer and the electron emission flux from the cathode. In the absence of electron emission by the cathode, current saturation occurs at a point whereby the ion flux at the sheath edge is but a small fraction of the one-way random thermal ion flux in the plasma.

* Work supported by the AFOSR, Grant No. 83-0108.

GC-4 Thickness of the ion-sheath surrounding a Langmuir probe, G. GOYETTE and M. NACHMAN, Dept. of Electrical Eng., Ecole Polytechnique of Montreal, Canada. It is the purpose of this paper to report on an experimental study of the thickness of the ion-sheath surrounding an electron retarding cylindrical probe, as a function of the dc-bias applied to this probe. The experiments were conducted in a low pressure diffusion-type argon plasma. A movable, point-like secondary probe at plasma potential was used for exploring the sheath around the dc-biased Langmuir probe, to which a low frequency, low voltage ac-signal was superimposed. The modulation in the electron density induced by this ac-signal resulted in a peak in the ac-component of the secondary probe current at the sheath-plasma boundary. Measurements on the dependence of the sheath thickness on the dc-bias applied to the probe were carried out for probes of different radiuses, at several plasma densities. The experimental results were compared with existing theories^{1,2}.

1. J.G. Laframboise, UTIAS Rept. 100 (1966).
2. J.L. Nightingale, E.R. Ault and A.A. Mondelli, J.Appl.Phys. 53, 886 (1982).

GC-5 Space Charge, Double Sheaths and Particle Emission at Plasma Boundaries,* T. INTRATOR, M.H. CHO, E.Y. WANG, University of Wisconsin-Madison -- We have measured the local plasma potential and density inside a hot cathode-plasma system, so that a comparison with the Child-Langmuir Law is possible. At the boundary between a plasma and a charged particle current source, space charge effects determine the steady state balance of current flow, particle density and potential. A double sheath plus the presheath determines the charge flux that can be extracted from a cathode (anode) or, for instance a plasma virtual cathode (anode) for processing applications. Plasma diodes of this type have been studied for many years from the outside, by measuring total current and voltage applied at the boundaries of the system. The local plasma potential inside the system measured with electrostatic emissive probes is compared with an extended Child-Langmuir law¹, that takes into account hot cathode electrons, thermal plasma electrons and streaming plasma ions.

*Work supported by NSF Grant ECS-8314488 and NASA Grant NAGW-275.

¹C.D. Child, Phys. Rev. 32, 492 (1911).

GC-6 Dynamics of an Ionic Non Collisional Sheath created by a R.F. Potential, A.M.POINTU, Lab. Phys. Gas and Plasmas (Univ. Orsay, France) --The dynamics of an ionic non collisional sheath created by an AC potential of frequency f can be simply described when f is either low or high as compared to ionic plasma frequency. In the first case, the sheath is constantly in the static equilibrium state described by Bohm's theory. In the second case, Poisson's equation involves at any point, x , electrons oscillating in the instantaneous potential, $V(x,t)$, and ions which are "frozen" in the mean potential, $V_0(x)=\langle V(x,t) \rangle$. The solution, $V(x,t)=V_0(x)+V_4(x,t)$, extends from the wall to the sheath edge. One can show that such an edge is stationary and corresponds to Bohm's criterion for the mean potential $V_0(x)$. Assuming a thick sheath, $V_0(x)$ obeys the Child-Langmuir law and the $V_4(x,t)$ potential decreases roughly linearly between the sheath edge where it is equal to zero and the wall. Thus, knowledge of dV_4/dt at the wall allows one to calculate the displacement current. A treatment extending the model of ref[1] will later be presented to describe R.F. discharges for complex sheaths impedances.

[1]A.M.Pointu,Appl.Phys.Lett. 48,762(1986).

GC-7 Measurement of Plasma Potential Profiles with RF Applied to Conducting Boundaries,* M.H. CHO, N. HERSHKOWITZ, E.Y. WANG, T. INTRATOR, University of Wisconsin-Madison -- There have been many attempts to understand plasma behavior affected by boundaries with time varying potentials. Here we present experimental measurements of time varying spatial plasma potential profile associated with an RF signal applied to two parallel conducting plates. Argon plasma is produced by hot-filament discharge in a multi-dipole device, and typical plasma parameters are $n_e = 10^8 \sim 10^9 \text{ cm}^{-3}$, $T_e \approx 2 \text{ eV}$, $T_i \approx 0.2 \text{ eV}$ and neutral pressure $\approx 1 \times 10^{-4} \text{ Torr}$. It is observed that the plasma potential response is no longer DC-like above a few KHz. Data are taken using emissive probes with time averaged and time resolved sampling techniques. Dependence on different plasma parameters and boundary conditions are discussed. Results are compared to the theory and other similar experiments.

*Supported by NSF Grant ECS-8314488.

SESSION HA

4:00 PM - 5:30 PM, Wednesday, October 8

Lakeshore Room - Wisconsin Center

SPECTROSCOPY OF ATOMS, MOLECULES, AND IONS

Chairperson: F. A. Sharpton, University of Wisconsin-Madison

HA-1 Metastable Autodetaching States of Negative Ions,* Y. K. BAE and J. R. PETERSON, SRI International.---

Metastable autodetaching states of negative ions have attracted both theoretical and experimental studies for some time. These states can be classified into three groups, such as electronically excited,¹ vibrationally excited,² and planetary (or Wannier) states.³ Studies of these ions provide stringent tests for sophisticated calculations as well as deeper understanding of spin related couplings, non-Born-Oppenheimer couplings, and correlation effects of two excited electrons. They also can be used for self-neutralizing ion beams and XUV lasers. We present an overview of what we have learned recently and suggest some potentially illuminating experiments.

*Work supported by NSF and AFOSR.

¹Y. K. Bae, J. R. Peterson, A. S. Schlachter, and J. W. Stearns, *Phys. Rev. Lett.* 54, 789 (1985).

²Y. K. Bae, P. C. Cosby, and J. R. Peterson, *Chem. Phys. Lett.* 126, 266 (1986).

³S. J. Buckman, P. Hammond, F. H. Read, and G. C. King, *J. Phys. B* 16, 4039 (1983).

HA-2 The Hopfield Helium Continuum and He₂(X¹Σ_g⁺) Potential,* J. R. PETERSON, SRI International, and H. H. MICHELS, UTRC -- The VUV spectrum of the Hopfield helium continuum arises from the transitions: He₂ [A¹Σ_u⁺] → He₂ [X¹Σ_g⁺] and He₂ [D¹Σ_u⁺] → He₂ [X¹Σ_g⁺]. We have fitted the optical data of Huffman, et al. with spectra calculated using accurate wavefunctions for the upper states and several versions of the X¹Σ_g⁺ ground state potential. The simulations show contributions from excited vibrational levels of the A and D states. The semi-empirical potential of Foreman et al.² yields a somewhat better overall fit than the recent ab initio potential of Ceperley and Partridge.³ We find a repulsive energy of 3.4 ± 0.1 eV for the ground X¹Σ_g⁺ state of He₂ at R=1.04 Å.

*Supported by NSF Grant PHY-8410980 and AFOSR Contracts F49620-85-K-0017 and F49620-85-C-0095.

¹R. E. Huffman, J. C. Larrabee and D. Chambers, *Appl. Opt.* 4, 1145 (1965).

²P. B. Foreman, P. K. Rol and K. F. Coffin, *JCP* 61, 1658 (1974).

³D. M. Ceperley and H. Partridge, *JCP* 84, 820 (1976).

HA-3 Radiative Lifetimes of the 0_u^- Sublevels of the Rare Gas Excimers,* DAVID L. HUESTIS, SRI International. The observed low-lying excited states of the rare gas dimers, Ne_2^* , Ar_2^* , Kr_2^* , and Xe_2^* , are frequently referred to as 0_u^+ and 1_u (arising from $1\Sigma_u^+$ and $3\Sigma_u^+$ respectively). In kinetic studies the third component of the $3\Sigma_u^+$ state, designated 0_u^- , has been supposed either to be entirely metastable, or has been otherwise ignored. By including rotational coupling among the $1,3\Sigma_u^+$ and $1,3\Pi_u$ states we have calculated separate radiative lifetimes for all three components of the $3\Sigma_u^+$ state (the 1_u is split into two distinct levels). The calculated 0_u^- thermally-averaged radiative lifetimes are 26, 14, 3, and 9 μs for Ne_2^* , Ar_2^* , Kr_2^* , and Xe_2^* respectively. Lifetimes from high-pressure gas experiments, in which the three triplet components should be well mixed by collisions, are 3-4 times shorter than those calculated. We will discuss the possible resolution of this difference by including the atomic p^5d configuration in the calculations.

*Supported by ONR and LLNL

HA-4 Atomic Transition Probabilities for ScI and ScII*, E.A. DEN HARTOG, G. MARSDEN and J.E. LAWLER, U. of Wisconsin, J.T. DAKIN and V. ROBERTS, General Electric Co..—An accurate and comprehensive set of atomic transition probabilities for ScI and ScII are being measured. The results are needed for reliable radiation transport calculations in metal halide discharge lamps. Radiative lifetimes for 59 levels in ScI and 15 levels in ScII are measured using time-resolved laser-induced fluorescence on a sputtered atom/ion beam. All 15 of the ScII and 40 of the ScI levels are odd parity levels which are populated using single-step laser excitation. The remaining 19 levels in ScI are of even parity and must be populated using two-step laser excitation. The single-step experiments are complete and the two-step experiments are underway. Branching ratios will be measured for all of these levels using the 1.0m Fourier Transform Spectrometer at the National Solar Observatory. The lifetimes and branching ratios will be combined to provide accurate absolute transition probabilities for approximately 150 of the strongest lines in ScI and 85 of the strongest lines in ScII.

*Supported by the General Electric Company and by NSF Grant AST85-20413.

HA-5 A Solution to the Problem of Missing Infrared Branches,* D.W. DUQUETTE[†], E.A. DEN HARTOG, and J.E. LAWLER[†], University of Wisconsin-Madison -- Much progress has been made in determining accurate atomic transition probabilities (gAs) for the elements in low stages of ionization. Time-resolved laser-induced fluorescence is used to determine reliable radiative lifetimes. Branching ratios are measured using a powerful Fourier transform spectrometer. The combination is producing a data base of gAs of unparalleled accuracy. The most serious remaining systematic uncertainty in the approach for determining gAs is the possibility of unknown IR branches. A new technique is reported for testing the completeness of emission branching ratios, and, if necessary, determining the total gA of unknown IR branches. The technique is based on comparison of non-infrared fluorescence produced by laser excitation of two upper levels from the same lower level. The technique is applied to many levels in HfI, NbI, WI, and TaI. The decay of the z^5F levels in HfI is found to be dominated by IR branches. The reliability of this technique is confirmed by direct identification and measurement of the dominant branches on IR emission spectra.

[†]Guest observer, National Solar Observatory, Tucson, AZ.

*Supported by NSF Grant AST85-20413.

HA-6 The Absolute Accuracy of the Electron-Impact Photoemission Cross Sections for the VUV Radiometric Standard, R. C. G. LIGTENBERG, P. J. M. VAN DER BURGT, W. B. WESTERVELD and J. S. RISLEY, North Carolina State University.* --A method was developed to measure absolute emission cross sections in the VUV (30-150 nm) using synchrotron radiation.¹ Previous measurements of the photoemission cross sections for dissociative excitation of H_2 followed by emission of Ly α radiation and for the 92.0 nm and 93.2 nm emission lines of Ar II demonstrated that our method is reproducible to within 0.5%. Currently, our efforts concentrate on the absolute accuracy which can be obtained by measuring the photoemission cross section of the He ($1^1S - 2^1P$) excitation process. Above 300 eV electron energy, measured excitation cross sections² for this transition are within a few percent of the Bethe and Born approximations, thus allowing accurate intercomparisons. Our measurements are taken at sufficiently low pressures to eliminate effects due to self-absorption and re-emission of resonance radiation.

*Supported in part by the Aeronomy program of NSF, grant no. ATM85-01865.

¹A. McPherson et al., *Appl. Opt.* **25**, 298-310 (1986).

²M. A. Dillon and E. N. Lassetre, *J. Chem. Phys.* **62**, 2373-90 (1975).

SESSION HB

4:00 PM - 5:30 PM, Wednesday, October 8

Room 313 - Wisconsin Center

DISCHARGES IN ELECTRONEGATIVE GASES

Chairperson: S. R. Hunter, Oak Ridge National Laboratory

HB-1 Electron Attachment in Weakly Attaching Gases.
J.DUTTON, A.K.LUCAS and A.W.WILLIAMS, Department of Physics, University College, Swansea, U.K. -- In order to measure the low values of attachment coefficient which are characteristic of some practically important mixtures, a pulsed drift-tube apparatus has been developed which uses a microprocessor controlled digital recording system to enable very small signal currents to be extracted from background noise by signal averaging. To calibrate this apparatus, measurement of electron and negative ion pulses have been used to obtain values for the electron attachment coefficient in oxygen. Measurements were carried out over a range $1.25 < E/N < 36 \times 10^{-17} \text{V cm}^2$ for pressures in the range 3.6 to 18.1 torr. The attachment coefficients were found to be independent of pressure for E/N values down to approximately $8 \times 10^{-17} \text{V cm}^2$, while for E/N values from 8 to $1.25 \times 10^{-17} \text{V cm}^2$ the values of the attachment coefficient increased and were pressure dependent. The results are in good agreement with the compilation of data given by Gallagher et al¹. It is expected that results for more weakly attaching gases will be available for presentation at the meeting.

¹J.W.Gallagher, E.C.Beaty, J.Dutton and L.C.Pitchford, J.Phys. Chem. Ref. Data 12, 109-152 (1983).

HB-2 The Influence of Transverse Magnetic Fields on the Current-Voltage Characteristics of Glow Discharges,* K.H. SCHOENBACH, S.T. KO, T.J. POWERS and V.K. LAKDAWALA, Old Dominion University, Norfolk, VA -- Measurements of the steady-state current-voltage characteristics of abnormal glow discharges in transverse magnetic fields have been performed in He and He/SF₆ mixtures at a pressure of 8 Torr. The discharge voltage in He/SF₆ increases by a factor of two with applied magnetic field of less than 0.3 T. In He the discharge voltage decreases with increasing magnetic field. Monte Carlo codes were used to determine the rate and transport coefficients in the positive column and in the cathode region. With the obtained values the spatial variation of charged particle densities and the electric field between plane-parallel electrodes was calculated using a continuum model.

* Work supported by the Office of Naval Research under contract number N00014-85-K-0602

HB-3 Switching of Conduction Current by Photodetachment and Photodissociation Processes Occurring in the SOCl₂-N₂ Gas Mixture,* W. C. WANG and L. C. LEE, San Diego State U. --An ArF laser (pulse width 10 ns) was used to study electrical switching in a negative point-to-plane Corona discharge containing SOCl₂-N₂ gas mixture. An increased current pulse (pulse duration ~ 1 μs) was observed in a DC discharge current when the discharge medium was irradiated by an ArF laser. The current increase is due to an increase of electrons that are produced from the photodetachment of negative ions in the discharge by the laser photons. After the increased current pulse, the discharge current is nearly cut-off. The current decrease is caused by the increase of electron attachment rate due to the photofragments (Cl, Cl₂, SO) and their excited products produced by laser excitation of SOCl₂. The dependence of the current switching on the laser power, SOCl₂ concentration, and laser beam size will be discussed.

*Work supported by AFOSR under Grant No. AFOSR-82-0314.

HB-4 Breakdown of a Wire-to-Plane Discharge - Time-wise Development,* K. RAMAKRISHNA, I. M. COHEN, and P. S. AYYASWAMY, MEAM Dept., U. of Pennsylvania, Philadelphia, PA 19104-6315 -- A wire-to-plane discharge is considered in the early phases of the EFO used to melt the wire and form a ball used in ball bonding of semiconductor chips. Unsteady diffusion flux equations with coupled energy conservation and Poisson's equation for the self-consistent electric field are formulated in prolate spheroidal coordinates with the wire electrode simulated as a slender hyperboloid of revolution. Three different time scales enter into the computation: the ionization/breakdown time, the electron diffusion time, and the ambipolar diffusion time. In practice, the electronic flame-off (EFO) occurs in atmospheric pressure air or argon with gold or aluminum wire. The computational simulation starts with an impressed voltage between the electrodes which establishes a very nonuniform electric field according to Laplace's equation (with very few charges in the gap). A curve fit to data for Townsend's first ionization coefficient is used locally in terms of the self-consistent electric field to show that ionization proceeds outwards from the wire tip where the electric field intensity exceeds the threshold value until breakdown is completed in the entire gap.

*Work supported by the National Science Foundation.

HB-5 Oxyfluoride Yields from Corona Discharges in Gas Mixtures of SF₆ with O₂¹⁸ and H₂O¹⁸, * R.J. VAN BRUNT and M.C. SIDDAGANGAPPA, National Bureau of Standards--The absolute yields of the gaseous oxyfluorides SOF₂, SO₂F₂, and SOF₄ from negative corona discharges in mixtures of sulfur hexafluoride with O₂¹⁸ and H₂O enriched with varying amounts of O₂¹⁸ and H₂O¹⁸ have been measured with a gas chromatograph-mass spectrometer. The SF₆ oxidation mechanisms have been revealed by a determination of the relative O¹⁸ and O¹⁶ content of the observed oxyfluorides. The results indicate that SOF₂ and SO₂F₂ derive oxygen predominantly from H₂O and O₂ respectively in slow, gas-phase reactions involving SF₄, SF₃, and SF₂ that occur outside of the discharge region. The species SOF₄ derives oxygen from both H₂O and O₂ through reactions in the discharge region involving free radicals or ions such as OH, and O, with the lower valence sulfur fluorides SF₅ and SF₄.

*Supported in part by U.S. Department of Energy

HB-6 Limit-Field Behavior of Various Gas Mixtures Described in Terms of the Relevant Microscopic Collisional Processes, M.F. Fréchette and J.P. Novak, IREQ, Varennes, Québec, Canada--Theoretical limit fields for SF₆/N₂, CCl₂F₂/N₂, CCl₂F₂/SF₆ and CCl₂F₂/SF₆/N₂ gas mixtures obtained from a Boltzmann-equation analysis are compared with experimental values measured in a steady-state discharge and with data from other swarm experiments as well as with breakdown-potential measurements taken from the literature. Good agreement is found between experimental and calculated limit-field values; the largest relative difference in magnitude, which occurs for the case of the ternary mixtures, is of the order of 10%. Discussion based on considerations of the electron energy distribution functions and collision integrals such as the ionization and attachment frequencies demonstrates that the theoretical model can successfully relate the limit-field behavior to the interplay of the microscopic processes involved.

HB-7 Effect of O₂ on By-Product Formation in Spark Decomposition of SF₆*. I. SAUERS, Oak Ridge National Laboratory, Oak Ridge, Tennessee--The yields of SOF₄, SO₂F₂, SOF₂, and SO₂ have been measured as a function of O₂ content in SF₆/O₂ mixtures, following spark discharges. All experiments were made at a spark energy of ~8.7 Joule/spark, a total pressure of 133 kPa, and for O₂ additions of 0, 1, 2, 5, 10, and 20%. Even for the case of no added O₂, trace amounts of O₂ and H₂O result in the formation of the above by-products. However, addition of O₂ significantly increases the yields of SOF₄ and SO₂F₂, while SOF₂ and SO₂ are only mildly affected. Reaction mechanisms will be discussed, and comparison of these yields with the yields from other types of discharges (corona and arc) will be made.

*Research supported by the Division of Electric Energy Systems, USDOE, under contract DE-AC05-84OR21400 with Martin Marietta Energy Systems, Inc.

SESSION JA

8:00 AM - 9:45 AM, Thursday, October 9

Lakeshore Room - Wisconsin Center

ELECTRON-ATOM/MOLECULE COLLISIONS II

Chairperson: P. D. Burrow, University of Nebraska

JA-1 Partial Cross Sections for Na 3S-3P Excitation by Electrons, X. L. HAN, G. W. SCHINN and A. GALLAGHER, JILA, Univ. of Colorado and NBS.--Partial cross sections for Na $3S_{1/2}(M_S) \rightarrow 3P(M_L, M_S)$ excitation by electrons are measured by optically exciting the electron-excited $3P(J, m_J)$ states to the 5S state in a 230 Gauss magnetic field. (The Na beam is optically pumped into the $M_S = 1/2$ state.) The $3P(J, M_J) \rightarrow 5S_{1/2}(M_S)$ transition frequencies are spectroscopically separated in the magnetic field, so that a scan of the 3P-5S laser frequency yields the partial cross sections. The 5S excitation is detected by collecting a large solid angle of cascade $4P \rightarrow 3S$ (330 nm) fluorescence, and a very high S/N is achieved from threshold to high electron energies. Results, and the possibilities for also obtaining these partial cross sections as differential cross sections in electron scattering angle will be discussed.

JA-2 Elastic 3P-3P Excited State Scattering of Electrons by Sodium⁺. M. ZUO, G. F. SHEN*, B. STUMPF**, L. VUŠKOVIĆ AND B. BEDERSON, New York University. We have measured the elastic 3P-3P excited state cross section for low energy electron scattering on sodium. This is, to our knowledge, the first elastic cross section direct measurement for an excited atomic species. The experimental method utilizes an atomic beam "double recoil" technique, in which laser-excited sodium atoms are spatially separated from unexcited atoms using photon-recoil; these atoms then suffer recoil in electron scattering¹. A quantitative analysis of transverse laser deflection² enables us to obtain the absolute excited state beam density, and consequently absolute excited state cross sections. The differential elastic 3P-3P cross section, measured at $E = 10$ eV, rises from about 150 to 300 Å²/srad as the scattering angle varies from 17 to 22°. This is 5 to 15 times larger than the corresponding 3S-3S cross section.

+ Supported by NSF. * Present address: University of California, Riverside. ** Present Address: University of Windsor, Windsor, Ont. 1 B. Jaduszliwer et al, Phys Rev A 21, 808 (1980); G.-F. Shen et al, XIV ICPEAC, Palo Alto, Abst's of Cont'd Papers, p. 200 (1985). 2 B. Jaduszliwer et al, J de Physique, Supp 1 46, C1-241 (1985); B. Jaduszliwer et al, Phys Rev A 33, 3792 (1986).

JA-3 Electron Scattering from Atomic Oxygen,*
J.P. DOERING, E.E. GULCICEK, and S. O. VAUGHAN, Dept. of Chemistry, Johns Hopkins U. --Absolute differential and integral electron scattering cross sections have been measured for the $^3P \rightarrow ^3S^0$ transition of atomic oxygen at incident energies from 16.5 to 200 eV. Optical oscillator strengths for the seven most intense dipole-allowed transitions have also been determined. An apparatus using a variable angle and incident energy electron spectrometer coupled to a microwave discharge free supersonic jet expansion source was developed for this work. The source produces an intense jet of O, O₂, and H seeded in He with a typical O/O₂ ratio >2.5. All excited states of OI below 12 eV as well as many higher-lying states have been detected and cross section work is proceeding for a number of these forbidden and allowed transitions.

*Work supported by National Science Foundation Grant ATM-8605992.

JA-4 Excitation of the Electronic States of Helium by Electron Impact,† D. C. CARTWRIGHT and G. CSANAK, Los Alamos National Laboratory, S. TRAJMAR and D. REGISTER†† JPL, Calif. Inst of Tech--Differential cross sections (CSs) for electron-impact excitation of all electronic states of helium with principal quantum numbers $n = 2$ and 3 (and some with $n = 4$) have been measured at incident electron energies of 30, 50 and 100 eV using an electron spectrometer. In addition, First-Order Many-Body (FOMBT) calculations of the differential and integral CSs have been completed for all the $n = 2, 3$ and 4 states at these and other incident electron energies for which experimental and/or theoretical data exist. Comparisons have been made between the results from FOMBT, close-coupling (CC) methods and experiment at all possible incident electron energies. Comparisons between the results from CC, FOMBT and experiment provide insight into the role of various physical interactions for describing this type of inelastic collision process.

†Work partially supported by the NSF, DOE and NASA.

††Present address; Phillips Petroleum Co., Bartlesville, OK.

JA-5 Further Measurements of Small-angle Scattering by Alkali Halides, G. F. SHEN⁺, M. ZUO, B. STUMPF*, L. VUŠKOVIĆ, AND B. BEDERSON, New York University** We are continuing our studies of small-angle scattering of low-energy electrons by selected alkali halide molecules using a crossed-beam recoil technique¹. In the angular (3-30°) and energy (5-20 eV) ranges studied the interaction is primarily the inverse r^2 potential. Since recoil measurements can be made absolute, i.e., need not be normalized to, say, the Born Approximation, they can be directly compared to BA and other calculations. We will present new measurements, particularly using LiBr, and compare to both available theory and to previous measurements. Attempts to perform similar measurements on (LiBr)₂ are being made (the primary interaction is the inverse r^4 polarizability potential), and we expect to present preliminary dimer results as well.

+ Present address: University of California, Riverside

* Present address: University of Windsor, Windsor, Ont.

** Supported by US Dept. of Energy (OBES)

1 B. Jadászliwer et al, Phys Rev A 30, 1255, 1269 (1984);

G.-F. Shen et al, Bull. Am. Phys. Soc. 31, 961 (1986)

SESSION JB

8:00 AM - 9:45 AM, Thursday, October 9

Room 313 - Wisconsin Center

SPECTROSCOPY OF ARC LAMPS

Chairperson: J. J. Lowke, CSIRO

JB-1 Self-reversed lines, and what we can learn from them, D.O. WHARMBY, THORN EMI Lighting, UK
-- Lines and other spectral features which are self-reversed provide markers in the spectrum of predictable optical depth. They can therefore be used to provide information about number densities and about temperatures in hot and cold regions of plasma. The diagnostics become particularly straightforward in LTE plasmas. The methods of Bartels and Cowan and Dieke were developed for this purpose. The physical concepts which underly these methods will be demonstrated with the help of radiation transport calculations which indicate the effects of temperature profiles and linewidth assumptions. With the normal assumptions, these methods cannot be applied to resonance lines. Direct radiation transport calculations, which do not require these assumptions, enable resonance lines to be used, so that plasmas may then be probed at very low temperatures. Measurement methods will be discussed together with errors which arise from measurements and the assumptions, particularly those about line profiles.

JB-2 Line and Continuum Emission from Optically Dense Sodium (Na + Hg + Xe) Plasmas, J.J. DE GROOT, Philips Lighting Division, Eindhoven, Netherlands; J. SCHLEJEN and J.P. WOERDMAN, Huygens Laboratory, University of Leiden, Netherlands-- The high-pressure sodium (HPS) discharge is a typical example of an optically dense plasma. Self-absorption and extreme line-broadening play a crucial role in determining the radiated spectrum, which is dominated by the self-reversed Na D-lines. In recent years the insight has grown that the very far wings of the D-lines are of (quasi-)molecular origin, originating from short range Na-Na interaction. Similarly the buffer gases mercury and xenon influence the wings of the D-lines, because of Na-Hg and Na-Xe interaction.

In the quasi-static approximation the absorption coefficient of bound as well as quasi-molecules can be calculated from the relevant potential energy curves of the NaNa, NaHg and NaXe molecules. From the spectral absorption coefficient, for atomic as well as (quasi-)molecular radiation, combined with the plasma temperature distribution, the emission spectrum can be calculated from the one-dimensional radiative transfer equation. Good agreement is found with measured ultraviolet-visible-near infrared spectra.

JB-3 Extensions to Bartels' Theory of Radiative Transfer.
P. A. REISER - GTE Products Corporation and P. A. VICHARELLI - GTE Laboratories -- A generalization of Bartels' solution of the equation of radiative transfer¹ for a self-absorbed emission line from an LTE plasma with a symmetric temperature profile is presented. The solution is presented as an asymptotic series of increasing powers of the generally small parameter $d = kT_0/E$, E being an energy associated with the line and T_0 being the temperature at the center of the plasma. The theory is extended to include resonance lines, overlapping lines and multiple broadening mechanisms. A discussion of Bartels' model for the relative source function and competing models (e.g. Cowan and Dieke²) is given. In the regime of large optical depth, where Bartels' theory breaks down, a series solution in inverse powers of the optical depth is presented. The impact of this solution upon the choice of models for the relative source function in a Bartels-type theory is discussed.

¹ H. Bartels, Z. Phys. **125**, 597 (1949); **126**, 108 (1949); **127**, 243 (1950); **128**, 546 (1950).

² R.D. Cowan and Gh. H. Dieke, Rev. Mod. Phys. **209**(2), 418 (1948).

JB-4 Sensitivity Analysis of Lineshape Diagnostics in Optically Thick Plasmas, P.A. VICHARELLI, W.P. LAPATOVICH and C. STRUCK, GTE Laboratories Incorporated, Waltham, MA -- Modern diagnostic methods for finding arc temperature profiles using optically thick lines are usually based on the solution of the radiation transport equation with the aid of some analytic temperature function with adjustable parameters.¹ These parameters are varied until satisfactory agreement is obtained between calculated and observed lineshapes. In this paper we use a modified version of this method to extract radial temperature and number density profiles for a high pressure Hg discharge using the 435.8 nm self-absorbed line. We discuss the sensitivity of the fitted lineshapes to the model parameters and establish uncertainty limits for the extracted information. Our results are compared with a temperature profile determined from optically thin side-on measurements of the 577.0 nm line.

1. H.-P. Stormberg and R. Schafer, J. Quant. Spectrosc. Radiat. Transfer **33**, 27(1985).

JB-5 Model and Diagnostics of the High Pressure Mercury Arc with Sodium and Scandium Iodide Additives,*
R.P. GILLIARD and J.T. DAKIN, General Electric Lighting Business Group and General Electric Corporate Research and Development-- Spectroscopic data from a high-pressure mercury arc with sodium and scandium iodide additives are compared with model calculations. The arc tube is rotated about its own horizontal axis. High-resolution line of sight spectra are recorded for principal spectral features and for a series of offsets from the arc axis. Measurements of arc physical parameters (e.g. temperature and species densities) are extracted from the spectra using standard techniques. The model provides self consistent solutions to the energy, radiation, and chemical transport equations assuming local thermodynamic equilibrium. Direct comparison between the data and the model are made for the high-resolution spectra at various offsets as well as for arc physical parameters.

JB-6 Estimation of the Broadening Constants for the 3S-3P Sodium Resonance Line in a Sodium-Mercury Arc, P. A. REISER and E. F. WYNER, GTE Products Corporation -- In Reference 1, measurements of the D-line radiation from a high pressure sodium lamp were reported and a model developed characterizing this radiation as a function of various lamp parameters and published values of the quasistatic broadening constants C_3 and C_6 . Using Moyre and Pichler's analysis² of alkali resonance radiation in the quasistatic regime, the experimental data have been re-evaluated without reference to a particular value of C_3 or C_6 in an attempt to determine more accurate values for the broadening constants as they apply to high pressure sodium lamps. It was determined that the constraints upon C_3 and C_6 resulting from our measurements, the analysis of the radiation, and the vapor pressure of the Na-Hg amalgam¹ gives an approximately linear relationship between the choices for $\ln(C_3)$ and $\ln(C_6)$.

¹ P. A. Reiser and E. F. Wyner, J. Appl. Phys. 57(5), 1623 (1985).

² M. Moyre and G. Pichler, J. Phys. B 10, 2631 (1977), J. Phys. B 13, 697 (1980).

SESSION KA

10:00 AM - 11:30 AM, Thursday, October 9

Lakeshore Room - Wisconsin Center

MODELING OF TRANSPORT AND KINETICS

Chairperson: J. N. Bardsley, University of Pittsburgh

KA-1 A Novel Method for Solving a Boltzmann Equation, N. Ikuta, A. Takeda and Y. Murakami*, Tokushima U., *NHK, Japan, --Using energy distributions $\Psi_S(\epsilon_0)$ and $\Psi_C(\epsilon')$, just after and just before collisions, a Boltzmann equation for charged particles in hydrodynamic stage under an electric field is written in a simple form as $d\Psi_S(\epsilon_0)/dt = d\Psi_C(\epsilon')/dt = 0$. $\Psi_S(\epsilon_0)$ is obtained by operating $S(\epsilon_0, \epsilon')$ $H(\epsilon', \epsilon_0)$ to an initial energy distribution iteratively. Here, $S(\epsilon_0, \epsilon')$ and $H(\epsilon', \epsilon_0)$ are energy dispersion functions at collision and in flight respectively. Once $\Psi_S(\epsilon_0)$ is determined, the l th order term of usual energy distribution function $F_l(\epsilon)$ and those at collision $\Psi_{Cl}(\epsilon')$ are easily calculated by operating the energy dispersion functions $H_{fl}(\epsilon, \epsilon_0)$ and $H_l(\epsilon', \epsilon_0)$ to $\Psi_S(\epsilon_0)$. Transport coefficients defined in velocity space and in configuration space are calculated easily by $F_l(\epsilon)$ and directly from $\Psi_S(\epsilon_0)$ using transport functions. Distinctive feature of this method is the applicability for systems with heavy anisotropy in the velocity distribution and for those having discontinuities in the collision frequency $\nu(\epsilon)$. This method is also suitable for the analysis of the ion transport. Results for electrons in model gases will be presented.

N. Ikuta and Y. Murakami: J. Phys. Soc. Jpn. submitted.

KA-2 Microwave Transient Conductivity of Electrons in Helium. B. SHIZGAL and S. RANGANATHAN, Univ. of British Columbia - The transient microwave conductivity of electrons in helium calculated recently by Koura (1) with a Monte Carlo simulation method is much slower than that determined experimentally by Warman and de Hass (2). The present work considers an alternate theoretical approach based on the appropriate Fokker-Planck equation. With a quasi-static assumption, the Fokker-Planck equation for an external oscillatory electric field reduces to a form similar to that employed in the calculation of the transient mobility in a steady field (3). The transient conductivity is determined rigorously for the well known e-He momentum transfer cross section with the methods employed previously (3) and good agreement with the experimental results is obtained. The calculated relaxation time for the decay of the conductivity to within 10% of the thermal value, for an initial delta function electron distribution at 0.864 eV with $T=295K$, $P=760$ torr, $E=4.4$ V/cm. and frequency 8.84 GHz, was 54 ns, whereas the experimental value (2) is 50 ns, and the value determined by Koura (1) is 76 ns.

(1) K. Koura, J. Chem. Phys. 84, 6227 (1986).
 (2) J. Warman and M. P. de Hass, J. Chem. Phys. 63, 2094 (1975).
 (3) D. R. A. McMahon and B. Shizgal, Phys. Rev. A31, 1894 (1985).

KA-3 A Diffusion Length Formula Modification Accounting for Particle Reflection and Long Mean Free Paths. P.J. CHANTRY, Westinghouse R&D Center -- In many applications the wall loss of active species produced in the volume of a container may be adequately represented using the container's fundamental mode diffusion length, Λ . However, Λ_0 , the value calculated assuming the species density is zero at the wall, can be seriously in error if the diffusion mean free path, λ_m , is comparable to the dimensions. This constraint on λ_m is more severe when the reflection coefficient, $R > 0$.^m These effects can be accounted for with a boundary condition based on the linear extrapolation length, $\lambda = 2(1+R)\lambda_m/3(1-R)$, whose inverse is the logarithmic gradient of the particle density at the boundary.¹ Application of this approach to spheres, right circular cylinders, and rectangular parallelepipeds reveals a useful scaling variable, $\ell_0 \lambda/\lambda_0^2$, where ℓ_0 is the ratio of container volume to surface area.² For all cases considered the simple approximation $\Lambda = (\Lambda_0 + \ell_0 \lambda)$ gives the modified diffusion length Λ to within 10%.

1. P. J. Chantry, A. V. Phelps and G. J. Schulz, Phys. Rev. 152, 81 (1966).

KA-4 Use of the Proportionality Condition for Simplifying Ambipolar Diffusion Coefficients. G.L. ROGOFF, GTE Laboratories Inc. -- Expressions for ambipolar diffusion coefficients can be simplified significantly¹ if the proportionality relationship holds for the charged particles. A necessary condition has been derived for this to be the case in collisional gas discharge plasmas containing electrons, one type of singly-charged negative ion, and one type of singly-charged positive ion. That condition is

$$\frac{\phi_e}{n_e}(\mu_- D_+ + \mu_+ D_-) - \frac{\phi_-}{n_-}(\mu_e D_+ + \mu_+ D_e) + \frac{\phi_+}{n_+}(\mu_e D_- - \mu_- D_e) = 0,$$

where, for a given species, n is the number density, μ is the (uniform) mobility, D is the (uniform) free diffusion coefficient, and $\phi = [(\text{net local production rate}) - \partial n / \partial t]$. A similar condition has been derived for three-component plasmas containing two types of positive ions. For both cases, simple necessary and sufficient conditions are obtained if the two species of the same charge have equal characteristic energies. In general, the conditions are quite restrictive, both for active discharges (steady-state or time-varying) and afterglows.

¹G.L. Rogoff, J. Phys. D: Appl. Phys. 18, 1533 (1985).

KA-5 Effect of a High Frequency Field on the Diffusion Rate of Electrons in Molecular Nitrogen*. D.F. Hudson, Naval Surface Weapons Center-White Oak and P.H. E. Meijer, Catholic U.-- We have calculated the effect which a high frequency (10 and 24 GHz.) field has on the diffusion rate of electrons in molecular nitrogen. The diffusion rate was computed by first solving the two term expansion of the Boltzmann transport equation using an iterative technique and then evaluating the transport integral. Compared to constant ,dc, field results, our calculations indicate an enhancement of the diffusion rate by 10 - 20 percent in the region 1 -3 Td.Results and possible explanations for the deviations will be presented.

* Supported in part by the Naval Surface Weapons Center Independent Research Fund.

KA-6 Time-dependence of the Atomic Level Populations in a Pulsed, High-Current Hydrogen Discharge*, B. M. Penetrante, E. E. Kunhardt, S. C. Kuo, J. Fuhr and Th. Aschwanden, Weber Research Institute, Polytechnic University -- Knowledge of the time-dependence of the excited-state populations is necessary for the interpretation of both time-integrated and time-resolved line intensity measurements. To obtain these populations, we have solved the time-dependent transition rate equations for the case of a pulsed, high-current, hydrogen discharge. By considering various values for the current rise time, we have been able to establish conditions for which a steady-state modeling of the conduction phase is valid. Furthermore, we have been able to better determine the contribution of the excited states to the properties of the discharge as a function of time and final steady-state current density.

*Work supported by the Defense Nuclear Agency.

SESSION KB

10:00 AM - 11:30 AM, Thursday, October 9

Room 313 - Wisconsin Center

LASER DIAGNOSTICS OF SHEATHS

Chairperson: J. B. Gerardo, Sandia National Laboratory

KB-1 Spectroscopic Studies of the Cathode Fall Region, J. E. LAWLER and D. A. DOUGHTY, Univ. of Wisconsin-Madison*--Laser excitation of a carefully chosen Helium transition is used to release excess ion-electron pairs at a well defined position in the negative glow or cathode fall region. A known fraction of the excited atoms are associatively ionized producing the ion-electron pairs. The simultaneous fluorescence signal provides a calibration of the number of excess ion-electron pairs. The ratio of the optogalvanic signal to fluorescence signal is independent of position in the negative glow and is strongly position dependent in the cathode fall region. This normalized optogalvanic effect provides a measure of the electron avalanche produced by releasing excess electrons at a point in the cathode fall. These measurements and independent measurements of the local electric fields are a direct probe of the non-hydrodynamic behavior of the electrons in the cathode fall region.

*Research supported by the U. S. AFOSR and U. S. ARO under Grant AFOSR 84-0328

KB-2 Measurement of Electric Field Profile in a Glow Discharge Cathode Fall Region, B. N. Ganguly, J. Shoemaker, B. L. Preppernau and A. Garscadden, APL, Wright-Patterson Air Force Base. -- The electric field profile in the cathode fall region of a low pressure helium dc glow discharge has been measured by optogalvanic Rydberg state Stark spectroscopy. The Stark manifold splittings of the triplet atomic helium Rydberg states from $n = 15$ to 20 with $\Delta m_j = 0$ and $\Delta |m_j| = 1$ polarizations have been used to measure the electric field. The accuracy of the electric field measurement from this technique is $\pm 30\text{V/cm}$. The experimental data show that the Stark splittings of higher orbital angular momentum states ($l > 5$) are hydrogenic for spectra of both polarizations and that the spectral intensity distributions of the Stark manifold for only $\Delta |m_j| = 1$ polarization are approximately hydrogenic for $n > 17$ at electric fields $\leq 700\text{V/cm}$. The relative metastable density profile has also been measured by optogalvanic spectroscopy.

KB-3 Stark Spectroscopy of a Double Sheath at a Discharge Constriction, B. N. Ganguly and A. Garscadden, APL, Wright-Patterson Air Force Base. -- In the diffusion controlled glow discharge, the electron temperature and the electron density are functions of the discharge tube radius. At an abrupt change in tube dimensions, in order to satisfy current continuity, a double sheath forms. This sheath region is difficult to examine with probes. We have therefore performed Stark spectroscopy in a helium discharge of the double layer region at the transition from an 18 mm radius to 3 mm radius tube. The method permits measurements of the electric fields and metastable populations in, and adjacent to, the sheath. The results illustrate that the fields increase significantly on both sides of the transition. As there is a transition in the radial component of the discharge field as well as in the axial component, the sheath assumes a meniscus type profile. Rydberg polarization spectroscopy permits tracking of the electric field vector. At transitions from a small radius to a large radius, the experiments show that an extended region of low electric field is created. In contrast to the negative glow, this is a region of reduced excitation.

KB-4 Double Layers, Breathing Sheaths, and Chemistry in BCl_3 /Rare Gas Radio Frequency Discharges, RICHARD A. GOTTSCHO and GEOFFREY R. SCHELLER, AT&T Bell Laboratories -- Using laser-induced fluorescence (LIF) and optical emission spectroscopy, the properties of low frequency (dc to 1 MHz) discharges through mixtures of BCl_3 and He, Ar, or Kr have been investigated. LIF is used to monitor the magnitude of the local electric field in the electrode sheaths and the concentrations of BCl and Ar metastables. Feedstocks with more than 5% BCl_3 exhibit double layers at the plasma-sheath boundary, whose position is nearly invariant during a cycle. The formation of double layers is understood in terms of field-dependent attachment and detachment rates. For discharges containing less BCl_3 , the sheath fields are monotonic but are observed to "breathe" periodically. As a function of Ar and Kr concentration in BCl_3 , the BCl density exhibits a maximum at 80% rare gas. Although, the BCl density decreases monotonically as He is added to the discharge, the decrease is less than what would be expected from simple dilution. By contrast, the Ar $1s_5$ metastable density decreases dramatically when only trace amounts of BCl_3 are added to an Ar discharge. These findings suggest that energy transfer from rare gas metastables is an efficient mechanism for dissociation of BCl_3 .

KB-5 Temporal and Spatial Electric Field Measurements in a 15KHz Glow Discharge, B. L. PREPPERNAU and B. N. GANGULY, APL, Wright-Patterson AFB. -- Using the method of optogalvanic spectroscopy we have measured electric field strengths via the Stark effect on Rydberg states as a function of phase and position in a 15KHz, low pressure, low power Helium glow discharge. The Stark effect is observed for atomic triplet Helium Rydberg states from $n=17$ to 26. The technique does not rely upon an amplitude response as we tune through each optically pumped transition; instead we observe a temporal response in the optogalvanic signal which is analogous to the spectral signal found in DC optogalvanic work. Electric fields on the order of 300 volts/cm have been measured with a resolution of ± 20 v/cm, a spatial accuracy of ± 200 microns, and a temporal accuracy of 2% over 80% of the RF cycle. These low-frequency electric field profile measurements agree with the DC approximation.

SESSION LA

1:00 PM - 4:00 PM, Thursday, October 9

Robert P. Lee Lounge - Wisconsin Center

POSTERS; SPECTROSCOPY

Chairperson: J. E. Lawler, University of Wisconsin-Madison

LA-1 Laser Double Resonance Measurements of the Vibrational Energy Transfer Rates and Mechanisms of DF(v=1,2), J.M. ROBINSON, K.J. RENSBERGER, M.A. MUYSKENS, and F.F. CRIM, U. of Wisconsin --Overtone vibration-laser double resonance measurements determine the self-relaxation rate constants for DF(v=1,2) to be $k_1 = (0.37 \pm 0.03) \times 10^{-12} \text{ cm}^3 \text{ molecule}^{-1} \text{ s}^{-1}$ and $k_2 = (22.0 \pm 0.6) \times 10^{-12} \text{ cm}^3 \text{ molecule}^{-1} \text{ s}^{-1}$, respectively. These experiments show that DF(v=2) relaxes solely by vibration-to-vibration energy transfer; in contrast, the fraction of HF(v=2) molecules that relax by V-V energy transfer is 0.59. The results demonstrate that the magnitude of the energy defects for the available pathways determines the energy transfer mechanism for the relaxation of DF(v=2) and HF(v \geq 2). A comparison of the v=1 rate constants for DF and HF indicates that rotational degrees-of-freedom are the primary receptor modes for the vibration-to-translation, rotation energy transfer process.

LA-2 Studies of Vibrational-Rotational Populations in Nitrogen Discharges Using Crossed-Beam CARS. P. P. YANEY, C. J. EMMERICH and D. D. HODSON, U. of Dayton,* and S. W. KIZIRNIS, USAF Aero Propulsion Lab.-- The narrow-line, scanned CARS technique permits the rotational structure of the vib-rot manifold of the N₂ ground state to be resolved. This feature is used to measure the apparent vibrational and rotational temperatures in low pressure discharges wherein the vibrational temperature typically is high.¹ The crossed-beam scheme permits spatial resolutions of less than 0.001 mm³ while the 10 ns laser pulse provides high temporal resolution in switched and pulsed discharges. The experimental setup which will permit time-resolved measurements is described. The initial studies are being carried out on a dc N₂ positive-column discharge the results of which are reported.

*Supported by USAF Contract F33615-81-C-2012.

¹W.F. Lynn, P.P. Yaney, L.P. Goss and S.W. Kizirnis, Proc. First Intern. Laser Sci. Conf., Nov. 18-22, 1985 (to be published).

LA-3 Collisional Relaxation of DF/HF(v=1) by the DF Dimer through Complex Formation, K.J. RENSBERGER, J.M. ROBINSON and F.F. CRIM, U. of Wisconsin -- Overtone vibration-laser double resonance measurements determine the vibrational relaxation rates of DF(v=1) and HF(v=1) by the DF dimer. Both monomers are efficiently relaxed by the dimer at a rate that is 20% of the gas kinetic rate. The similarity of the rate constants for the two systems which have very different energy defects indicates that the relaxation occurs by collision complex formation and energy redistribution, rather than direct vibration-to-vibration energy transfer from the monomer to the dimer.

LA-4 Magnetically Induced Circular Polarization,* K.L. STRICKLETT, D.J. BURNS, and P.D. BURROW, U. of Nebraska--Helium atoms are aligned by electron impact in a configuration involving an electron beam parallel to a variable magnetic field (120-350 Gauss). The circular polarization of the $3^3D \rightarrow 2^3P$ radiation is examined. Kemp et al.¹ have postulated that alignment of the atoms may be followed by an evolution of the atomic state into an oriented one with finite orbital angular momentum along the magnetic field direction. An induced circular polarization component of the radiation should then be observed. Circular polarization fractions of several per cent are measured and the field strength dependence agrees qualitatively with calculations by Nehring.² The polarization fraction is pressure dependent indicating that collisional energy transfer and cascade must be included to completely describe the effect. This orientation process is of astrophysical interest in the determination of the magnetic fields within sunspots¹ and may have similar application as a plasma diagnostic.

*Supported by NSF.

¹J.C. Kemp, J.H. Macek, and F.W. Nehring, *Astrophys. J.* 278, 863 (1984).

²F.W. Nehring, Ph.D. thesis, U. of NE., Lincoln (1979).

LA-5 Effect of Radiation Trapping on the Polarization of an Optically Pumped Alkali Metal Vapor,*

D. TUPA, L.W. ANDERSON, D.L. HUBER, and J.E. LAWLER, U. of Wisc.--We present rate equations describing the electron spin polarization of an optically pumped alkali metal vapor in a large magnetic field with the presence of radiation trapping. Solving these equations gives the time evolution of the polarization and predicts the limitations imposed by radiation trapping on the polarization. It is found that, with Na densities up to 10^{19} atoms/m³, a ground level relaxation time of 150 μ s, and a cylindrical geometry of radius 7.5×10^{-3} m, polarizations of 90% are possible. An experiment to test such predictions is described.

*Work supported in part by the United States Department of Energy.

SESSION LB

1:00 PM - 4:00 PM, Thursday, October 9

Alumni Lounge - Wisconsin Center

POSTERS; LASERS AND R. F. DISCHARGES

Chairperson: J. E. Lawler, University of Wisconsin-Madison

LB-1 Direct Observation of 157.5 nm "Laser" Photons from the $f^3\Pi_g$ State of F_2 ,* D. SPENCE, H. TANAKA, M. A. DILLON,^g and K. LANIK, ARGONNE NATIONAL LABORATORY

--Since the discovery of lasing action¹ in F_2 , it has long been conjectured (based on analogy with I_2)² that the laser radiation corresponds to a transition from a $^3\Pi_g$ upper level to a $^3\Pi_u$ lower level. Using variable-energy high-resolution electron impact techniques, we have directly observed for the first time 157.5 nm emission from the $f^3\Pi_g$ state of F_2 thus confirming the laser mechanism. Emission at 157.5 nm is also observed from higher lying $^1\Sigma_u^+$ states, but these are optically coupled to the ground state and decay into an energy region containing repulsive states and thus could not give rise to the observed discrete laser spectrum.

*Work supported by the U.S. Dept. of Energy, Office of Health and Environmental Research under Contract W-31-109-Eng-38.

¹J. K. Rice, R. A. K. Hays, and J. R. Woodworth, Appl. Phys. Lett. 31, 31 (1977).

²J. R. Woodworth and J. K. Rice, J. Chem. Phys. 69, 2500 (1978).

LB-2 Lithium Plasma Generation by ArF* Laser,⁺ S. LIN, K. Y. TANG and R. O. HUNTER, Jr., Western Research Corporation -- A new method of generating a high-density lithium plasma was demonstrated in a proof-of-principle experiment. A low energy UV laser was utilized to photoevaporate and ionize the lithium target at the same pulse. The lithium plume blow-off and its footprints are presented. The laser energy density at the target surface is very low, found only at the 200 mJ/cm² level. Laser pulse width is 15 nsec. Various lithium emission lines have been observed by a spectrometer and optical multichannel analyzer system. Data from the Stark-broadened 4603 Å lithium line indicates the existence of a very high density $\geq 10^{17}$ cm⁻³ lithium plasma, which is confined in a very thin layer estimated to be about several mm thick. No hydrogen impurities were observed from the spectroscopic data. Preliminary studies on the time resolved lithium light emission history indicated that the lithium neutral atoms existed in a much longer time scale than the laser pulse.

⁺Work supported by Sandia National Laboratory under contract 65-2278.

LB-3 Laser Diagnostic in Surface Wave Helium Discharge, C. BOISSE-LAPORTE, G. GOUSSET and A. GRANIER, Lab. Phys. Gas and Plasma (Univ. Orsay, France) -- Two diagnostics of excited metastable states $n=2$ ($2^1S, 2^3S, 2^1P, 2^3P$) are performed in pure Helium discharges at low pressure (0.1 to 10 torr in a 5mm tube diameter), sustained by surface wave (2.45GHz, $P < 100W$, length 20cm). First, a method of optical longitudinal absorption technics is used. The light source is delivered by a pulsed dye laser P.A.R. (1.0ns duration). The wavelength of laser line is tuned to one of transitions falling to the $n=2$ He states (587, 389, 668 or 502nm). As the electron density decays from the excitation gap along the surface wave discharge, this measurement gives only the mean value of the $n=2$ population density. Therefore, L.I.F. intensity measurements have been performed perpendicularly to the axis, providing the axial variation of this population. From the L.I.F. results, we find, for example, that the 2^3P density decreases like the electron one. Typically, for a pressure of 1.25 Torr, we obtain $5 \cdot 10^{10} \text{ cm}^{-3}$ for the density of 2^3P level at the excitation gap ($P=40W$, electron density at the gap = $7 \cdot 10^{12} \text{ cm}^{-3}$).

LB-4 Spatially Resolved Emission Profiles of a Parallel Plate Rf Glow Discharge, R. M. ROTH, Amoco Corporation -- An apparatus is described which can acquire, in less than a second, a spectrally resolved, spatial profile of the light emitted from a parallel plate, rf glow discharge. This is achieved by imaging the discharge emission onto the entrance slit of a monochromator with its spatial integrity preserved. Then a spatially resolved image is detected by an optical multichannel detector which is oriented parallel to the entrance slit. Results from argon and nitrogen discharges are presented. In an argon discharge, different emission profiles from neutral states, ionic doublet states, and ionic quartet states are resolved.

LB-5 A Fluid Model of the R. F. Discharge at 13.56 MHz,
D.B. GRAVES, Dept. of Chemical Engineering, Univ. of California --The fluid model presented consists of continuity equations for a single positive ion species and electrons, an equation for the mean electron energy and Poisson's equation for the self-consistent electric field. A parallel plate electrode, one-dimensional geometry is used.

A key part of this work is the numerical method used to solve the highly non-linear and stiff system of equations that make up the model. A spectral-Galerkin method is used to discretize the equations in space and time. This technique involves expanding the unknown functions in terms of a Fourier series in time and finite element basis functions in space. The Fourier series representation assures time-periodic solutions and the finite elements simplify spatial mesh refinement to treat rapidly varying functions at the plasma-sheath boundary.

The model results reveal details of the interaction between the electron current, density profile and mean energy, and the structure of the self-consistent electric field profile throughout the discharge. The structure of the plasma-sheath boundary is emphasized.

LB-6 Diffusion Theory of Surface Wave Produced Plasmas with Ionization from Metastable States, C.M. FERREIRA and A.B. Sá, Centro de Electrodinâmica, Lisbon Tec. U. --Recently developed models¹ of low pressure plasma columns sustained by the propagation of a surface wave (SW) have disregarded stepwise ionization processes in the discharge ionization balance. The theory is currently being extended by taking into account the effects of ionization from metastable states in the case of argon discharges. The basic set of equations now includes the continuity equation for the metastables in addition to the continuity and momentum transfer equations for the electrons and the ions and the SW-field equations previously used. These equations have been solved to determine the spatial distributions of the metastable density, plasma density, and electric field intensity, and the maintaining field at the axis as a function of the operating parameters (angular frequency, ω ; gas pressure, p ; tube radius, a ; mean electron density \bar{n}_e). The maintaining field and the average absorbed power per electron required for the steady state discharge operation are appreciably smaller than predicted when predominant direct ionization is assumed.

¹C.M. Ferreira, J. Phys. D 16, 1673 (1983).

LB-7 Microwave Discharges sustained by Surface Wave in Argon-Oxygen Mixtures C. BOISSE-LAPORTE, P. LEPRINCE, R. DARCHICOURT, J. MAREC, S. PASQUIERS Lab Phys Gaz et Plasma Orsay France -- Macroscopic characteristics as ν (electron-neutral collision frequency), θ (power needed to maintain an electron) and the effective electric field E_{eff} are determined in Ar-O₂ mixtures versus the O₂ percentage at 390MHz. Influence of tube diameter ($d=8$ to 76 mm) and pressure (0.1 to 5 Torr) is studied. In pure argon and oxygen, scaling laws giving the dependence of ν , θ and E_{eff} on the pressure and the tube radius enable to predict the energy balance for various discharge parameters. In Ar-O₂ mixtures, ν (or the absorbed power) is decreasing in a weak ratio of 1.5 as the O₂ percentage is increasing while θ and E_{eff} are strongly increasing, in a ratio of 2 to 200 for θ and 2 to 20 for E_{eff} . Hence, for the same input power the electron density is decreasing. Typically, in a 8 mm tube at 0.5 Torr, ν is about $1.1 \cdot 10^9$ s⁻¹ in pure argon and $7 \cdot 10^8$ s⁻¹ in pure oxygen whereas θ varies from $1.5 \cdot 10^{-12}$ W to $1.5 \cdot 10^{-11}$ W and E_{eff} from 2.5 to 6 V/cm. Due to the O₂ dissociation, ν , θ and E_{eff} are strongly varying as soon as the oxygen is introduced. Discharge kinetics will be further investigated. Such studies will be useful for polymers' surfaces treatment.

LB-8 Standing wave discharge (SWD). Application to ion argon laser, Z. RAKEM*, P. LEPRINCE, J. MAREC and S. SAADA, Lab. Phys. Gaz et Plasma (Univ. Orsay, France) -- Travelling Wave Discharges (TWD) exhibit a decreasing electron density along the column. If the wave is reflected before the end of the column, we obtain a SWD exhibiting a spatially modulated density which the mean value is quite flat. SWD have been studied in Argon plasma at 2.45 GHz in capillary tubes at low pressure (0.5 to 3 torrs). From measurements both of ArI and ArII lines intensities and outside power, we determine the wave components and the characteristics of the discharge as neutral and electron densities, maintaining electric field... We find them modulated with the same spatial period. Equilibrium conditions of SWD are determined and a modelling of wave propagation in such a variable medium is proposed. Under the same conditions, SWD provides a higher electron density than TWD (10^{13} instead of 10^{12} cm⁻³ for $P=73$ W at $p=0.5$ torr). An Argon ion Laser has been built with a SWD structure in a Ar/He mixture. Best efficiency ($\sim 3 \cdot 10^{-5}$) has been obtained for 1:1 mixtures. Enhanced emission of ArII lines is probably due to Penning ionisation.

* H. Commissariat aux Energies Nouvelles-Alger

LB-9 Effects of Alkali-Metal Seeding on the Performance of the CuCl Laser,* S.W. KIM, J.B. ATKINSON and L. KRAUSE, U. of Windsor, Canada -- We have recently reported an extended temperature regime of operation of the CuCl double-pulse laser,¹ and have studied the effects of introducing metallic Na or K into the laser plasma on the performance of the laser². These phenomena have now been investigated further by examining the laser performance when NaCl, KCl or CsCl was mixed with the CuCl. It was found that small admixtures of NaCl increased the pulse energy which remained constant over a temperature range 450°C - 850°C while CsCl addition caused a stable laser discharge to persist beyond 900°C. The effect of NaCl, KCl and CsCl addition on the optimum delay time between the dissociating and pumping discharge pulses was also studied.

* Research supported by the Canadian Department of National Defence.

¹ W. Winiarczyk and L. Krause, Appl. Optics 21, 2659 (1982).

² W. Winiarczyk and L. Krause, Optics Comm. 43, 47 (1982).

SESSION LC

1:00 PM - 4:00 PM, Thursday, October 9

Robert P. Lee Lounge - Wisconsin Center

POSTERS; RECOMBINATION

Chairperson: J. E. Lawler, University of Wisconsin-Madison

LC-1 Detailed Investigation of the Thomson Model of Termolecular Recombination,* E. J. MANSKY and M. R. FLANNERY, School of Physics, Georgia Tech-- The quasi-steady-state rate of ion-ion recombination in a gas M is given by the net downward current in energy space across a band of highly excited bound energy levels of the ion pair (A^+-B^-), including the dissociation neck at zero energy. The contribution to the one-way equilibrium current across this neck that arises from the range $[0-R]$ in internal separation R of the ion pair (A^+-B^-) exhibits a rapid monotonic increase with R, and diverges for large R. Calculations which illustrate this divergence are provided for various ion-gas interactions. Comparison with exact calculations of the net current illustrates the effectiveness of a modern Thomson-style model for equal-mass species.

* Research supported by U. S. Air Force Office of Scientific Research under Grant No. AFOSR-84-0233.

LC-2 Ion-Ion Recombination in SF_6 and in Mixtures of CH_4 and SF_6 , M. C. CORNELL and I. M. LITTLEWOOD, University of Missouri-Rolla.--The ion-ion recombination rate in SF_6 and in mixtures of SF_6 and CH_4 has been studied in gas discharges. The rate constant was determined by analyzing the rising edge of the discharge current pulse. Measurements were made as a function of E/N between 12 and 150 Td, gas pressure between 100 and 600 Torr, and gas mixture composition. The rate was found to decrease with increasing E/N, and to be mixture dependent. However over the pressure range used in the study, no dependence on the total gas pressure was observed. When the rates in mixtures of SF_6 and CH_4 were plotted as a function of an effective ion temperature, T_{eff} , then for $T_{eff} \geq 450^\circ K$, the recombination rate obeyed a simple power law.

LC-3 Ion-Pair Production in Li-Cs Collisions,
S. Y. TANG, D. P. WANG and R. H. NEYNABER, Univ. of
Calif., San Diego and La Jolla Institute. * -- A beam-gas
technique is used to measure absolute and relative
cross sections, Q , for the ion-pair production reaction
 $\text{Li} + \text{Cs} \rightarrow \text{Li}^- + \text{Cs}^+ - 3.27 \text{ eV}$, where the atoms and ions
are in the ground state. The measurements are made
with Li as a projectile over the laboratory energy range
from 1000 to 5500 eV. The data show that Q is a mono-
tonically increasing function of the relative velocity
with values ranging from 0.79 to 9.2 \AA^2 . The Q -curve
can be qualitatively explained by the poor coupling in at
least the first step of a ladder climbing process be-
tween the incoming covalent and outgoing ionic poten-
tials.

* Supported by NSF Grant No. CBT83-10965 and
AFOSR.

LC-4 Contributions of Atom-Atom Collisions in
Weakly-Ionized Argon Plasmas, * C. BRAUN and
J. A. KUNC, U. of Southern California - An analy-
tical solution of a collisional-radiative model,
including both inelastic electron-atom and
atom-atom collisions, for non-equilibrium,
weakly-ionized and steady state argon plasmas
is presented. The model includes three atomic
levels (the ground level, one excited level and
continuum) and assumes a Maxwellian distribu-
tion function for electrons and atoms. Calcula-
tions are made for plasmas with atomic den-
sities from 10^{14} - 10^{20} cm^{-3} , for ionization de-
grees less than 10^4 , electron and atom temper-
atures less than 8,000 K and for different de-
grees of radiation trapping. The results (den-
sities of electrons and excited atoms) clearly
indicate the importance of atom-atom inelastic
collisions in weakly-ionized argon plasmas.

* Work supported by the Air Force Office of
Scientific Research and by the National Science
Foundation.

LC-5 Steady-State Townsend Experiment: Measured and Predicted Electron Swarm Properties of CCl_2F_2 and $\text{CCl}_2\text{F}_2/\text{N}_2$ Mixtures, M.F. Fréchette and J.P. Novak, IREQ, Varennes, Québec, Canada--Spatial growth of ionization currents has been measured in CCl_2F_2 and $\text{CCl}_2\text{F}_2/\text{N}_2$ by the steady-state Townsend method over the range of reduced fields $50 \leq E/p_{20} \leq 200 \text{ Vcm}^{-1}\text{Torr}^{-1}$. Experimental values for pure CCl_2F_2 compare well with those found in the literature while the measured transport coefficients for $\text{CCl}_2\text{F}_2/\text{N}_2$ mixtures differ markedly from those published by Maller.¹ However, the present experimental data, i.e., limit field $(E/p_{20})^*$, ionization (α), attachment (η) and effective ionization ($\bar{\alpha}$) coefficients are in good agreement with our earlier calculated values² obtained from a Boltzmann-equation analysis. This satisfactory comparison provides further supporting evidence for the applicability of the proposed set² of electron scattering cross sections and, in particular, favours the attachment cross sections by Illenberger et al.

¹V.N. Maller, IEEE-IAS Annual Meeting, New York, IAS78:7F (IEEE, New York, 1978).

²J.P. Novak and M.F. Fréchette, J. Appl. Phys. **57**, 4368 (1985).

LC-6 Dissociative Electron Attachment to the Isotopes of Molecular Hydrogen,* J. M. WADEHRA, Wayne State U.--Using a local width model, the cross sections for dissociative electron attachment to rovibrationally excited isotopes (HD, HT, D₂, DT and T₂) of H₂ are obtained. For a given rovibrational level, the factor by which the peak attachment cross section alters on isotope substitution, varies from about 10 to 65000. For a given isotope, the factor by which the peak attachment cross section is altered on exciting the molecule vibrationally from $v=0$ to $v=1$, varies from about 39 to 61. For a given isotope, the factor by which the peak attachment cross section is altered on exciting the molecule rotationally from $J=0$ to $J=10$, varies from about 12 to 6. The reasons for these observations will be given.

*Supported by AFOSR Grant Number 84-0143.

LC-7 Cs Ion - Electron Recombination in the Presence of the Rare Gases. A. T. PRITT, JR. Rockwell International-Science Center -- A pulsed excimer laser operating at 308 nm was used to directly photoionize atomic cesium in the presence of selected rare gases. The laser induced electron density was monitored by recording the transmission of a 35 GHz radiation source through the plasma immediately following the photolysis. First, second, and third order rates were extracted from the transient behavior of the electron density. From plots of these rates vs. species concentration, electron-stabilized and neutral-stabilized, three-body, electron-ion recombination rate constants were determined. The experimental rate constants for neutral-stabilized recombination are compared to model calculations, including a quantum mechanical treatment describing the interaction of the ion and the third body.

LC-8 Dissociative Attachment in the Chloromethanes*, S.C. CHU, K.L. STRICKLETT and P.D. BURROW, U. of Nebraska, Lincoln--The dissociative attachment cross sections for CH_3Cl , CH_2Cl_2 , CHCl_3 and CCl_4 are examined using an electron beam method with particular attention to low energy structure. Each compound displays a sharp peak near zero energy and a broad second peak below one eV. Recent beam studies by Scheunemann et al.¹ report the yield of fragment ions from CCl_4 to be approximately 250 times that of CH_3Cl near zero energy. Our measurements indicate this ratio to be about 800,000:1, in much closer agreement with swarm studies. The energy dependence of the CH_3Cl and CH_2Cl_2 cross sections given by Scheunemann et al. suggest that their apparatus may have been contaminated by CCl_4 .

*This work was supported by NSF.

¹H.-U. Scheunemann, E. Illenberger and H. Baumgaertel, Ber. Bunsenges. Phys. Chem. 84, 580 (1980).

LC-9 Assessment of the He_2^- Potential from the Auto-detachment Spectrum,* Y. K. BAE and J. R. PETERSON, SRI International, and H. H. MICHELS, UTRC--We have measured and analyzed the electron energy spectrum from the spin-forbidden autodetachment of the recently discovered¹ metastable $\text{He}_2^- 4\Pi_g$ ion. The spectrum shows a single-peaked continuum with a maximum at 15.7 eV, resulting from a vertical transition to the repulsive wall of the $\text{He}_2 X^1\Sigma^+$. The spectrum is inconsistent with predictions based on current values of the potentials of the $\text{He}_2^- 4\Pi_g$ and the $\text{He}_2 X^1\Sigma^+$. A separate analysis of the known He_2 singlet continuum² has confirmed the ground-state potential, suggesting an increase in the equilibrium internuclear separation of He_2^- .

*Supported by NSF and AFOSR.

¹Y. K. Bae, M. J. Coggiola, and J. R. Peterson, *Phys. Rev. Lett.* 52, 747 (1984).

²R. E. Huffman, J. C. Larrabee and D. Chambers, *Appl. Opt.* 4, 1145, (1965).

LC-10 Angular and Energy Distributions of Electrons Detached in H^- - He Collisions (50 eV-2keV). F. PENENT, J.P. GROUARD, R.I. HALL and J.L. MONTMAGNON. LPOC* Univ. Paris VI, France -- The energy and angular distributions of electrons detached in H^- - He collisions have been directly measured using an electrostatic analyser. There is now a large discrepancy between these observations and both TOF¹ and theoretical² results. The angular observations indicate that the emitting frame for the detached electrons is the center of mass even at 2keV where the molecular picture of the collision is no longer valid. At small angles sharp structures are observed near electron energies corresponding to the projectile velocity. These are attributed to resonances near the H n=2 state threshold.

*

Associated to the Centre National de la Recherche Scientifique (UA.774).

¹ Vu Ngoc Tuan, J.P. Gauyacq and V.A. Esaulov. *J. Phys. B.* 16, L 95 (1983).

² J.P. Gauyacq. *J. Phys. B.* 13, 4417 (1980).

LC-11 Rate for F⁻ Exchange in SF₆⁻ + SOF₄ Collisions,*
 I. SAUERS, Oak Ridge National Laboratory, L.W. SIECK
 and R.J. VAN BRUNT, National Bureau of Standards,
 M.C. SIDDAGANGAPPA, Indian Institute of Science--The
 temperature (T) and electric field-to-gas pressure
 (E/p) dependences of the rate constant, k, for the
 reaction SF₆⁻ + SOF₄ + SOF₅⁻ + SF₅ have been measured.
 For T < 270 K, k approaches a constant of
 2.1 x 10⁻⁹ cm³/s, and for 433K > T > 270K, k decreases
 with T according to k(cm³/s) = 0.124 exp(-3.3 lnT(K)).
 For E/p < 60 V/cm·Torr, k has a constant value of
 about 2.5 x 10⁻¹⁰ cm³/s, and for 130 V/cm·Torr > E/p >
 60 V/cm·Torr, the rate is approximately given by
 k(cm³/s) ~ 7.0 x 10⁻¹⁰ exp(-0.022 E/p). This reaction
 is shown to be important in controlling the yield of
 SOF₄ from corona discharges in SF₆/O₂, SF₆/N₂, and
 SF₆/Ne gas mixtures containing trace amounts of water
 vapor. Information about the rate constant obtained
 here is used in a computer model that predicts the
 behavior of SOF₄ production in a negative, point-plane
 corona.

*Supported by U.S. Department of Energy

SESSION LD

1:00 PM - 4:00 PM, Thursday, October 9

Alumni Lounge - Wisconsin Center

POSTERS; ION-NEUTRAL COLLISIONS

Chairperson: J. E. Lawler, University of Wisconsin-Madison

LD-1 Ionization of Rydberg Atoms in Thermal Collisions with Polar Molecules,* TOSHIZO SHIRAI,[†] ARGONNE NATIONAL LABORATORY -- Ionization collisions ($A^* + M \rightarrow A^+ + e + M$) between Rydberg atoms (A) and rotationally excited molecules (M) have been investigated within the impulse approximation. Calculations so far reported use the Born approximation for the e - M rotationally inelastic scattering.¹ We have now carried out calculations with use of the Glauber amplitude² for the electron-polar molecule scattering. The new calculations give smaller cross sections for the ionization collisions than the earlier calculations. The plot of the ionization rate against the principal quantum number n now shows a saw-like structure rather than a step-like structure.

*Work supported by the U.S. Dept. of Energy, Office of Health & Environmental Research under Contract W-31-109-Eng-38.

[†]Japan Atomic Energy Research Institute, Japan.

¹M. Matsuzawa and W. A. Chupka, Chem. Phys. Lett. 50, 373 (1977);

²O. Ashihara, I. Shimamura, and K. Takayanagi, J. Phys. Soc. Jpn. 38, 1732 (1975).

LD-2 Thermal-Energy Charge Transfer in Ar-Zn System. Y. TAMIR and R. SHUKER, Ben-Gurion U. of the Negev, Israel -- A thermal-energy charge transfer (T.E.C.T.) process between ground state argon ions and ground-state Zn atoms is observed confirming Chubb's¹ assumption. The emission spectrum of the system in pulsed and C.W. discharges is studied. We found that the T.E.C.T. process ending at the $4p^2P^0_{1/2}$ level of the ZnII is preferred over that ending at the $4p^2P^0_{3/2}$ one. This is in contrast with the direct electron collision excitation which populates the levels according to their (2J+1) multiplicities. The total cross-section of these two T.E.C.T. processes is estimated from the ratio of the relevant emission line intensities and is in the range of $10^{-17} - 10^{-16} \text{ cm}^2$. This is consistent with the value calculated from the modified Landau-Zener model² using isoelectronic molecular energy curves for (Ar-Zn)⁺ system.

¹D. L. Chubb, J. Appl. Phys., 47, 2462 (1976).

²A. R. Turner-Smith, J. M. Green and C. E. Webb, J. Phys. B: Atom. Molec. Phys., 6, 114 (1973).

LD-3 Collisional Processes in XeF(X),[†] G. BLACK, L. E. JUSINSKI, and D. L. HUESTIS, SRI International -- Collision-induced dissociation of XeF(X) has been studied with He, Ne, Ar, Kr, Xe, N₂, SF₆, and XeF₂ as collision partners, giving dissociation rate constants of 0.58, 0.62, 0.76, 0.68, 0.75, 1.13, 1.05, and 7.3(±10%)×10⁻¹² respectively. The values for He and Ne are in agreement with those found previously.^{1,2} Except for XeF₂, there is only a slight dependence on the nature of the collision partner, in line with theoretical expectations. We produce the XeF(X) by photodissociation of XeF₂. By following the approach to association/dissociation equilibrium in Xe, we are able to determine that the yields of bound XeF(X) at 193 and 248 nm are only 0.54% and 0.08% respectively, with fragmentation to give three atoms the dominant pathway. Vibrational relaxation is observed, and studied in detail for collisions with XeF₂, with which it is found to be very fast.

[†]Work supported by ONR.

1. S. F. Fulghum, I. P. Herman, M. S. Feld, and A. Javan, Appl. Phys. Lett. **33**, 926 (1978)
2. S. F. Fulghum, M. S. Feld, and A. Javan, Appl. Phys. Lett. **35**, 249 (1979).

LD-4 Laser-pumped He⁴ as a Spin-dependent Probe of Atomic and Molecular Collisions,* L. D. SCHEARER and C. L. BOHLER, U. of Missouri-Rolla and M. LEDUC, Laboratoire de Spectroscopie Hertzienne, Paris--Spin-polarized He(2³S₁) atoms have been used to probe the symmetry of collisions with atoms and molecules, electrons, and surfaces. To orient the spins of helium metastable atoms, optical pumping with conventional laboratory resonance lamp is used. The relatively low-intensity resonance lamps limit the degree of the polarization that is obtained. Laser sources have a much greater spectral brightness, but until recently tunable lasers at the helium resonance wavelength have not been available. We describe recent advances in the development of such laser sources and their application to the helium optical pumping process. We will also describe our work involving spin-dependent Penning collisions, dissociative excitation, and polarized electron scattering in He beams and afterglows.

*Work supported in part by NATO and the NSF.

LD-5 Reactions of He₂⁺ and He(2³S) with Ne, Ar, Kr, Xe, H₂, N₂, O₂, CO₂, and N₂O at Atmospheric Pressures,* J.M. POUVESLE, A. KHACEF, and J. STEVEFELT, U. of Orléans, France, and V.T. GYLYS, H. JAHANI, and C.B. COLLINS, U. of Texas at Dallas --Results are reported from a continued reexamination of the significance of three-body effects that enhance the reaction rates for non associative energy transfer and ion-molecule reactions in high pressures of inert gas diluent. Two experimental systems were employed, each exploiting the large dynamic range and high data acquisition rates available with preionized pulsed discharge excitation, but using substantially different energy deposition to enhance the ionic and the metastable reactions, respectively. The results for the ion-molecule reactions generally confirm earlier measurements, showing the critical importance of termolecular channels. For the reactions of He(2³S), these channels have been well characterized, and they occur at rates around 10⁶ cm³ s⁻¹.

*Supported in part by NSF Grant ECS.83 146 33 and in part by NATO Grant 655/84.

LD-6 S and P State Excitation During Hard Collisions in the Ar⁺ on Kr System - Metastable Production, K. B. MCAFEE, JR., and R. S. HOZACK, AT&T Bell Laboratories --Hard ion - molecule collisions at intermediate impact energies have been observed to yield a richly detailed momentum and charge transfer spectrum. At large scattering angles during charge transfer reactions of rare gas species, excitation of the products to 4s, 5s, and 6s levels occurs with significant intensity despite an internal energy defect of about 10 eV. Some p-state excitation is also observed. Momentum transfer is the principal energy loss mechanism in intermediate energy impacts, since photon emission is known to occur in less than 10% of the collisions. Under high energy and angular resolution the production of eleven transitions to 4s metastable states of argon has been identified with large cross-section. These metastable states ionize most gaseous species and have had an important impact both from the standpoint of the science of collisional excitation transfer and practically in detection and surge devices, plasmas, sputtering, and ion etching.

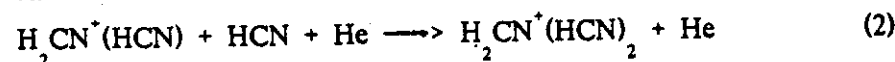
LD-7 Clustering Reactions of H_2CN^+ Ions with HCN*

B. CHATTERJEE AND R. JOHNSEN, University of Pittsburgh --

Rate coefficients for the three-body clustering reactions



and



have been measured in a variable-temperature drift tube apparatus at temperatures from 185K to 300K. We find that the rate coefficients can be expressed by power laws of the form:

$$k_1(T) = (6 \pm 1) (300/T)^{4.0} \times 10^{-28} \text{ cm}^6/\text{sec} \quad \text{and}$$

$$k_2(T) = (6.5 \pm 0.7) (300/T)^{4.4} \times 10^{-28} \text{ cm}^6/\text{sec}$$

*Research supported by NASA.

LD-8 Excitation Mechanisms in keV He^+ - H_2/D_2 Collisions*, C.L. ENGELHARDT and D.H. JAECKS, University of Nebraska-Lincoln--Cross-section measurements have been made for $He(3^3P)$ and $He(3^1P)$ magnetic substate levels resulting from low keV He^+ + H_2/D_2 collisions. In addition, preliminary results of He-photon coincidence measurements for these collisions are presented. The observed isotopic shift and other features are discussed within the quasi-diatomic model, which provides a reasonable extension of ion-atom collision mechanisms to those of ion-molecule collisions.

*Work supported by National Science Foundation.

LD-9 Three-body Reaction of XeCl* to Form Xe₂Cl₂,[‡]

D. C. LORENTS, R. L. SHARPLESS, D. L. HUESTIS, SRI INTERNATIONAL -- Synchrotron measurements of the decay rate of XeCl* and the formation rate of Xe₂Cl₂ in Ne/Xe/Cl₂ and Kr/Xe/Cl₂ mixtures is composed of three components: radiation, two-body quenching and three-body reaction. The measurements at pressures up to 5000 Torr show that the reaction, XeCl* + Xe + Ne → Xe₂Cl₂ + Ne, is not a linear function of the [Xe][Ne] product and therefore is not a simple three body reaction. Measurements at Xe pressures of 50 and 150 Torr and Ne pressures ranging from 0 to 5000 Torr can be fit with the simple pressure dependent three-body rate constant given by $k_p = 7 \times 10^{-31} \frac{[Xe][Ne]}{\{1 + 10^{-20}[Ne]\}}$. This result can be qualitatively understood in terms of the Lindemann mechanism that implies that the reaction proceeds through an intermediate complex that is relatively long-lived.

[‡] Work supported by ONR

LD-10 Dissociation of Diatomic Molecules, PHILIP C. COSBY and HANSPETER HELM, SRI International.^{*} --A new apparatus has been constructed to measure the electron impact dissociation cross sections of small molecules. The molecules are produced in a fast beam by charge transfer of the corresponding molecular ion at several keV energy. Each pair of dissociation fragments is detected in coincidence using a unique detector based on the recent FOM design¹, which allows the intensity, angular distribution, and dissociation energy of the fragments to be simultaneously determined. Initial tests of the detector using fragments produced by photodissociation of H₂⁺ demonstrates rotational resolution of the molecule's initial state from the fragment translational energy spectrum. Recent results on electron impact dissociation of H₂ will be presented.

^{*}Supported by Aero Propulsion Lab, Aeronautical Systems Div., USAF

¹D. P. de Bruijn and J. Los, Rev. Sci. Instrum. 53, 1020 (1982).

LD-11 Total Quenching Cross Sections of Metastable Atoms and Molecules by Mercuric Halides*--J. L. Daniels, University of Wisconsin-Platteville--The total quenching cross sections of thermal beams of Ar, He, and N₂ metastables by HgBr₂, HgCl₂, and HgI₂ have been measured. The metastable beam passes through an oven constructed of glass and stainless steel which contains the saturated vapor of the mercuric halide. The fluorescence of the collision products is monitored from two equal, separate, and contiguous regions of the cell containing the heated halide vapor. An analysis of the ratio of the fluorescence signals as a function of the halide density provides the total quenching cross section. The metastable beam energies range between 45 and 66 meV. The measured cross sections are of the order of 10⁻¹⁵ cm².

*Work performed at the University of Missouri-Rolla.

LD-12 Polarization of the Na 3d→3p and the Na 3p→3s Radiation Induced by the Collisional Excitation of Na by Fast H⁺ and H⁻ Ions, JAMES S. ALLEN, L.W. ANDERSON, CHUN C. LIN, U. of Wisc. --Apparent cross sections have been measured for the excitation of Na from the ground 3s level to the 3p and 3d levels by fast H⁺, H₂⁺, H₃⁺, H⁻, or H⁰ with energies in the range 1-25 keV. The polarization of the Na 3d→3p and the Na 3p→3s radiation induced by the collisional excitation of Na by H⁺ and H⁻ ions with energies in the range 5-25 keV is reported. The polarization of the Na 3d→3p radiation for incident H⁺ ions rises from 0.04 ± 0.02 at 10 keV to 0.12 ± 0.05 at 15 and 20 keV and then decreases to 0.07 ± 0.03 at 24 keV. The polarization of the Na 3d→3p radiation for incident H⁻ ions rises from 0.18 ± 0.04 at 5 keV to 0.24 ± 0.04 at 10 keV and then decreases to 0.13 ± 0.02 at 25 keV. The polarization of the Na 3p→3s radiation is between 0.00 and -0.02 for 5-25 keV incident H⁻ ions and it is between 0.00 and -0.03 for 6-25 keV H⁺ ions.

SESSION LE

1:00 PM - 4:00 PM, Thursday, October 9

Robert P. Lee Lounge - Wisconsin Center

POSTERS; ELECTRON-ATOM/MOLECULE COLLISIONS

Chairperson: J. E. Lawler, University of Wisconsin-Madison

LE-1 Electron-Silene Interactions at 30-500 eV Using a Parameter-Free Energy-Dependent Spherical-Complex-Optical-Potential (SCOP) Model, A. JAIN, Phys. Dept., KSU, Manhattan, KS—We report ab initio calculations on the total (σ_t), elastic, absorption, momentum transfer and differential (DCS) cross sections for e-SiH₄ scattering in the range 20-500 eV. A recently proposed Spherical-Complex-Optical-Potential(SCOP) model approach¹ is adopted, in which the real part consists an exact static, free-electron-gas (FEG) exchange and a parameter-free polarization potentials. The imaginary part is derived from a quasifree-scattering model with Pauli blocking in which the molecular electrons are treated as a free-electron-gas.² This potential is energy-dependent and is a function of static-exchange energy and the polarized target charge density.¹ The absorption cross sections are peaked around 70-80 eV. The absorption effects reduce the DCS significantly. Our σ_t results compare very well with the recent measurements of Sueoka.³

¹A. Jain, Phys. Rev. A34 (in press); *ibid*, J. Chem. Phys. 81, 724 (1984).

²Staszewska et al., J. Phys. B16, L281 (1983).

³O. Sueoka (private communication).

LE-2 Effects of Helium Upon Electron Beam Excitation of N₂⁺ at 391.4 nm and 427.8 nm,* M. L. BRAKE, T. REPETTI, K. PEARCE, R. M. GILGENBACH, R. F. LUCEY JR., AND P. SOJKA[†], U. of Michigan, Ann Arbor, MI 48109 -- Relativistic electron beam interactions with very small ratios of nitrogen to helium (10⁻¹ to 10⁻⁴) have been found to produce extremely large N₂⁺(B²Σ_u⁺ → X²Σ_g⁺) intensities at 391.4 nm and 427.8 nm, compared to line intensities originating from helium. These results occurred in the total pressure regime of 0.1 torr to 500 torr. The pressure scaling results presented here are inconsistent with previously proposed kinetic mechanisms for the N₂⁺ laser pumped by helium. With a simple model of the chemical kinetics, we show that this effect is due to the collisional transfer of energy between excited states of helium atoms and the ground state of N₂⁺.

*Work supported by NSF and AFOSR

[†]Purdue University, West Lafayette, IN 47907

LE-3 The Generalized Oscillator Strength for One-Electron Diatomic Molecules, * M. KIMURA, ARGONNE NATIONAL LABORATORY and RICE UNIVERSITY --The generalized oscillator strength (GOS) is the central property describing the response of an atom or molecule in the scattering of high-energy electrons.¹ However, theoretical study of the GOS for molecular system is scarce in contrast to that for atomic system. Furthermore, study of the molecular GOS involving continuum is virtually untouched. We have conducted a systematic and comprehensive study of the molecular GOS for discrete-discrete and discrete-continuum transitions, for one-electron-diatomic molecular (OEDM) systems for the first time. Although this study of the molecular GOS for OEDM systems may appear somewhat academic because of the present difficulty of a relevant experiment, it is a necessary step toward full elucidation of the molecular GOS in general. We have examined characteristic features of OEDM-GOS's as a function of orientation of molecule, ejected electron energy and internuclear distance.

*Work supported by the U.S. Dept. of Energy, Office of Health & Environmental Research under Contract W-31-109-Eng-38.

¹M. Inokuti, Rev. Mod. Phys. 43, 297 (1971).

LE-4 Dissociation of Etchant Gas Plasma Constituents by Controlled Electron Impact, A.E. TABOR* and K. BECKER, Dept. of Physics, Lehigh University -- Discharges containing molecules such as NF_3 , CF_4 and SF_6 are widely used in the etching of silicon compounds. We have studied the fragmentation of these molecules by controlled electron impact under single collision conditions in a crossed-beam apparatus. The initial work focuses on the formation of fluorine fragments which are the etch-active species. Absolute emission cross sections have been measured from threshold to 500 eV impact energy for various FI and FII lines in the uv and visible range of the spectrum. A comparison of the measured appearance potentials with spectroscopic and thermochemical data provides insight into the dissociation mechanisms. This elucidates the fundamental atomic and molecular processes that occur in the initial break-up of the main plasma constituents. In the case of SF_6 comparisons will be made with data from VUV emission work¹ and time-of-flight studies².

*Recipient of a Sherman-Fairchild Summer Scholarship

1. J.L. Forand et al., Can. J. Phys. 64, 269 (1986)

2. J.J. Corr et al., Bull. Am. Phys. Soc. 31, 961 (1986)

SESSION MA

8:45 AM - 10:15 AM, Friday, October 10

Lakeshore Room - Wisconsin Center

LASER KINETICS

Chairperson: H. T. Powell, Lawrence Livermore National Laboratory

MA-1 Analytical Time-Dependent Treatment of Electron Degradation: Electronic Excitation of N₂ Molecule by Subexcitation Electron in He or Ne Gases, * M. A. DILLON, M. KIMURA[†], and M. INOKUTI, ARGONNE NATIONAL LABORATORY

--The electron degradation spectrum (EDS) is the key element in the description of the elementary processes induced by ionizing radiation. The original study by Spencer and Fano¹ gave a time-independent representation, applicable to the stationary irradiation. However, recent experiments follow the kinetics of formation and decay of excited states in pulse-irradiated gases.² Stimulated by this work, we developed a time-dependent version of the Spencer-Fano equation. The new equation has been applied to model the moderation of subexcitation electrons in He or Ne and the competing formation of the C³Π_u state of N₂ solute. We have tested the sensitivity of the EDS to cross-section data used to derive the EDS.

*Supported by the U.S. Dept. of Energy, Office of Health & Environmental Research, Contract W-31-109-Eng-38.

[†]Rice University, Houston, Texas.

¹L. V. Spencer and U. Fano, Phys. Rev. 93, 1172 (1954).

²R. Cooper et al., J. Phys. Chem. 86, 5093 (1982).

MA-2 Excited-State Lifetime Measurements in Nitrogen at High Pressures, P. BLETZINGER, AF Aeronautical Labs, WPAFB, Ohio, and D. F. GROSJEAN, Systems Research Labs, Dayton, Ohio. -- The long-lived A-triplet state in nitrogen and its energy transfer reactions to other species have been previously investigated extensively at low pressures. We have used a pulsed e-beam to excite nitrogen at atmospheric pressure containing from 2.6 to 65 ppm of NO. The decay of the NO-Gamma bands was measured as a function of NO concentration. Extrapolating to zero added NO, the lifetime of the state transferring its energy to the NO A-state exceeds 6msec at atmospheric pressure, increases as the N₂ pressure is lowered, and is independent of e-beam current. The two main excitation reactions -- electron pumping and cascade resulting from atom-atom recombination -- have been modeled along with the major loss mechanisms. The dependence of the NO Gamma-band intensity and temporal pulse shape on the NO concentration suggests that direct electron excitation dominates. However, the relevant quenching rates predicted from low-pressure data must be reduced considerably in order to obtain agreement between experiment and model predictions. Excitation via a dielectric-barrier discharge at atmospheric pressure has also been investigated.

MA-3 Quenching of NF(b¹Σ) by F₂, IF, and I₂ from 330K to 572K, R. A. YOUNG, R. BOWER, C.L. LIN, and J. BLAUER, Rockwell Intl, Rocketdyne Div. -- The rate coefficient for quenching NF(b¹Σ) by F₂, IF and I₂ has been measured from 330K to 572K in a low pressure flow system. None has a strong temperature dependence. The temperature dependence of the rate coefficient can be fitted by $k = (BT^{1/2}) \exp(-E/RT)$ with $B = 1.0 \times 10^{-12} \text{ cm}^3 \text{ s}^{-1} \text{ K}^{-1}$, $E = 0.39 \text{ kcal mol}^{-1}$, for F₂ and $B = 3.7 \times 10^{-10} \text{ cm}^3 \text{ s}^{-1} \text{ K}^{-1}$, $E = -0.16 \text{ kcal mol}^{-1}$, for IF and $B = 6.4 \times 10^{-12} \text{ cm}^3 \text{ s}^{-1} \text{ K}^{-1}$, and $E = -0.07 \text{ kcal}$ for I₂. This implies that the efficiency of energy transfer from NF(b) to the potential lasing species, IF, would be 7% at 800K. The rate coefficient at 330K is $4.4 \times 10^{-12} \text{ cm}^3 \text{ s}^{-1}$, $1.0 \times 10^{-10} \text{ cm}^3 \text{ s}^{-1}$ and $1.6 \times 10^{-10} \text{ cm}^3 \text{ s}^{-1}$ for F₂, IF, and I₂. NF(b) was made by reaction of argon metatables with NF₂ and its concentration measured by its emission near 528 nm.

MA-4 Criteria for the Transient Generation of Homogeneous Ozone-Synthesis Plasmas,* L.A. ROSOCHA, Los Alamos National Laboratory -- In addition to its use in water purification, ozone gas (O₃) has recently been shown to be an effective saturable absorber¹ at the KrF laser wavelength (248 nm). An O₃ saturable absorber may offer system design advantages such as retro-pulse shutters and long-pulse shaping for KrF ICF drivers (e.g., Aurora² at Los Alamos). O₃ can be produced by chemical reaction, electrical discharges, or electron beams. Discharge and e-beam production both offer the possibility of in-situ production, with discharges offering the added advantage of easily separating the electronic phase (O₂ dissociation) from the formation phase. Calculated values are presented for the necessary voltage rise times and preionization electron densities that are required for the initiation of homogeneous discharge plasmas in pure O₂. These values depend on the electronic and transport properties of the gas and the gas pressure.

*Work performed under the auspices of USDOE.

¹S. J. Thomas and I. J. Bigio, Proc. IQEC, June 1986.

²L.A. Rosocha et al, Laser and Particle Beams 4, 55 (1986).

MA-5 Pump Rate Dependence of Rare-Gas Halide Excimer Laser Efficiencies Using Self-Sustained Discharge Pumping of Ne Diluent Mixtures, M. OHWA and M. OBARA, Keio U. -- Of all the rare-gas halide excimer lasers using self-sustained discharge pumping, KrF* laser is the most powerful and efficient especially in case of the resonant-charge-transfer type discharge pumping. We have developed a computer model for a self-sustained discharge KrF* laser of Ne/Kr/F2 laser mixtures and compared it with available experimental data to obtain close agreement between experimental values and calculated results. The model has allowed us to predict pump rate dependence of the KrF* laser efficiency. It is found that for a 4-atm mixture of 98.6% Ne/1.3% Kr/0.1% F2 a pump rate of more than 1.5 MW/cm³ is essential to high-efficiency operation of the KrF* laser, which is so high pump rate that it is not so easy to maintain large volume glow discharge. A discussion of high-efficiency operational conditions of the KrF* laser in comparison with those of the XeCl* and ArF* lasers will also be presented.

MA-6 Non-Uniform Optical Extraction as a Source of Discharge Instability in E-Beam Sustained Discharge Excimer Lasers,* Mark J. Kushner †, Spectra Technology Inc. -- E-Beam Sustained Discharge (EBSD) excimer lasers pumped at levels exceeding 100-200 kW/cm² will operate stably for only short pulse lengths (< 1 μs). Current instabilities resulting from multistep ionization, and discharge constriction resulting from non-uniform e-beam pumping prematurely terminate laser oscillation. With results from a multi-dimensional model for an EBSD KrF laser [1], another aspect of discharge instability will be discussed; non-uniform laser extraction. Due to photo-detachment of electrons from F⁻, non-uniform laser extraction creates local regions of high conductivity which, having sharp corners, results in local enhancement of the electric field. Such local enhancement, if aligned along the bulk electric field, will propagate and can initiate an arc.

* Work supported by Los Alamos National Laboratory, Contract No. 9-X65-W1478-1

† Present address: University of Illinois, 607 E. Healey, Champaign, Illinois 61820

1. M. J. Kushner and A. L. Pindroh, to be published in J. Appl. Phys. (August 1986)

SESSION MB

8:45 AM - 10:15 AM, Friday, October 10

Room 313 - Wisconsin Center

PLASMA CHEMISTRY

Chairperson: C. Zarowin, Perkin-Elmer Corporation

MB-1 Plasma Chemistry in Metal Etching, D. W. Hess, Univ. of California, Berkeley -- As metal pattern sizes shrink toward 1 μm , dry etching processes are required for microelectronic device fabrication. The etching or patterning of these films in glow discharges is dependent upon the reaction of halogen atoms and/or molecules with the metal film. Unfortunately, such processes are complicated by the high reactivity of metal surfaces with oxygen and water vapor. Therefore, an etch gas must be capable of removing the native oxide coating, scavenging oxygenated species in the gas phase, and etching the metal film. Comparison of plasma etch studies with atom and molecule reactions on metal surfaces downstream of a discharge can generate insight into important chemical reactions during etching. Examples of such studies for aluminum etching in chlorine- and bromine-containing plasmas will be discussed. Preliminary investigations of tungsten and tungsten silicide etching using chlorine- and fluorine-containing plasmas will also be described.

MB-2 Reactions Leading to the Formation of Large Clusters in SiH_4/Ar RF Plasmas. * Mark J. Kushner †, Spectra Technology Inc. -- Plasma deposition of amorphous silicon (a-Si:H) is performed with RF glow discharges in gas mixtures containing silane (SiH_4) and/or disilane (Si_2H_6). Interesting deposition rates (≥ 1000 Å/min) can be obtained with high pressures of silane (≥ 0.5 Torr) and high power deposition (> 100 mW/cm²). These conditions, though, often lead to formation of gas phase particulates. A validated RF discharge, plasma chemistry, and surface deposition model [1] is used to examine the important reactions and conditions which lead to the formation of large clusters and particulates in SiH_4/Ar RF discharges. The size and rate of formation of clusters are discussed for polymerization chains initiated by reactions of Si_nH_m ($n \geq 2$) molecules with SiH_m radicals, Si_nH_m radicals, and by sputtering from surfaces.

* Work supported by Army Research Office, Contract No. DAAG29-85-C-0031

† Present address: University of Illinois, 607 E. Healey, Champaign, Illinois 61820

1. M. J. Kushner, Plasma Processing Symposium, Materials Research Society Spring Meeting, Palo Alto, CA 1986.

MB-3 The Surface of Growing Hydrogenated Amorphous Silicon Films, J. R. Doyle, G. H. Lin, M. Z. He and A. Gallagher,* JILA, Univ. of Colo. and NBS. — The species on the surface of freshly-deposited hydrogenated amorphous silicon (a-Si:H) films are studied by argon sputtering and mass-spectrometer detection of the sputtered neutral molecules. The results show that the Si atoms with multiple H bonds form about one monolayer for deposition on a room-temperature cathode of a silane dc discharge, while they form slightly more than one monolayer for an rf discharge film. However, at the 240°C substrate temperature typical of film production, the density of these hydrogen-enriched molecules decreases to about one tenth of a monolayer for the films prepared by either method. The dynamics of discharge deposition and Ar sputtering are briefly discussed, based on three processes: film deposition, ion sputtering and surface self organization.

*Staff Member, Quantum Physics Division, National Bureau of Standards.

MB-4 Oxygen Species in Ne-O₂ and Ar-O₂ rf Sputter Deposition Discharges and Their Effect on Pt-O Alloy Film Growth,* Carolyn Rubin Aita, Materials Department and Laboratory for Surface Studies, U. Wisconsin-Milwaukee, P.O. Box 784, Milwaukee, WI 53201: Ne-O₂ and Ar-O₂ rf (13.56MHz) sputter deposition discharges were previously studied using optical emission spectroscopy. For the same nominal O₂ content in the sputtering gas, oxygen species (O, O₂⁺) in Ne exist in more highly excited states than in Ar. Pt-O alloy film formation by sputter deposition from a Pt target in Ne-O₂ and Ar-O₂ discharges is discussed in terms of these findings. Pt target surface oxidation appears to be the factor that controls Pt-O bond formation in the film. Direct evidence of PtO molecules in the negative glow was found using glow discharge mass spectrometry.

*Work partially supported under U.S. ARO Grant No. DAAG29-84-0126.

1. C.R. Aita and M.E. Marhic, J. Appl. Phys. 52, 6584 (1981); J. Vac. Sci. Technol. A 1, 69 (1983).

SESSION N

10:30 AM - 11:40 AM, Friday, October 10

Lakeshore Room - Wisconsin Center

RECENT DEVELOPMENTS IN EXCIMER KINETICS

Chairperson: J. J. Ewing, Mathematical Sciences Northwest Inc.

N-1 Electron Density Measurements of XeCl, XeF and KrF Laser Mixtures,* W.D. KIMURA, D.R. GUYER, S.E. MOODY, J.F. SEAMANS, AND D.H. FORD, Spectra Technology, Inc., -- Time-dependent electron density measurements of e-beam pumped XeCl, XeF and KrF laser mixtures (nonlasing) are performed using a CO₂ (10.6 μm) interferometer with a quadrature detector system. The electron beam pulse length is <0.6 μsec, and the current density at the foil is >10 A/cm². For a 0.16% HCl/0.5% Xe/99.3% Ne mixture at 3000 torr, the electron density, n_e, peaks near the beginning of the pulse at ~7 x 10¹⁴ cm⁻³, decreases to 3 x 10¹⁴ cm⁻³, then gradually increases to ~6 x 10¹⁴ cm⁻³ at the end of the pulse. The XeF and KrF mixtures do not display this peak in n_e at the beginning of the pulse and tend to have lower electron densities. As the halogen density is decreased and/or "burns up", n_e increases dramatically, reaching >10¹⁵ cm⁻³.

*Work supported by the Office of Naval Research, Contract No. N00014-85-C-0843, and Los Alamos National Laboratory, Contract No. 9-X65-W1478-1.

N-2 Model Comparisons of Electron Density Measurements in KrF, XeF, and XeCl,* E.T. SALESKY, North East Research Associates, and W.D. KIMURA, Spectra Technology, Inc., -- Code predictions are compared with recent electron density measurements [1] of e-beam pumped excimer laser mixtures. The code uses a Boltzmann transport solution for the secondary electron processes. It is found that a non-zero local electric field (E/N ~ 1-2 Td) is necessary in order to predict the measured electron densities. Even with a non-zero E/N, the code still slightly underpredicts the electron density. The electron density measurements were performed under nonlasing conditions, the code predicts higher electron densities during lasing as a result of metastable photoionization [2].

* Work supported by the Office of Naval Research, Contract No. N00014-85-C-0843, and Los Alamos National Laboratory, Contract No. 9-X65-W1478-1.

1. W.D. Kimura, D.R. Guyer, S.E. Moody, J.F. Seamans, and D.H. Ford, 39th Gaseous Electronics Conference, Madison, WI, 1986.
2. E.T. Salesky and S. Singer, 38th Gaseous Electronics Conference, Monterey, CA, 1985.

N-3 Implication of Attachment Rates on KrF Laser Performance In Light of Recent Measurements of Electron Density.* Mark J. Kushner †, Spectra Technology Inc.

-- Measured rate constants for dissociative attachment of electrons to F_2 and those used in models for KrF e-beam pumped lasers vary by as much as an order of magnitude. These models, though, are all validated; that is, they reproduce experimentally measured laser characteristics. The rates of e-beam power deposition and electron attachment largely determine the electron density, implying that models using different rates of attachment yield different electron densities. Recent measurements of electron densities in an e-beam pumped KrF laser are now available with which to further validate models [1]. The implication of varying the rate of attachment and its effect on laser performance is discussed in light of these measurements. Sources of agreement and discrepancy between models will be presented.

* Work supported by Los Alamos National Laboratory.
Contract No. 9-X65-W1478-1

† Present address: University of Illinois, 607 E. Healey,
Champaign, Illinois 61820

1. W. D. Kimura, D. R. Guyer, S. E. Moody, J. F. Seamans, and D. H. Ford, 39th Gaseous Electronics Conference, Madison, WI 1986.

N-4 Current Understanding of the XeCl Laser,
D. L. HUESTIS, SRI International-- Rare gas halide excimer lasers are now eleven years old. Their development has required the investigation of a unique combination of electrical, chemical, and optical processes. Nevertheless, numerous surprises await us. We will review the present state of misunderstanding of kinetic processes in XeCl lasers. The laser works well, yet there is almost no aspect of its kinetics and spectroscopy about which we can feel comfortable.

INDEX OF AUTHORS

A

ABAYARATHNA, S., DA-3
 AITA, C.R., FA-7, MB-4
 AJELLO, J.M., GA-1
 ALLEN, G., EB-7
 ALLEN, J.S., BA-5, LD-12
 ANDERSON, L.W., AA-2, BA-5, GA-4
 LA-5, LD-12
 APRUZESE, J.P., EA-7
 ARAI, T., FC-9
 ASCHWANDEN, TH., FC-10, KA-6
 ASMUSSEN, J., FB-4
 ATKINSON, J.B., LB-9
 AYYASWAMY, P.S., HB-4

B

BAE, Y.K., HA-1, LC-9
 BARDSLEY, J.N., CA-3
 BARTNIKAS, R., BB-6
 BEARD, J., DB-5
 BECKER, K., LE-4
 BEDERSON, B., JA-2, JA-5
 BEELER, R.G., DB-5
 BENSON, T.P., EA-5
 BERNSTEIN, E.M., EB-4
 BHATTACHARYA, A.K., EA-5, FC-4
 BIES, W.D., DB-6
 BIONDI, M.A., CA-2
 BLACK, G., LD-3
 BLAIR, R.J., CB-6
 BLAUER, J., MA-3
 BLETZINGER, P., DB-2, MA-2
 BLUMBERG, W.A.M., AA-5
 BOHLER, C.L., DA-3, LD-4
 BOISSE-LAPORTE, C., LB-3, LB-7
 BOWER, R., MA-3
 BRAKE, M.L., FB-4, LE-2
 BRAUN, C., LC-4
 BURNS, D.J., LA-4
 BURROW, P.D., LA-4, LC-8

C

CALEDONIA, G.E., DA-5
 CARTWRIGHT, D.C., JA-4
 CASTAGNA, T., FA-5
 CHANTRY, P.J., DA-4, KA-3
 CHATTERJEE, B., LD-7
 CHEN, C.L., DA-4
 CHEN, H.L., DB-5
 CHEN, D., GA-8
 CHO, K.Y., EA-4
 CHO, M.H., AB-1, FB-6, GC-5, GC-7

CHRISTOPHOROU, L.G., CA-5, CA-7
 CHU, S.C., LC-8
 CHUANG, T.J., FA-4
 CHUNG, S., GA-3
 COHEN, I.M., HB-4
 COLLINS, C.B., FC-1, LD-5
 COLLINS, G.J., AB-6, CB-3
 CONRAD, J.R., FA-5
 CORNELL, M.C., LC-2
 COSBY, P.C., LD-10
 CRAM, L.E., EA-1
 CREASY, W.R., DA-7
 CRIM, F.F., LA-1, LA-3
 CSANAK, GY., JA-4

D

DAKIN, J.T., HA-4, JB-5
 DANIELS, J.L., LD-11
 DARCHICOURT, R., LB-7
 DATSKOS, P.G., CA-7
 DAVANLOO, F., FC-1
 DAVIES, A.J., GB-7
 DAVIS, J., EA-7
 De GROOT, J.J., DB-5, JB-2
 DEN HARTOG, E.A., HA-4, HA-5
 DICKINSON, J.S., CA-8, CA-9
 DILLON, M.A., GA-9, LB-1, MA-1
 DOERING, J.P., JA-3
 DOUGHTY, D.A., KB-1
 DOWNES, L.W., FC-7
 DOYLE, J.R., MB-3
 DRUMMEY, J.P., FB-5
 DULANEY, J.L., CA-2
 DULLNI, E., EA-8
 DUQUETTE, D.W., HA-5
 DURRANI, S.M.A., DB-7
 DUSTON, D., EA-7
 DUTTON, J., GB-7, HB-1

E

ECKSTROM, D.J., CA-8, CA-9
 EDDY, T.L., EA-2, EA-3, EA-4
 EMMERICH, C.J., LA-2
 EMMERT, G.A., GC-1
 ENGELHARDT, C.L., LD-8
 ERNIE, D.W., CB-5, GC-2
 ESKIN, L.D., GC-3

F

FARMER, A.J.D., EA-1
 FEHRING, E., DB-5
 FERREIRA, C.M., GA-10, LB-6

FEUERSANGER, A.E., FB-5
FILIPELLI, A.R., GA-6
FLANNERY, M.R., BA-2, LC-1
FLEMMING, M.J., DB-2
FORAND, J.L., AA-4
FORD, D.H., N-1
FOREST, C., FB-6
FRECHETTE, M.F., HB-6, LC-5
FUHR, J., FC-10, KA-6

G

GABRIELE, P., DB-5
GAEBE, C.E., FB-2
GALLAGHER, A., JA-1, MB-3
GALLUP, G.A., GA-8
GANGULY, B.N., KB-2, KB-3, KB-5
GARSCADDEN, A., BA-4, KB-2, KB-3
GASTINEAU, J.E., GA-4
GELLERT, B., EA-8
GENTRY, W.R., BA-1
GERARDO, J.B., BB-2
GILGENBACH, R.M., LE-2
GILLIARD, R.P., JB-5
GISLASON, E.A., BA-3
GODYAK, V., CB-4
GOHIL, P., EB-4
GOTO, T., FC-9
GOTTSCHO, R.A., FB-2, KB-4
GOUSSET, G., FC-6, LB-3
GOYETTE, G., GC-4
GRAHAM, W.G., EB-4
GRANIER, A., LB-3
GRAVES, D.B., LB-5
GREEN, B.D., AA-5
GREEN W.B., FC-3
GROSJEAN, D.F., MA-2
GROUARD, J.P., LC-10
GULCICEK, E.E., JA-3
GUYER, D.R., N-1
GYLYS, V.T., LD-5

H

HAALAND, P.D., BA-4
HADDAD, G.N., EA-1
HAKHAM-ITZHAQ, M., FB-3
HALL, D.R., DB-7
HALL, R.I., LC-10
HAMMOND, P., AA-3, GA-2
HAN, X.L., JA-1
HARGIS, Jr., P.J., EB-5
HAUCK, J.P., CB-6
HAYES, T.R., FB-2
HAYS, G.N., BB-2

HE, M.Z., MB-3
HEBNER, G.A., DB-4
HEDDLE, D.W.O., AA-1
HEIDEMAN, H.G.M., GA-7
HELM, H.H., CA-4, GB-6, LD-10
HERSHKOWITZ, N., AB-1, FB-6, GC-7
HESS, D.W., MB-1
HITCHON, W.N.G., FA-6
HLAHOL, P.G., FC-4
HODGES, R.V., GB-5
HODSON, D.D., LA-2
HOPWOOD, J., FB-4
HOWALD, A.M., BA-5
HOZACK, R.S., LD-6
HUBER, D.L., LA-5
HUDSON, D.F., KA-5
HUESTIS, D.L., HA-3, LD-3, LD-9, N-4
HUNTER, Jr., R.O., LB-2
HUNTER, S.R., CA-5, CA-6
HUTCHISON, S.B., FA-1

I

IIJIMA, T., FC-9
IKUTA, N., GB-2, GB-3, KA-1
INOKUTI, M., MA-1
INTRATOR, T., AB-1, FB-6, GC-5, GC-7

J

JAECKS, D.H., LD-8
JAFFE, S.M., CA-1
JAHANI, H., LD-5
JAIN, A., GA-12, LE-1
JELENKOVIC, B.M., BB-1
JOHNSEN, R., CA-2, LD-7
JUSINSKI, L.E., LD-3

K

KEEFFE, W., EB-7
KHACEF, A., LD-5
KHAKOO, M.A., AA-3
KIM, S.W., LB-9
KIMURA, M., LE-3, MA-1
KIMURA, W.D., N-1, N-2
KIZIRNIS, S.W., LA-2
KLINE, L.E., DB-6
KNUDTSON, J.T., FC-3
KO, S.T., HB-2
KRAUSE, L., LB-9
KUBINEC, M., FB-4
KUNC, J.A., LC-4
KUNHARDT, E.E., BB-3, BB-4, FC-10
KA-6

KUNKEL, W.B., EB-4
KUO, S.C., FC-10, KA-6
KUSHNER, M.J., MA-6, MB-2, N-3

L

LAGUSHENKO, R., CB-4, EB-7
LAKDAWALA, V.K., HB-2
LANIK, K., LB-1
LAPATOVICH, W.P., JB-4
LAWLER, J.E., HA-4, HA-5, KB-1
LA-5

LEDUC, M., LD-4
LEE, E.T.P., GA-3
LEE, L.C., FA-4, HB-3
LEE, S.-P., FB-1
LEPRINCE, P., LB-7, LB-8
LEUNG, K.N., EB-4
LI, Y.M., BB-2, CB-3
LIGTENBERG, R.C.G., HA-6
LIN, C.C., AA-2, BA-5, GA-3, GA-4,
GA-5, GA-6, LD-12
LIN, C.L., MA-3
LIN, G.H., MB-3
LIN, S., LB-2

LITTLEWOOD, I.M., DA-3, LC-2
LIU, C.S., DA-4
LORENTS, D.C., CA-4, LD-9
LOUREIRO, J., GA-10
LOWKE, J.J., EA-1
LUCAS, A.K., HB-1
LUCEY, Jr., R.F., LE-2

M

MALEKI, L., EB-3
MANSKY, E.J., LB-1
MARCUM, S.D., FC-7
MAREC, J., LB-7, LB-8
MARINELLI, W.J., AA-5, BB-6
MARSDEN, G., HA-4
MAYA, J., CB-4, EB-7
McAFEE, Jr., K.B., LD-6
McCONKEY, A.G., GA-2
McCONKEY, J.W., AA-3, AA-4, GA-2
McCOY, L.E., GB-5
McELVANY, S.W., DA-6
MEIJER, P.H.E., KA-5
MENTEL, J., EA-6
METZE, A., CB-5
MEYER, J., AB-6, CB-3
MICHELS, H.H., HA-2, LC-9
MIERS, R.E., BA-5
MILLER, T.A., EB-1
MITCHELL, M.J., FA-4

MITCHNER, M., CA-1
MONTMAGNON, J.L., LC-10
MOODY, S.E., N-1
MORATZ, T.J., AB-5
MOSKOWITZ, P., EB-6
MURAKAMI, Y., KA-1
MUYSKENS, M.A., LA-1

N

NACHMAN, M., GC-4
NEYNABER, R.H., LC-3
NIHIRA, K., FC-9
NOVAK, J.P., BB-5, HB-6, LC-5

O

OBARA, M., MA-5
OHWA, M., MA-5
OKA, T., EB-2
O'KEEFE, A., DA-6, DA-7
OSKAM, H.J., CB-5, GC-2
OVERZET, L., FC-5

P

PAI, R., CB-4
PAN, F.-S., EB-2
PANAFIEU, P., FC-6
PARLANT, G., BA-3
PARTLOW, W.D., DB-6
PASQUIERS, S., LB-7
PEARCE, K., LE-2
PENENT, F., LC-10
PENETRANTE, B.M., BB-3, BB-4,
CA-3, FC-10, KA-6
PETERSON, J.R., HA-1, HA-2, LC-9
PEYRAUD, N., CB-1
PHELPS, A.V., BB-1, DA-2, GB-4
PINNADUWAGE, L.A., CA-5
PIPER, L.G., BB-6, DA-5
PITCHFORD, L.C., BB-2
POINTU, A.M., FB-7, GC-6
POUVESLE, J.M., LD-5
POWERS, T.J., HB-2
PREPPERNAU, B.L., KB-2, KB-5
PRITT, JR., A.T., LC-7
PUECH, V., GA-11

R

RAKEM, Z., LB-8
RALL, D.L.A., AA-2, GA-6
RAMAKRISHNA, K., HB-4
RANEA-SANDOVAL, H.F., CB-2

RANGANATHAN, S., KA-2
RECK, G.P., FB-1
REESOR, N., CB-2
REGISTER, D., JA-4
REISER, P.A., JB-3, JB-6
RENSBERGER, K.J., LA-1, LA-3
REPETTI, T., LE-2
RICARD, A., FA-3
RICHARDSON, W., EB-3
RIEMANN, K.U., AB-3, GB-1
RILEY, J.F., GB-5
RISLEY, J.S., HA-6
ROBERTS, V., HA-4
ROBINSON, J.M., LA-1, LA-3
ROCCA, J.J., CB-2
ROGOFF, G.L., AB-7, FB-5, KA-4
ROSOCHA, L.A., MA-4
ROSSI, M.J., CA-4, GB-6
ROTH, R.M., LB-4
ROTHER, E.W., FB-1
ROTHWELL, Jr., H.L., FB-5

S

SÁ, A.B., LB-6
SAADA, S., LB-8
SALESKY, E.T., N-2
SANDERS, L., DA-1
SAPOROSCHENKO, M., GB-6
SAUERS, I., HB-7, LB-11
SAVAS, S.E., AB-4, DB-3
SCHADE, E., EA-8
SCHAPPE, R.S., GA-5
SCHEARER, L.D., DA-3, LD-4
SCHELLER, G.R., KB-4
SCHEUER, J.T., GC-1
SCHINN, G.W., JA-1
SCHLACHTER, A.S., EB-4
SCHLEJEN, J., JB-2
SCHOENBACH, K.H., HB-2
SCHULMAN, M.B., AA-2, GA-5
SCOTT, D.A., GB-4
SEAMANS, J.F., N-1
SEDGHINASAB, A., EA-3
SELF, S.A., CA-1, GC-3
SHARPLESS, R.L., LD-9
SHARPTON, F.A., AA-2, GA-5, GA-6
SHEMANSKY, D.E., GA-1
SHEN, G.F., JA-2, JA-5
SHI, B., AB-6
SHIRAI, T., LD-1
SHIZGAL, B., KA-2
SHOEMAKER, J., KB-2
SHUKER, R., FB-3, FC-2, LD-2
SIDDAGANGAPPA, M.C., HB-5, LC-11

SIECK, L.W., LC-11
SIELKER, R., EA-6
SOJKA, P., LE-2
SPENCE, D., GA-9, LB-1
SPENCER, M.N., CA-8, CA-9
STEARNS, J.W., EB-4
STEEFELT, J., LD-5
STEVENS, R., EB-4
STRICKLETT, K.L., LA-4, LC-8
STRUCK, C., JB-4
STUMPF, B., JA-2, JA-5
STUTZIN, G., EB-4
SUTO, M., FA-4
SUTTON, D.G., FC-3
SZAPIRO, B., CB-2

T

TABOR, A.E., LE-4
TAKEDA, A., GB-3, KA-1
TAMIR, Y., FC-2, LD-2
TANAKA, H., GA-9, LB-1
TANG, K.Y., LB-2
TANG, S.Y., LC-3
TONKYN, R., DA-1
TORCHIN, L., GA-11
TOUPS, M.F., GC-2
TOUZEAU, M., FC-6
TRAJMAR, S., JA-4
TUPA, D., LA-5
TURRI, R., GB-7

V

VAN BRUNT, R.J., HB-5, LC-11
VAN DER BURGT, P.J.M., GA-7, HA-6,
VAN ECK J., GA-7
VAUGHAN, S.O., JA-3
VERDEYEN, J.T., BB-1, BB-2, DB-4, FC-5
VIALLE, M., FC-6
VICHARELLI, P.A., JB-3, JB-4
VIDAUD, P., DB-7
VON DADELSZEN, M., AB-2
VÚSKOVIĆ, L., JA-2, JA-5

W

WADEHRA, J.M., LC-6
WALKER, K.G., GA-4
WANG, D.P., LC-3
WANG, E.Y., AB-1, FB-6, GC-5, GC-7
WANG, W.C., HB-3
WATERS, R.T., GB-7
WEDDING, A.B., DA-2
WEISSHAAR, J.C., DA-1

WELLS, W.E., FC-7
WERNSMAN, B., CB-2
WESTERVELD, W.B., HA-6
WHARMBY, D.O., JB-1
WILLIAMS, A.W., HB-1
WINANS, J.G., FC-8
WOERDMAN, J.P., JB-2
WOOLDRIDGE, J., DB-5
WOOLSEY, J.M., AA-4
WORMHOUDT, J., FA-2
WORTH, G., EB-4
WU, C., BB-3, BB-4
WYNER, E.F., JB-6

Y

YAMAMOTO, K., GB-2
YANEY, P.P., LA-2
YANG, Z., CB-3
YOUNG, R.A., MA-3
YU, Z., AB-6, CB-3

Z

ZAROWIN, C.B., DB-1
ZELLER, P., FB-7
ZUO, M., JA-2, JA-5

Thirty-Ninth Annual Gaseous Electronics Conference

October 6-10, 1986

University of Wisconsin-Madison

Monday, October 6

6:00 - 8:00 Reception and registration Wisconsin Center

Tuesday, October 7

8:00 - 9:50 AA Electron-Atom/Molecule Collisions I (R. M. St. John)..... Lakeshore Room
8:00 - 9:50 AB Sheaths: Theory and Experiment (T. Benson)..... Room 313
10:10 - 11:50 BA Ion-Neutral Collisions (W. A. M. Blumberg)..... Lakeshore Room
10:10 - 11:50 BB Transient Discharge Phenomena (J. Dutton)..... Room 313

1:00 - 2:50 CA Electron Recombination and Attachment (R. S. Freund)..... Lakeshore Room
1:00 - 2:50 CB D.C. Glows (G. L. Rogoff)..... Room 313
3:10 - 5:00 DA Heavy Particle Collisions and Clusters (J. P. Doering)..... Lakeshore Room
3:10 - 5:00 DB R.F. Glows (D. Graves)..... Room 313

7:30 - 8:30 Popular lecture - Geysers (L. W. Anderson) 1300 Sterling

Wednesday, October 8

8:00 - 10:00 EA Radiation Transport in Arcs (P. A. Vicharelli)..... Lakeshore Room
8:00 - 10:00 EB Laser Diagnostic Techniques (B. Ganguly)..... Room 313

10:30 - 3:45 FA Posters: Processing (J. Ingold)..... Robert P. Lee Lounge
FB Posters: Diagnostics (S. Chung)..... Alumni Lounge
FC Posters: Spectroscopy (J. Ingold)..... Robert P. Lee Lounge
GA Posters: Electron-Atom/Molecule Collisions (S. Chung)..... Alumni Lounge
GB Posters: Breakdown and Transport (J. Ingold)..... Robert P. Lee Lounge
GC Posters: Sheaths (S. Chung)..... Alumni Lounge

4:00 - 5:30 HA Spectroscopy of Atoms, Molecules, Ions (F. A. Sharpton)..... Lakeshore Room
HB Discharges in Electronegative Gases (S. R. Hunter)..... Room 313

I Lakeshore Room and 313 available Wednesday evening

Thursday, October 9

8:00 - 9:45 JA Electron-Atom/Molecule Collisions II (P. D. Burrow)..... Lakeshore Room
8:00 - 9:45 JB Spectroscopy of Arc Lamps (J. J. Lowke)..... Room 313
10:00 - 11:30 KA Modeling of Transport and Kinetics (J. N. Bardsley)..... Lakeshore Room
10:00 - 11:30 KB Laser Diagnostics of Sheaths (J. B. Gerardo)..... Room 313

11:30 - 12:00 Business Meeting Lakeshore Room

1:00 - 4:00 LA Posters: Spectroscopy (J. E. Lawler)..... Robert P. Lee Lounge
LB Posters: Lasers and R.F. Discharges (J. E. Lawler)..... Alumni Lounge
LC Posters: Recombination (J. E. Lawler)..... Robert P. Lee Lounge
LD Posters: Ion-Neutral Collisions (J. E. Lawler)..... Alumni Lounge
LE Posters: Electron-Atom/Molecule Collisions (J. E. Lawler)..... Robert P. Lee Lounge

6:30 - 10:00 Banquet Lowell Hall
After dinner speaker: Prof. Robert Greenler,
U. of Wis.-Milwaukee, "Optical Phenomena in the Atmosphere"

Friday, October 10

8:45 - 10:15 MA Laser Kinetics (H. T. Powell)..... Lakeshore Room
8:45 - 10:15 MB Plasma Chemistry (C. Zarowin)..... Room 313
10:30 - 11:40 N Recent Developments in Excimer Kinetics (J.J. Ewing)..... Lakeshore Room